DOKUZ EYLÜL UNIVERSITY
GRADUATE SCHOOL OF NATURAL AND APPLIED SCIENCES

PRODUCTION AND INDUSTRIAL APPLICATIONS OF HEAT RELEASING ELECTRONIC NANOCOMPOSITE MATERIALS FOR HEATING SYSTEMS

by
Mustafa EROL

December, 2013
İZMİR

PRODUCTION AND INDUSTRIAL APPLICATIONS OF HEAT RELEASING ELECTRONIC NANOCOMPOSITE MATERIALS FOR HEATING SYSTEMS

A Thesis Submitted to the
Graduate School of Natural and Applied Sciences of Dokuz Eylül University
In Partial Fulfillment of the Requirements for the Degree of Doctor of Philosophy in Metallurgical and Material Science Engineering

by
Mustafa EROL

December, 2013
İZMİR

Ph.D. THESIS EXAMINATION RESULT FORM

We have read the thesis entitled **PRODUCTION AND INDUSTRIAL APPLICATIONS OF HEAT RELEASING ELECTRONIC NANOCOMPOSITE MATERIALS FOR HEATING SYSTEMS** completed by **MUSTAFA EROL** under supervision of **PROF. DR. ERDAL ÇELİK** and we certify that in our opinion it is fully adequate, in scope and in quality, as a thesis for the degree of Doctor of Philosophy.

Prof. Dr. Erdal ÇELİK

Supervisor

Assoc. Prof. Dr. Mustafa TOPARLI

Thesis Committee Member

Assist. Prof. Dr. Ömer MERMER

Thesis Committee Member

Assoc. Prof. Dr. Zafer EVİS

Examining Committee Member

Assist. Prof. Dr. Işıl Birlik

Examining Committee Member

Prof. Dr. Ayşe OKUR

Director

Graduate School of Natural and Applied Sciences

ACKNOWLEDGMENTS

First of all, I would like to express my deep sense of gratitude to my advisor Prof. Dr. Erdal ÇELİK for his constructive ideas, help, constant support, guidance and contributions during my PhD research. I would also like to thank my committee members, Assist. Prof. Dr. Ömer MERMER and Assoc. Prof. Dr. Mustafa TOPARLI for reviewing my work and offering valuable suggestions and sharing their visions about the content of my thesis.

I wish to extend my sincere thanks to Assist. Prof. Dr. M. Faruk EBEOĞLUGİL, Assist. Prof. Dr. Işıl Birlik, Assist. Prof. Dr. Osman ÇULHA, Assist. Prof. Dr Yavuz ÖZTÜRK, Erhan ÖZKAN, Assist. Prof. Dr. Esra DOKUMACI, and Assist. Prof. Dr. Necmiye Funda AK AZEM for their collaboration in the laboratory studies and sharing their valuable experiences with me. In addition, I would like to thank Dr. Orkut SANCAKOĞLU, Tuncay DİKİCİ, Kadir Cihan TEKİN, Murat BEKTAŞ, Elif Zehra EROĞLU, Onur ERTUĞRUL, Haydar KAHRAMAN, Nihal ALTUĞ KAHRAMAN, Serhan KÖKTAŞ and Aslıhan SÜSLÜ, for their invaluable assistance and kind friendship who are my collegues in my department. I would also like to express my genuine gratitude to Çiğdem Gülay BAŞKURT, Serdar YILDIRIM, Fatma BAKAL, Selim DEMİRCİ, Güneş KURŞUN, Özlem CANPOLAT who are my collegues in Center for Fabrication and Application of Electronic Materials. I also want to thank to Haluk GÜRSES, Metin GEMİCİ, Dalyan ÖZKAN, Hamdi CİNAZ and Esra AKINCI who are the technical and official staff of my department. I would like to thank Salih GÜNNAZ, Berkan ÖZTÜRK, Erkan ÇAKIROĞLU, and Emre ÇİNKILIÇ for their assistance, support and kind friendship on my studies. Finally I want to thank to all my lecturers in the department whom encoureged me to afford this work. I would also like to express my genuine gratitude to each of people, although it would be impossible for me to name all.

Metin YURDDAŞKAL who is my project mate and also my brother, deserves biggest thank since we have finished the study togethers without any problems. This research was funded by SANTEZ program of Turkish Republic Ministry of Science, Industry and Technology and Ayçe Mühendislik between 2009 and 2011 with the

project number 00360.STZ.2009-1. Due to fact that I would like to thank the ministry and Çetin ÖZKUMUR for their economical and infrastructural supports.

Finally, a special thank goes to my fiancee Begüm DURUTÜRK and my family for their concern, confidence and support. The successful completion of this study would not have been possible without their constant love and encouragement.

Mustafa EROL

PRODUCTION AND INDUSTRIAL APPLICATIONS OF HEAT RELEASING ELECTRONIC NANOCOMPOSITE MATERIALS FOR HEATING SYSTEMS

ABSTRACT

Electrical heating technology is employed in many devices or device components nowadays. The technology is based on the heat generation of flowing current through metal thanks to its resistance.

Materials science as an interdisciplinary science can be defined as investigation and production of suitable material for devices to supply human needs. In the scope of thesis, it is aimed to produce conductive polymeric composite films with carbon based filler to be replaced present metallic heating elements.

Naturally insulating polymers were transformed to a conducting material via carbon based fillers. The produced films were characterized through XRD, XPS, FT-IR, DTA-TG, SEM and NI equipments. In addition to these characterizations, electrical properties and heating behaviors of films were determined. By using the optimum films, some applications as heat releasing fabrics, portable sauna, boiler and green house heating systems were produced.

In conducting polymer composites there is a insulator-conductor transition at a critical filler concentration named as percolation threshold. The concentrations were determined as 15 and 13 percentages for graphite and carbon black filled composite films respectively. In order to decrease percolation threshold, the films including graphite and carbon black together were produced. The synergetic effect which is defined as co-percolation supplied lower resistance values with lower filler content. If mass production objective is taken into account; decrease in the filler content will be important about production costs.

In addition to scientific results; it must be noted that the originality and innovation of the study was approved by some foundations. Firstly the study was protected by

Turkish Patent Institute with patent number 2009/05515. It was funded by SANTEZ program of Turkish Republic Ministry of Science, Industry and Technology between 2009-2011 (00360.STZ.2009-1).Finally it is selected the Best SANTEZ project in March 2013, and the prize was presented by the minister Nihat ERGÜN.

Keywords: Polymer composites, percolation, conducting polymer, heating element

ISITMA SİSTEMLERİ İÇİN ISI YAYAN ELEKTRONİK NANOKOMPOZİT MALZEMELERİN ÜRETİMİ VE ENDÜSTRİYEL UYGULAMALARI

ÖZ

Elektrikle ısıtma teknolojisi, günümüzde birçok cihaz ve cihaz bileşeninde kullanılmaktadır. Bu teknoloji genellikle iletken bir metal üzerinden geçen elektrik akımının metalin elektriksel direnci sebebiyle ısı üretilmesi prensibine dayanmaktadır.

Disiplinler arası bir bilim olan malzeme bilimi; insanlık ihtiyaçlarını karşılayacak cihazların geliştirilmesi için uygun malzemelerin araştırılması ve geliştirilmesi olarak tanımlanabilir. Bu tez kapsamında mevcut metalik ısıtma elemanlarının yerini alabilecek nitelikte karbon içerikli katkılara sahip polimerik kompozit filmlerin üretilmesi hedeflenmiştir.

Doğası gereği yalıtkan olan polimerler karbon içerikli katkılar yapılarak iletken hale getirilmiştir. Üretilen filmleri yapılarının aydınlatılabilmesi için; XRD, XPS, FT-IR, DTA-TG, SEM ve NI cihazları ile karakterize edilmiştir. Yapısal analizlere ek olarak üretilen filmlerin elektriksel özellikleri, ısıtma davranışları belirlenmiştir. Optimum filmler kullanılarak ısı yayan tekstiller, sauna, kombi ve sera ısıtma sistemleri gibi prototip uygulamalar gerçekleştirilmiştir.

Polimer kompozitlerde perkolasyon eşiği kavramı ile açıklanan, kritik bir katkı kompozisyonunda yalıtkan iletken geçişi söz konusudur. Kritik iletkenlik geçişi grafit ve karbon katkıları için sırasıyla ağırlıkça yüzde 15 ve 13 olarak belirlenmiştir. Bu nedenle üretilen filmlerle eşdeğer dirence sahip ancak daha az katkı miktarına sahip filmlerin üretilmesi hedeflenmiştir. Bu doğrultuda perkolasyon eşiğinin aşağı çekilebilmesi için koperkolasyon olarak tanımlanan, karbon ve grafit katkılarının birlikte farklı oranlarda kullanıldığı filmler üretilmiştir. Bu filmler ile hedeflendiği gibi; daha az katkı ile koperkolasyon da başarı sağlanmıştır. Kütlesel üretim amacı göz önünde bulundurulursa, katkı miktarında azalma üretim maliyetlerinde önemli olacaktır.

Bilimsel sonuçlara ek olarak; çalışmanın özgünlüğünün ve yenilikçiliğinin bazı kuruluşlarca onaylandığı belirtilmelidir. İlk olarak çalışma Türk Patent Estitüsü tarafından 2009/05515 patent numarası ile korumaya alınmıştır. Çalışma 2009-2011 yılları arasında Türkiye Cumhuriyeti, Bilim, Teknoloji ve Sanayi Bakanlığınca SANTEZ (00360.STZ.2009-1) kapsamında desteklenmiştir. Projenin sonlandırılmasını takiben 2013 yılı Mart ayı içerisinde en iyi SANTEZ projesi seçilmiş ve ödül bizzat bakan Nihat ERGÜN tarafından takdim edilmiştir.

Anahtar Kelimeler: Polimer kompozitler, perkolasyon, iletken polimer, ısıtma elemanı.

CONTENTS

Page

LIST OF FIGURES

Page

LIST OF TABLES

Page

CHAPTER ONE
INTRODUCTION

1.1 Scope of the Thesis

Materials constructed with two or more individual components acting as matrix and the filler are defined as composites. As known there are three main classes of engineering materials; metals, ceramics and polymers. All these three classes have important and distinct properties. In this manner if we draw a triangle with metal, ceramic and polymer corners, one can locate composites into the center of the triangle. In order to declare this situation on the basis of matrix phase, composites can be clasified into metal matrix composites (MMCs), ceramic matrix composites (CMCs), and polymer matrix composites (PMCs). It is also possible to classify composites on the manner of reinforcement type as particle, fiber and laminates.

PMCs are very popular due to their low cost and simple fabrication methods when compared with MMCs' and CMCs'. PMCs are particularly produced to improve polymers limited mechanical and electrical properties with reinforcement addition. In a composite most of the physical properties are functions of filler fraction. Several research groups focused on mechanical properties of PMCs by adding different fractions of harder reinforcements in order to increase their tensile strength (Cheang, & Khor, 2003, Schneider et al. 2013, Wang et al. 2006, Colloca et al. 2013, Erçin et al. 2013).

Polymers zare known as good insulators for electronic applications. Developments of the polymers together with new researches involve desired conductivities and a wide range of application for decades. Conductivity of polymer composites can be obtained by loading an electrically insulating matrix with conductive fillers (Erol, & Celik, 2013). The filler can be an inorganic powder such as a metal or a ceramic, or an organic material such as carbon (graphite, carbon black or a fullerene) or an intrinsically conducting polymer. For very low filler fractions, the mean distance between conducting particles is large and the conductance is

limited by the polymer matrix, which has a typically conductivity in order of 10-15 $\Omega^{-1}cm^{-1}$. Subsequent to increasing the content of the filler, distance between the particles decreases (Strümpler, & Reichenbach, 1999). At a critical filler content (critical particle distance), conducting network formed for electron mobility where conductivity obtained. In the literature survey, it is reported that there are many different filler matrix couples forming the composite structures as listed in Table 1.1.

Table 1.1 Some reported studies on conducting composites with different filler and matrix types.

Filler	Matrix	Material Type	References
Ni	Silicon	Bulk	Bloor et al. 2005.
	Tetrasulfonatedphthalocyanine	Film	Hamilton et al. 2003.
Cu	Polyolefin	Film	Przemyslaw et al. 2011.
	Polyester	Bulk	Teh et al. 2011.
Ag	Polyvinylidenefluoride copolymer	Film	Chun et al. 2010.
	Polycarbonate	Film	Moreno et al. 2001.
Carbon Black	Polypropylene	Film	Xu et al. 2008.
	Polyethylene	Bulk	Seo et al. 2011.
	Styrene–butadiene	Bulk	Wan et al. 2005.
	Polyurethane	Film	Chen et al. 2010.
Carbon nanotube and Carbon nanofiber	Polypropylene	Film	Shen et al. 2012.
	Polypyrrole	Bulk	Sivakkumar et al. 2007.
	Polyester	Bulk	Wu., 2010.
Graphite	Polyester	Film	Lu et al. 2006.
	Epoxy	Bulk	Li & Kim. 2007.
	Polyaniline	Bulk	Wang et al. 2011.

According to Table 1.1, it can be briefly declared that the matrix polymer and filler types can be varied widely to be employed as a conductive polymer composite (CPC). Recently carbonous filler composites have been drawing more attention than metallic ones thanks to their low production costs, lightweights and so on (Xu et al. 2008, Wang et al. 2011.).

Conductivity mechanisms of CPC's have been successfully explained by using a phenomenon called percolation. Percolation is a very general phenomenon applicable in almost every area of science as the simplest model for spatial disorder. It has been shown that percolation has application to a broad range of topics including but not limited to mathematics, physics, biology, geography, hydrology, petroleum, ecology, chemistry, and materials science (Belashi, 2011). In the scope of this study it was focused on implementation of percolation to electrical conductivity.

PMCs are very popular due to their low cost and simple fabrication methods if compared with MMCs' and CMCs'. PMCs are generally produced to increase polymers limited mechanical and electrical properties with reinforcement addition. In a composite, most of the physical properties are functions of filler fraction. The electrical resistance in a composite system comprising a network of conducting and insulating phases is the result of a large number of resistors combined in series and parallel.

There are different contributions to the resistance or conductance, with hopping and tunneling effect on conductance generally dominating the magnitude of the overall conductance. The hopping mechanism refers to the process in which a charge carrier is suddenly displaced from one occupied state to another equivalent empty donor state of higher energy. The tunneling mechanism is a manifested characteristic of the conductivity of nanocomposites. The conductivity of the percolating network in CPC's appears to be the result of electron transport between the nearest neighbor connections of one filler to another which denote the dominant conducting elements across the inter-particle tunneling distance. The tunneling distance is the average distance between the two closest separated points of adjacent particles and is only a few nanometers (Belashi, 2011). Obtained resistance at this minimum distance refers to critical filler content. At critical filler content resistance sharply decreases and this sharp change is defined as a percolation threshold. Conductive network formation, and percolation threshold and are illustrated in Figure 1.1 using microstructural demonstrations. There are different contributions to the resistance or conductance,

with hopping and tunneling effects on conductance generally dominating the magnitude of the overall conductance.

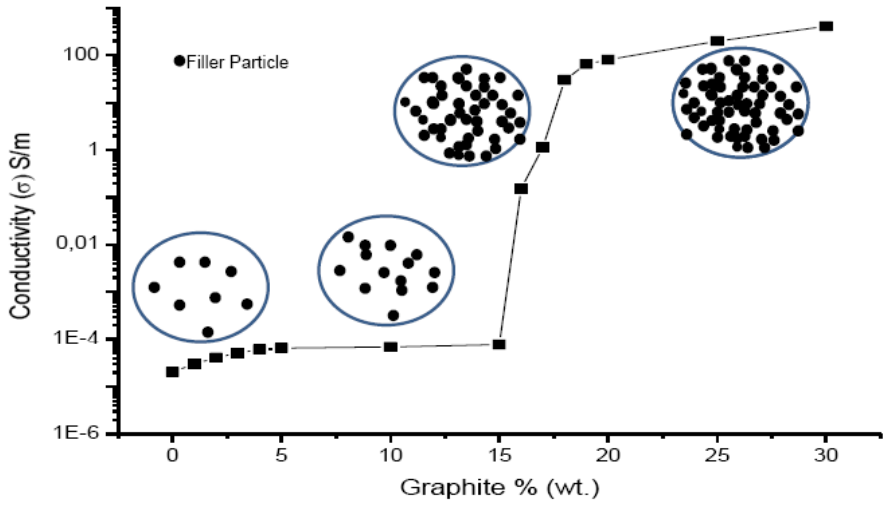

Figure 1.1 Schematic illustration of percolation phenomena.

In recent years, the CPC's have been widely investigated in terms of their low percolation thresholds for many different applications; as temperature or current sensors (Jeon et al. 2013., Shih et al. 2010.) flooring materials to dissipate static electric, charge, antistatic coating and electromagnetic radiation shielding (Gupta, & Choudhary (2011), Nam et al. 2012 and Klemperer, & Maharaj (2009)). Metallic materials have resistivities between 10^{-8} and 10^{-6} Ωm and they are also in a good relationship with ohm's law (inverse proportionality of resistance and current). Whenever an electric current flows through a material that has some resistance it creates heat. This resistive heating is the result of "friction," as created by microscopic phenomena such as retarding forces and collisions involving the charge carriers (usually electrons); in formal terminology, the heat corresponds to the work done by the charge carriers in order to travel to a lower potential. This phenomenon is defined as joule heating in 1841 by J. P. Joule and employed in many electric based heaters (for example, a toaster, an electric space heater, or an electric blanket). According to this manner, issue of using CPC's as joule heating elements is a promising idea. There are a few studies reported on CPC based heating elements which are the main objective of this thesis (Isaji et al. 2009, Erol, & Celik, (2013))

Most of the joules heating based devices mentioned above are constructed from different materials. Important materials selection criterias are melting point of the heating element and environmental conditions (corrosion attack, mechanical stresses and etc.).

Heating elements can be classified into two groups depending on their working temperatures; low temperature and high temperature. Low temperature applications generally for home usage included such metallic alloys with trade names Kanthal (FeCrAl), Nichrome 80/20, and Cupronickel. For industrial requirements generally for metal-alloy melting, ceramic sintering and for any high temperature industrial heat treatments one needs more affective elements with higher melting temperatures and desired resistances. In the cases where reducing atmospheres can be tolerated, graphite or refractory metals such as molybdenum and tungsten can be used, while platinum and its alloys can be used safely in air up to 1500^{o}C. Ceramics allow the use of air atmospheres at relatively low cost such as silicon carbide, molybdenum disilicide, lanthanum chromite, tin oxide, zirconia and so on (Moulson & Herbert 2003).

As a physical magnitude resistance of a heating element is directly affected from its resistivity, length and cross sectional area (ohm's law) and indirectly from temperature. The resistance of a material has a dependence upon a number of phenomena. One of them is the number of collisions that occurs between the charge carriers and atoms in the material. As the temperature increases so do the number of collisions and therefore it can be imagined that there will be a marginal increase in resistance with temperature. This may not always be the case because some materials have negative temperature coefficient of resistance. This can be caused by the fact that with increasing the temperature, further charge carriers are released which will result in a decrease in resistance with temperature. As might be expected, this effect is often seen in semiconductor materials. There are numerous uses for resistors with high values of the temperature coefficient of resistance (TCR) and they may be negative (NTC) or positive (PTC). TCR can be expressed from the equation; $R=R_{ref}[1+\alpha(T-T_{ref})]$ where R: the resistance at temperature, T, R_{ref}; the resistance at

temperature T_{ref}, α; the temperature coefficient of resistance for the material, T; the material temperature in ° Celcius, T_{ref}; (generally speaking 20 C) is the reference temperature for which the temperature coefficient is specified.

In manner of producing graphite and carbon black reinforced CPC's many researchers reported that CPC's show PTC effect (Xu et al. 2008, Seo et al. 2011, Isaji et al.2009, Chen et al. 2005, Erol, & Celik, 2013) Using graphite as a heating element to melt metallic scraps to produce secondary steel is an indispensable process in electrical arc furnaces. Most resistors for electrical and electronic applications are required to be ohmic and to have small temperature coefficients of resistance. The major requirement in electronics is for resistors in the range of 10^3–$10^8\Omega$, while materials with suitable electrical properties usually have resistivities less than 10^{-6} Ω. Fabrication of a 10^5 Ω resistor with length of 110 mm from a material with a resistivity of 10^{-6} Ω requires a cross-sectional area of 10^{-12} m^2, i.e. a strip 1 μm thick and 1 μm wide, for example. This is not a technical impossibility, but other more economic routes to resistor manufacture have been established based on the two principles. First; very thin conductive layers are deposited on an insulating substrate and large length-to-width ratios are obtained by etching a suitable pattern (thin film technology). Second; The conductive material is diluted with an insulating phase (composite technology).

All theoretical issues mentioned above as; using resistive elements to generate heat, employing graphite in scrap melting, PTC properties of carbonous CPC's, and producing CPCs as thin film composites; strengths the idea of graphite and/or carbon black reinforced polymer matrix films as a low temperature heating elements. Distinct from the reported studies in literature CPC's were deposited on polyester and glass substrates via spray deposition technique. Since decreasing filler content is cost effective and mechanically favored beside individual effect of graphite and carbon black, co-percolation studies were innovatively applied with the aim of decreasing weight of filler.

1.2 Organization of the Thesis

The primary purpose of this thesis is to convey insight into preparation characterization, development and application of three different classes of styrene acrylic copolymer matrix CPC films produced using spray deposition technique. Three different classes can be summarized as individual carbon black, individual graphite and binary carbon black and graphite reinforced CPCs. The approach is to explore both the science and technology of synergic effect of carbon black and graphite on electrical, mechanical and structural properties of CPCs.

In order to determine the thermal properties and chemical structure of the CPC films, Differential Thermal Analysis-Thermogravimetry (DTA-TG) and Fourier Transform Infrared (FTIR) devices were used respectively. Structural analysis of the produced films was performed using multipurpose X-Ray Diffraction (XRD) and X-Ray Photoelectron Spectroscopy (XPS) and surface morphology was investigated using Scanning Electron Microscopy/Energy Dispersive Spectroscopy (SEM/EDS). A Keithley-2400 sourcemeter was used for 2-probe resistance measurements of the CPC films to obtain filler versus resistance plots and percolation thresholds. Samples above percolation were selected to employ as a heating element. By this way a 0-60 V DC source meter and an IR thermal camera were used to record heating regime versus time. Finally in order to prove theory best performance CPC films were transformed in to some prototype heating devices such as floor heating pads, portable saunas, and central heating boilers (combi boiler) for houses and greenhouses.

In Chapter 2, polymeric composites, their production, type of fillers, type of matrixes characterization and applications were explained as a general introduction. Conduction mechanisms and its physical background in CPCs which are members of polymeric composites were presented. Additionally with an electrical manner, percolation theory and its basics were theoretically summarized; also joule heating and its theory, heating elements and applications were represented. Chapter 3 concerns with characterization performed on styrene acrylic copolymer matrix graphite and/or reinforced CPC films. All characterization techniques and

applications are described briefly. In Chapter 4 general results of characterization and application studies are given and interpreted. The obtained results were discussed with similar reported studies. Finally, the general conclusions of this study and future plans about the work are presented in Chapter 5.

CHAPTER TWO
THEORETICAL BACKGROUND

2.1 Polymer Matrix Composites (PMCs)

Composites are combinations of (at least two) materials such as matrix and reinforcement. The matrix material surrounds and supports the reinforcement materials by maintaining their relative positions. The reinforcements are embedded and arranged in specific internal configurations to obtain mechanical or other properties tailored to specific applications. In similar manner one can easily define polymer composites as; a well-established class of materials in which particles or fibers – used as reinforcing elements – are dispersed in the polymer matrix (Michler, 2008).

2.1.1 General Motivation

Polymer matrix composites consist of particles and/or fibers embedded in polymer matrices. The particles and/or fibers are introduced to enhance selected properties of the composite. The particles and/or fibers play a key role on many properties of the composite structure with their size, orientation, dispersion and geometry as well. In order to create a general classification based on these aspects; Figure 2.1 will be useful for demonstration.

Different material types can be used as particle reinforcements to form PMCs such as; ceramic, glass and minerals (SnO_2, SiO_2, talc and etc.), metallic particles (Fe, N, Cu and etc.), organic materials (chaffs, chitosan, and starch etc.), and carbon derivates (carbon black, graphite, active carbon and carbon nanotube etc.). Generally ceramics and minerals are used to increase mechanical properties of the matrix, to increase wear and abrasion resistance and surface hardness, to improve performance at elevated temperatures, to reduce friction and shrinkage, and to decrease the permeability of the matrix. Sometimes they are also just used to reduce the cost of

the polymer. In contrast, metal particles and carbon derivates are mainly used to improve the electrical conductivities of most insulating polymer matrices.

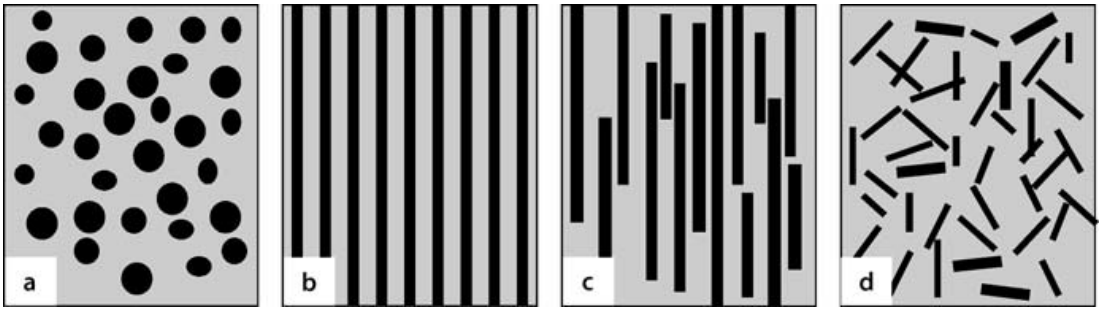

Figure 2.1 Schematic representations of polymer composites: (a) particle reinforcement, (b) fiber reinforcement with continuous and aligned fibers; (c) with discontinuous and aligned fibers; (d) with discontinuous and randomly oriented fibers (Michler, 2008).

Fibers, although strong and tough, are generally not very stiff because they are very small in diameter. Therefore, it would be impossible for a structure to be made only from small fibers. As mentioned in Chapter 1 similar material types can be employed to form fiber reinforced PMCs. Adding a matrix material ties the fibers together to form a structure, so that stress can be transferred from one fiber to another, sharing the load. Adding reinforcing fibers increases the modulus of the matrix material. The arrangement or orientation of the fibers relative to one another, the fiber concentration and their distribution all have a significant influence on the strength and other properties of fiber-reinforced composites. Applications involving multidirectional applied stresses normally use discontinuous fibers, which are randomly oriented in the matrix material (Michler, 2008).

2.1.2 Manufacturing types of PMCs

Processing is the science of transforming materials from one shape to the other. Because composite materials involve two or more different materials, the processing techniques used with composites are quite different than those for metals processing.

There are various types of composite processing techniques available to process the various types of reinforcements and resin systems. It is the job of a

manufacturing engineer to select the correct processing technique and processing conditions to meet the performance, production rate, and cost requirements of an application.

Generally speaking, aim of processing a PMC has basic steps as; obtaining and combining matrix and reinforcement. Matrix material in another saying polymer is usually used in liquid or gel form. Reinforcements and cross linking agents were added in to this non solid structure and homogenized. Subsequent to mixing, mixture is solidified to form PMC structure. According to mentioned every material possesses unique physical, mechanical, and processing characteristics and therefore a suitable manufacturing technique must be utilized to transform the material to the final shape. Ceramic parts are difficult to machine and therefore are usually made from powder using hot press techniques. In metals, machining of the blank or sheet to the desired shape using a lathe or CNC machine is very common. In metals, standard sizes of blanks, rods, and sheets are machined and then welded or fastened to obtain the final part. In composites, machining of standard-sized sheets or blanks is not common and is avoided because it cuts the fibers and creates discontinuity in the fibers. Exposed and discontinuous fibers decrease the performance of the composites. Moreover, the ease of composites processing facilitates obtaining near-net-shape parts. Composites do not have high pressure and temperature requirements for part processing as compared to the processing of metal parts using extrusion, roll forming, or casting. Because of this, composite parts are easily transformed to near-net-shape parts using simple and low-cost tooling. In certain applications such as making boat hulls, composite parts are made at room temperature with little pressure. This lower-energy requirement in the processing of composites as compared to metals offers various new opportunities for transforming the raw material to near-net-shape parts (Mazumdar, 2001).

In industrial and research applications, there are many types of PMC manufacturing. The most utilized ones can be listed as; Lay-Up Process (Hand Lay Up, Prepeg Lay Up), Filament Winding, Pultrision, Molding Techniques (Injection, Extrusion and Compression), and Spray Deposition.

2.1.2.1 Lay-Up Process

Complicated shapes with very high fiber volume fractions can be manufactured using Lay-Up Process. It is an open molding process with low-volume capability. In this process, prepegs are cut, laid down in the desired fiber orientation on a tool, and then vacuum bagged (Figure 2.2). After vacuum bagging, the composite with the mold is put inside an oven or autoclave and then heat and pressure are applied for curing and consolidation of the part. The process is widely used in the aerospace industry as well as for making prototype parts. Wing structures, radomes, yacht

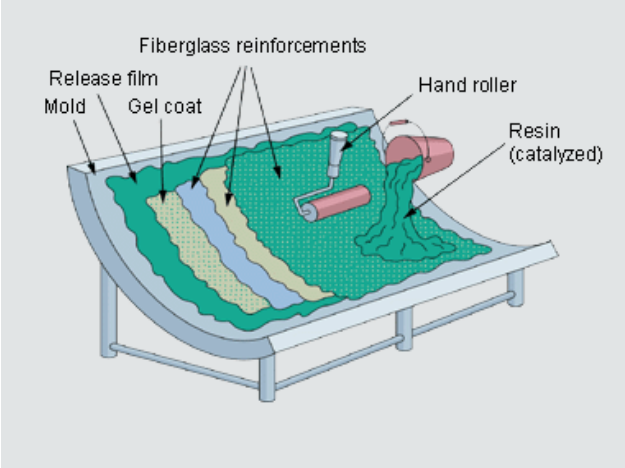

Figure 2.2 Schematic illustration of layup process (Wacker Chemie, 2013).

Figure 2.3 Variety of aircraft radomes (Mazumdar, 2001).

parts, and sporting goods are made using this process. Figure 2.3 depicts a variety of aircraft radomes such as shark nose, conical, varying lengths, solid laminates, and sandwich constructions with dielectrically loaded foam cores.

2.1.2.2 Filament Winding Process

Filament winding is a process in which resin-impregnated fibers are wound over a rotating mandrel at the desired angle. A typical filament winding process is shown in Figure 2.4, in which a carriage unit moves back and forth and the mandrel rotates at a specified speed. By controlling the motion of the carriage unit and the mandrel, the desired fiber angle is generated. The process is very suitable for making tubular parts. The process can be automated for making high-volume parts in a cost-effective manner. Filament winding is the only manufacturing technique suitable for making certain specialized structures, such as pressure vessels as seen in Figure 2.5.

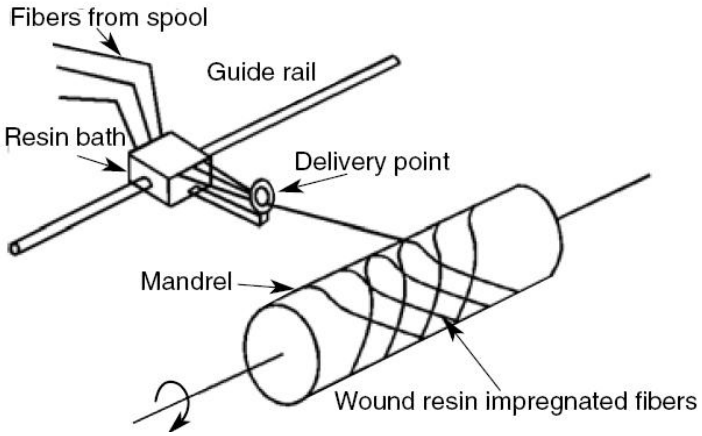

Figure 2.4 Schematic of the filament winding process (Mazumdar, 2001).

2.1.2.3 Pultrusion Process

The pultrusion process is a low-cost, high-volume manufacturing process in which resin-impregnated fibers are pulled through a die to make the part. The process is similar to the metal extrusion process, with the difference being that instead of material being pushed through the die in the extrusion process, it is pulled

through the die in a pultrusion process. Pultrusion creates parts of constant cross-section and continuous length.

Pultrusion is a simple, low-cost, continuous, and automatic process. Figures 2.6 and 2.7 illustrate a typical pultrusion process in which resin-impregnated yarns are pulled through a heated die at constant speed and its products, respectively. As the material passes through the heated die, it becomes partially or completely cured. Pultrusion yields smooth finished parts that usually do not require post-processing.

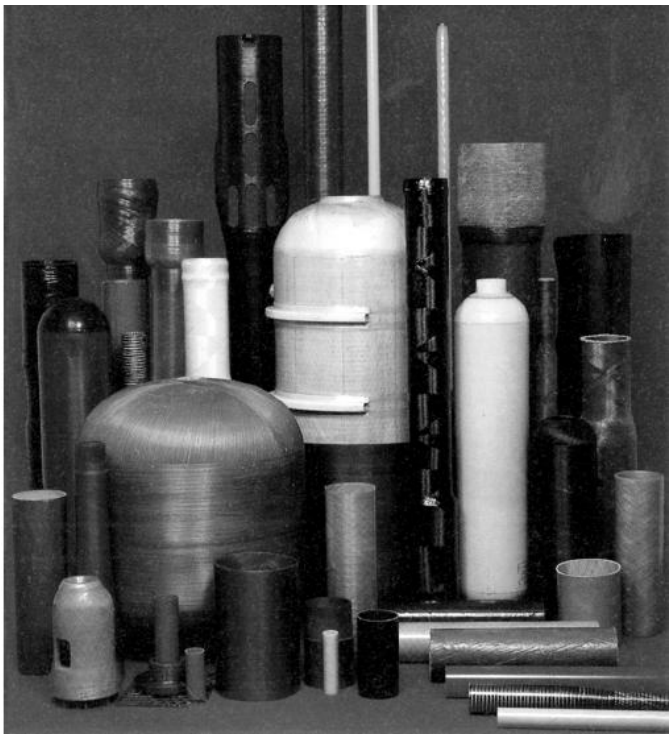

Figure 2.5 Filament wound parts (Mazumdar, 2001).

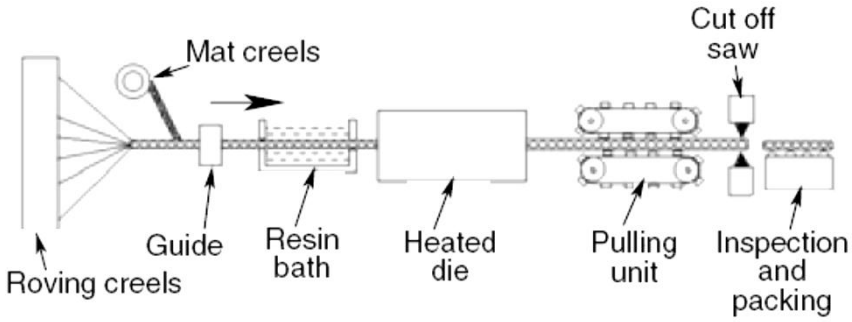

Figure 2.6 Illustration of a pultrusion process (Mazumdar, 2001).

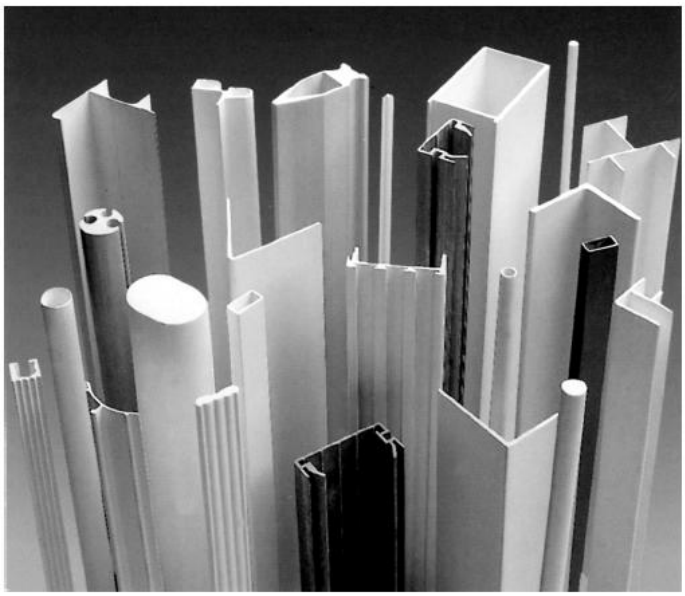

Figure 2.7 Typical pultruded shapes (Mazumdar, 2001).

2.1.2.4 Molding Processes

In engineering applications there are too many different molding processes employed for PMC production. This variety is present because final product needs, raw material suitability's, and cost etc.

Injection molding process is generally associated with processing the thermoplastics. However, with the development of the reciprocating screw type equipment, thermosets can also be injection molded. The basic process includes plasticizing, injection, cooling, and ejection. Typically, the granules are fed from a hopper into to a screw that rotates to feed the material into a heated chamber to allow the material to change to a molten state. The material is then forced through a nozzle into the mold cavity. A cooling time is necessary to allow the polymer to become solid, and then is ejected from the mold by mechanical ejector pins. Stages of injection molding are depicted in Figure 2.8.

Extrusion molding process, a continuous flow of molten material is forced through a die. The shape of the final product is determined by the shape of the die opening. Typically, thermoplastic molding power is fed from a hopper, similar to the

configuration of the screw system in injection molding as illustrated in Figure 2.9. The screw forces the material through a tapered opening in the die. The heat and friction causes plasticizing to occur, softens the material, and forces it through the die opening. The material is cooled by either air or water. The rate of cooling can be controlled and further forming is possible. For example, pvc pipe is extruded as well as electrical conduit. If allow to be immersed in hot water, the conduit can be bent at 90 degree angles. Typical products that are extruded include tubing, rods, bars, moldings, sheets and films. Extrusion is also used for coating wire and cable.

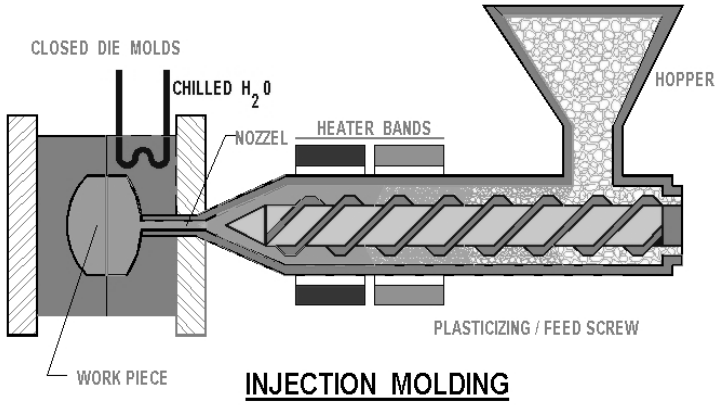

Figure 2.8 Schematic illustration of Injection molding (Western Carolina University, 2013)

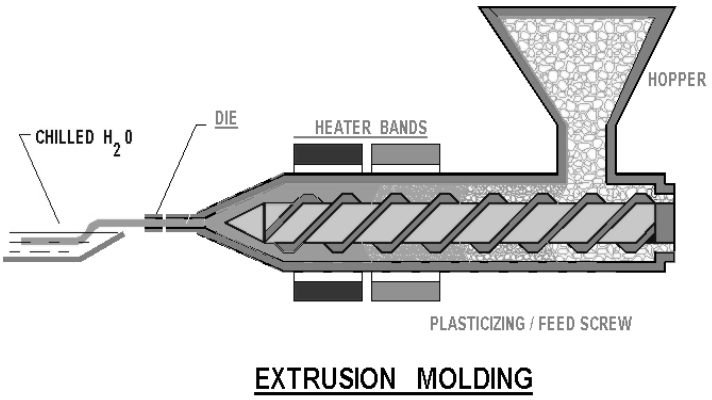

Figure 2.9 Schematic illustration of extrusion molding (Western Carolina University, 2013)

Compression molding process is used for forming thermosets by applying heat and pressure. As sequenced in Figure 2.10, measured amount of thermoset powder, granules or pellets, is fed into the mold cavity. Heat allows the material to soften and pressure to fill the cavity, then the material is cured. Heat actually causes the

polymer to soften and then harden into a highly cross-linked and networked structure. This process is primarily for thermosetting materials and is of limited use for thermosets owing to of the cooling time required of the mold. Typical products include electrical insulators, pot handles, and some automotive parts.

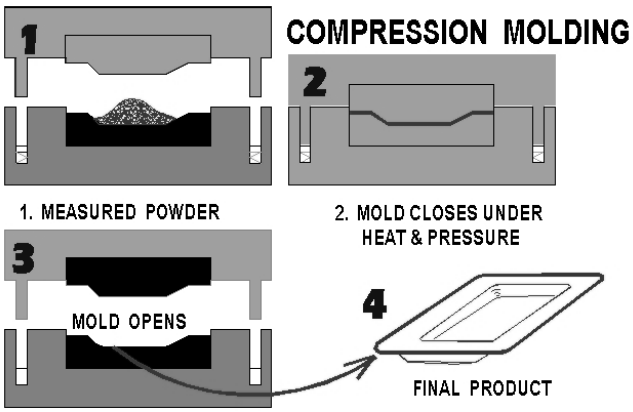

Figure 2.10 Schematic flow of compression molding (Western Carolina University, 2013).

2.1.2.5 Spray Molding and Deposition Processes

Spray deposition process is a method that deposits the mixture of pre-composite onto a substrate or mold as seen in Figure 2.11. In contrast to prior processes, this process also allows the deposition of composites in film form.

Increasing impact of thin film technology on many industries is also present in composite technology. Mostly in electronic, magnetic and optical devices, polymer composites are applied in deposited form (Oxford Vacuum Science, 2013). There are many methods involving thin film deposition of PMC films such as; printing, vacuum techniques, spraying, spin and dip coating. In addition, the spray deposition technique is well established in graphic arts, industrial coatings, and painting. This high-throughput large-area deposition technique ensures ideal coatings on a variety of surfaces with different morphologies and is often used for inline production. Moreover, the fluid waste is reduced to minimal quantities, and the deposition can be easily patterned by simple shadow masking. Also, the spray coating technique is able to access a broad spectrum of fluids with different rheologies, offering the opportunity to tune the system to deposit virtually any kind of solution and obtain the

desired film properties (Girotto et al, 2009). A schematic illustration of system is depicted in Figure 2.12 which was designed by a research group. In their study premixture of a composite (PFA/MWCNT) is fed in to syringe and accelerated by compressed air on to heated and shifting substrate (Zhao et al, 2009).

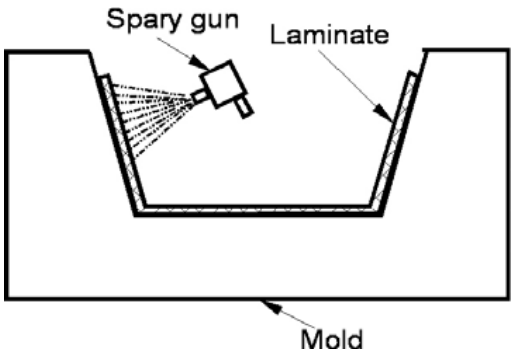

Figure 2.11 Schematic illustration of spray up molding (Mazumdar, 2001).

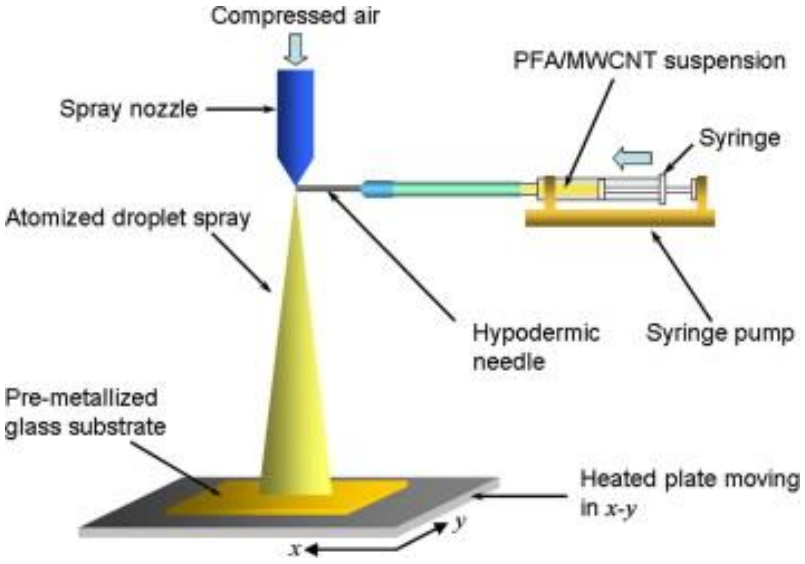

Figure 2.12 Schematic illustration of spray deposition process (Zhao et al. 2009).

2.1.3 Applications of PMCs

There are many reasons for the growth in composite applications, but the primary impetus is that the products fabricated by composites are stronger, lighter and more funtionalized. Today, it is difficult to find any industry that does not utilize the benefits of composite materials. In the past three to four decades, there have been substantial changes in technology and its requirement. This changing environment

created many new needs and opportunities, which are only possible with the advances in new materials and their associated manufacturing technology (Mazumdar, 2001). Broadly speaking, the composites market can be divided into the following industry categories: aerospace, automotive, construction, marine, corrosion resistant equipment, consumer products, appliance/business equipment, and others.

Composite shipments in 2000s are demonstrated in Figure 2.13 which includes mentioned industry categories. According to chart of a decade before one can easily note that the most shipped categories are transportation and construction.

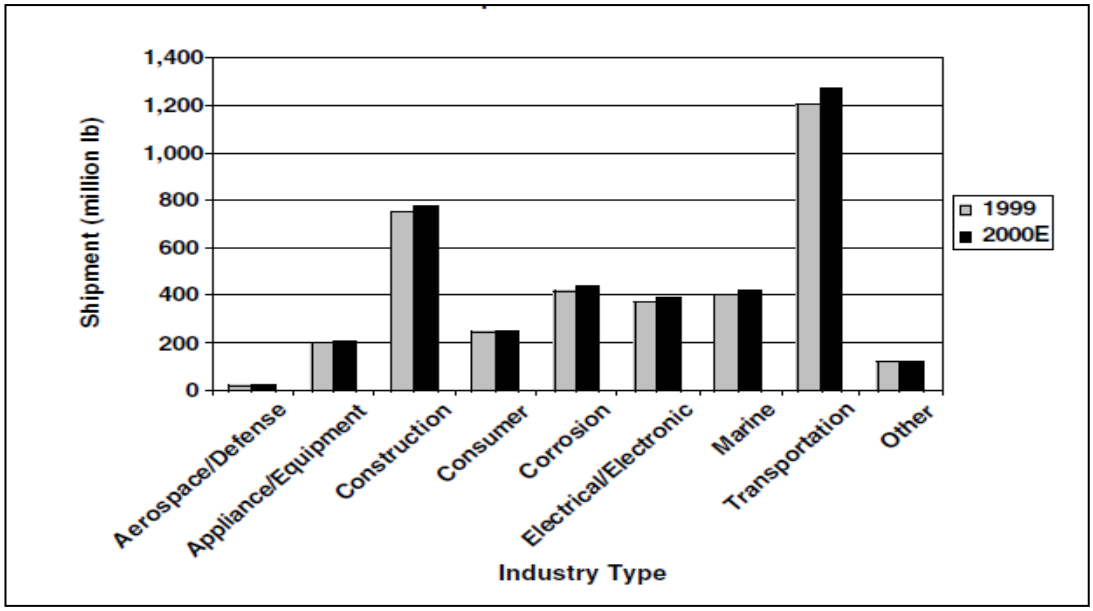

Figure 2.13 Composite shipments in various industries in 1999 and those projected for 2000 (Mazumdar, 2001).

Any electronic device which allows computing, communicating, controlling and being employed to humankind has an increasing role in every part of individual lives. Figure 2.14 represents the shipments for 2011 and predicted the shipments for 2017. If compared to trend in 2000s the increase in the piece of Electrical and electronics (E&E) must be noted. Comparison of this figure also provides us to understand that bulk and large materials have been replaced with small, smart and technological materials. Polymer composite science has evolved over the years by a need to produce new materials for new applications. As mentioned before some materials

have been on the market for a while, there exists a need to optimize their properties to meet specific requirements. And when it comes to developing new materials, more emphasis is being placed on controlling the manufacturing process to manipulate molecular weight or develop novel architectures. Polymers have experienced so much market success because it is possible to build properties into the material. Further advances in polymer research will enable the materials to meet the demand for highly specialized applications, such as those found in optics and electronics.

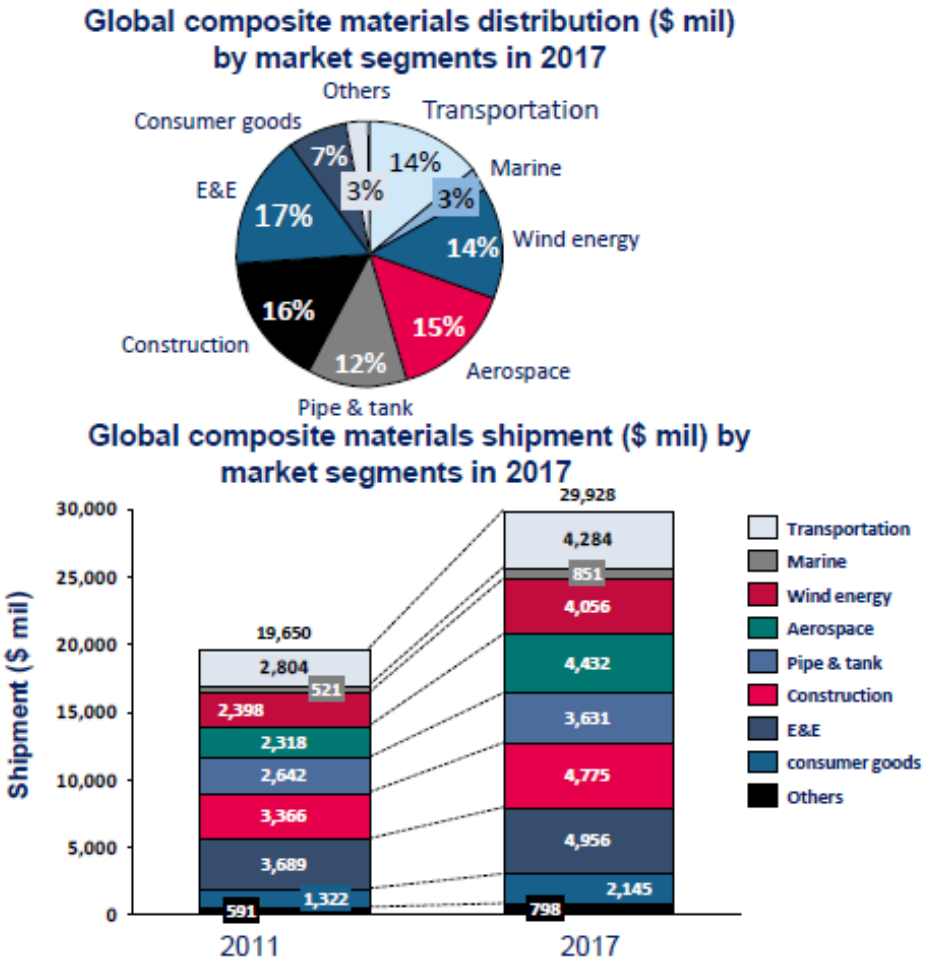

Figure 2.14 Composite shipments in various industries in 2011 and those predicted for 2017 (Lucintel, 2013).

Almost daily, new developments are emerging from advanced materials and polymer research labs around the world: novel electroactive polymer actuators; polymer nanofilms; self-healing polymers; electrically conducting tissue; embedded waveguide sensors in polymer membranes. Definition of composite encourages

researchers to develop new and unique materials in infinitive number and application types. The incorporation of nanomaterials can improve the various properties of the polymers such as its tensile strength, Young's modulus, impact and scratch resistance, electrical and thermal conductivity, thermal stability and fire resistance (Davtyan et al. 2012). Thus there are some studies with different property considerations applied are tabulated in Table 2.1.

2.2 Conducting Polymer Matrix Composites (CPCs)

As mentioned in the introduction part of the thesis, our objective is to produce carbon and/or reinforced conductive nanocomposite films and to investigate their application for low temperature heating elements. Thus manner of conduction, mechanism and types will be summarized in this section. When an electrically conducting phase is dispersed in sufficient quantity in a polymeric resin, a conductive composite is formed. The unique properties of such composites make them technologically superior to or more cost effective than alternative materials. Since the first experimental results were published decades ago, conducting polymer composites have been adapted to a variety of applications.

2.2.1 Conduction Mechanism and Percolation Phenomena in CPCs

An alternative method of inducing electrical conductivity in polymers is to make polymer composite materials with conductive additives or fillers. Typical examples of conductive components used to prepare this type of conducting polymer include conducting solids (carbon-black, carbon fibers, aluminum flake, stainless steel fibers, metal-coated fillers, metal particles, etc.) and conjugated conducting polymers. Inasmuch as the conductivity is introduced through the addition of the conducting components, various polymer materials including both amorphous polymers (polystyrene, PVC, PMMA, polycarbonate, acrylonitrile butadiene styrene (ABS), polyethersulphone, polyetherimides, etc.) and crystalline polymers (polyethylene, polypropylene, polyphenylene sulphide, nylons, etc.) can be made electrically conducting (Dai, 2004).

Table 2.1 PMC research and applications with different aims.

Property	Common Nanocomposite Approach	Potential Application	References
Chemical/Physical Gas/liquid Permability	Inclusion of impermeable, high aspect ratio silicate or graphite flake in resin.	Cryogenic tanks, durability to diffusion species	Ward, & Koros, 2011
Oxidative Resistance	Incorporate high temperature, oxidative resistant fillers (silicate, CNT,POSS, etc.) that form passivating layers.	Thermal protective systems, atomic oxygen resistance	Mahmoudian et al. 2013
Electrical Conductive	Incorporate high aspect ratio conductive particles such as CNT, graphite flake, metals, etc as percolated network in resin between conductive fibers.	Sensors, Electrodes, Heating Elements, Thermistors and etc.	Erol, & Celik, 2013.
Electro Magnetic Interferrence	Create films of highly percolated network of conductive nanofillers (nickel nanostrand veil, SWNT buckypaper, etc.) that can both absorb and dissipate broadband frequencies.	Bus compartment enclosure, electronic enclosures	Al-Saleh et al. 2013
Thermal Thermal Conductivity	Incorporate highly thermal conductive particles (CNT's, metals, etc.) into resin and optimize structure for heat transfer along continuous path to heat sink.	Adhesives, gaskets, radiators, doublers, electronics board, solid state laser heat removal	Baniassadi et al. 2011
Thermal Protection Systems	Use thermally conductive and insulating nanofillers within resin to assist larger structure components to direct heat away from protected systems.	Aircraft brakes, re-entry vehicles, missiles	Wang, & Ke, 2006
Coefficient of Thermal Expansion	Incorporate nanofillers with low expansion coefficients and good matrix bonding such as (functionalized CNT, CNF, silicates, etc.) into resin or as fiber sizing to reduce CTE mismatch.	Adhesives, space apertures	Yang et al. 2012.
Flame/Fire Flame Retardancy	Incorporate nano clay, metal oxide nanopowder and minerals with body physical water.	Shields, household goods, furnitures	Atay, & Çelik, 2010
Mechanical Toughness	Incorporate nanofillers like CNT into resin to increase energy dissipation on failure through deformation.	Membrane structures, damage tolerant structures	Timurkutluk et al. 2012
Modulus	Incorporate high modulus nanoparticles like continuous CNT yarns/sheets as reinforcement or grow reinforcements between plies to increase out of plane modulus.	Precision stable structures	Griebel, & Hamaekers. 2004
Strength	Incorporate high strength nanoparticles such as functionalized carbon nanotubes into the resin.	Propulsion tanks, fittings	Morais, 2006

The conductivity depends critically on the volume content (X) of the filler. For very low filler fractions, the mean distance between conducting particles is large and the conductance is limited by the polymer matrix. Figure.1.1). When a sufficient amount of filler is loaded, the filler particles get closer and form linkages, which result in an initial conducting path through the whole material. The corresponding filler content is called the percolation threshold (X_{th}) as represented in Figure 2.15.

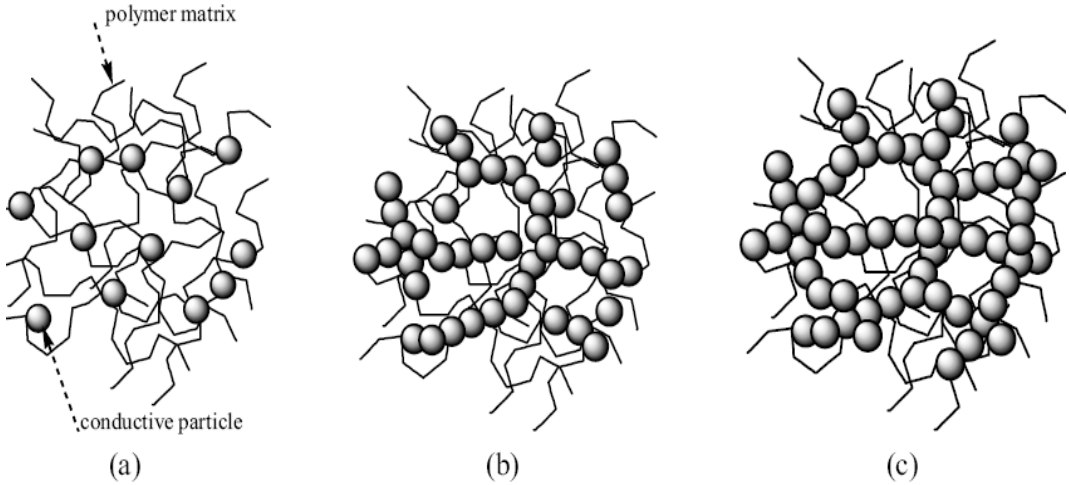

Figure 2.15 Schematic representation of conductive particles dispersed in a polymer matrix at different particle volume fractions: (a) X<Xth, (b) X=Xth, (c) X>Xth (Dai, 2004).

Percolation is a random probabilistic process which exhibits a phase transition. Different percolation systems may contain clusters of different sizes and shapes. Studying the statistics of the clusters helps to identify the critical value of density when formation of infinite or long-range connectivity in random systems first occurs. This is called the percolation threshold. Percolation is a very general phenomenon applicable in almost every area of science as the simplest model for spatial disorder. It has been shown that percolation has application to a broad range of topics including but not limited to mathematics, physics, biology, geography, hydrology, petroleum, ecology, chemistry, and materials science (Belashi, 2011).

The electrical resistance in a composite system comprising a network of conducting and insulating phases is the result of a large number of resistors combined in series and parallel. There are different contributions to the resistance or

conductance, with hopping and tunneling effect on conductance generally dominating the magnitude of the overall conductance (Belashi, 2011).

When an electric field is applied to two media in contact with each other, charge polarization occurs at the interface due to the differences between the ratios of the electrical properties such as resistivity. It has been shown that, at a specific low temperature, electrons are able to transfer between localized states through hopping conduction and electron tunneling. Hopping refers to the process in which a charge carrier is suddenly displaced from one occupied state to another equivalent empty donor state of higher energy.. Hopping conduction takes place via defects or impurities which form potential wells (traps or localized states) that are favorable for charge carriers (electrons and ions) to hop. The degree of hopping conductivity is dependent on donor and acceptor atom concentrations in the material. If the applied voltage is assumed to be alternating, the frequency of the field affects the hopping rate as well (Belashi, 2011).

The conductivity models described above are based on more or less idealized and simplified materials. In practice, the materials, which are available and used for conducting composites, exhibit special properties or morphologies. Beside critical concentration, filler particle size, shape, distribution, temperature, pressure and matrix polymer properties have important roles in conductivity of the composite structure.

As reported in literature; interparticle distance is shorter than the gap width that quantum tunneling effect permits, percolation takes place. Because interparticle distance decreases proportionally with decreasing particle diameter, the percolation threshold declines with decreasing particle diameters (Figure 2.16). Particle size is small enough, the percolation threshold will be extremely low (Jing et al. 2000).

Electrical tunneling effect is occurred at the interconnecting conductive particle surfaces. As known different shape of materials with same volume or mass has

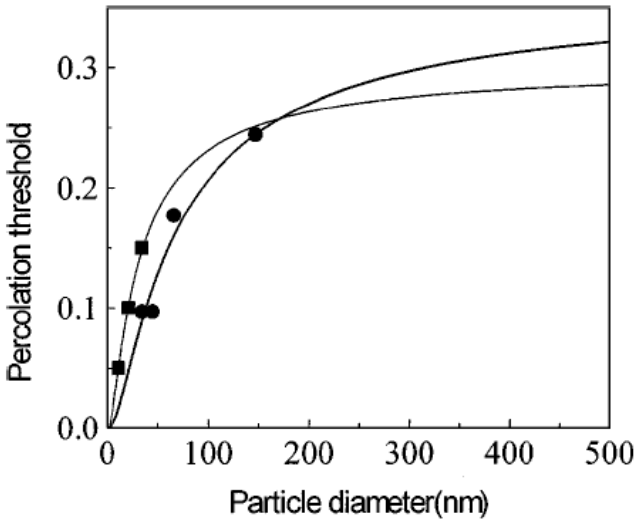

Figure 2.16 Plots of percolation threshold against particle diameter. Solid squares and solid circles are data taken from different studies respectively (Jing et al. 2000).

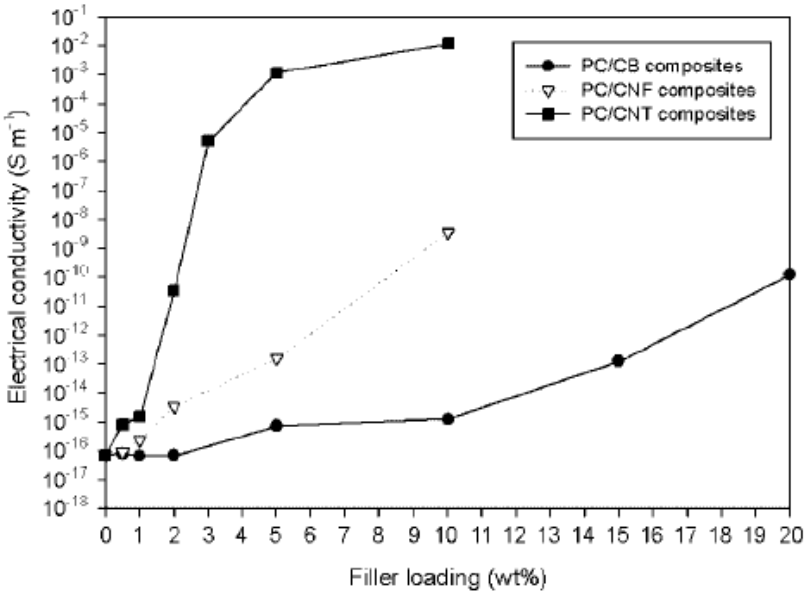

Figure 2.17 Electrical conductivity of the three types of PC composites with various carbon filler loadings (Lee et al. 2008).

different surface areas and aspect ratios. The aspect ratio of a filler particle is the ratio between the particle's largest dimension and its smallest. Thus surface area changes will change conductivity of the composite (Hao et al. 2008). A research study was handled by Lee et al. to verify this theory with an experimental proof (Figure 2.17). It is well known that the aspect ratio of CNTs is typically a hundred

times greater than that of conventional carbon fillers used to increase the electrical conductivity of polymer materials. Inasmuch as CNTs have higher aspect ratio and electrical conductivity than spherical CBs or CNFs of submicrometre size, a continuous conductive network structure is formed efficiently in PC-blend- CNT nanocomposites at very low loadings. The relatively low electrical percolation threshold is attributed to the geometrical characteristics such as high aspect ratio and surface area as well as the uniform dispersion of CNT particles in the polymer matrix (Lee et al. 2008).

Beside internal factors effecting the conductivity of CPCs, there are environmental factors such as temperature and pressure. The effect of temperature and pressure, on the electrical properties of CPCs has been reported in the literature (Mohanraj et al. 2007). The dependence of electrical resistivity on temperature for conductive polymer composites is quite a complex phenomenon. The temperature coefficient of resistance may be positive (PCT), negative (NCT), or zero, depending upon the concentration of filler and the nature of the polymers and the filler. The variation of volume resistivity with temperature for the system styrene–butadiene rubber (SBR) nanocomposites produced by Mohanraj et al. is shown in Figure 2.18. It is found that the DC resistivity of the nanocomposites increases with the increase in temperature (i.e. PCT effect). This behavior is similar to that of carbon black-filled polymer matrix composites and can be explained in a similar fashion. The resistivity of carbon black-filled composites progressively increases with the increase in temperature, i.e., PCT effect has been noticed. This behavior is explained based on three main theories of conduction, namely (1) conductive network rearrangement, (2) electron hopping/tunneling effect, and (3) electric field radiation. In fact, the actual conduction seems to be the net result due to the combined effect of different mechanisms described in these theories. The appreciable PCT effect is explained by the predominant breakdown of the conducting network structure due to higher thermal expansion of rubber matrix compared to the filler. Similarly, the increase in resistivity of SBR nanocomposites with the increase in temperature is mainly due to the increased gap between conducting elements with the increase in temperature, and this is because of the higher differential thermal expansion of the SBR matrix

compared to that of the Cu–Ni alloy nanofiller. The probability of electron tunneling and electric field radiation may also be reduced in this condition (Mohanraj et al., 2007).

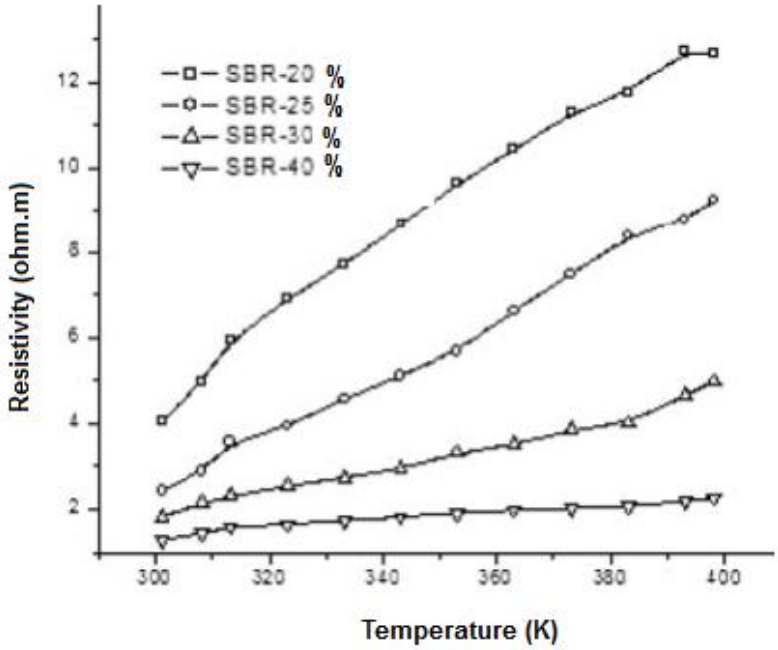

Figure 2.18 Effect of temperature on DC resistivity of SBR-nano composites (Mohanraj et al., 2007).

Similar manner for the thermal expansion of CPCs can be employed for the pressure changes. The application of compressive stress causes movement of the polymer chains, which in turn affects the movement of network structure of the conductive filler as depicted in Figure 2.19. The change in resistivity with applied pressure can be explained by considering two phenomena that simultaneously occur in the system: the breakdown of existing conductive networks and the formation of additional conductive networks. The formation of this continuous conducting path occurs not only by the direct contact between electrically conductive particles dispersed in the rubber matrix, but also when the interparticle distance is only a few nanometers and the electrons can easily jump across the gap. Thus, there exists a threshold value for the interparticle gap, which is electrically equivalent to the occurrence of interparticle contact. The formation of a continuous conducting network at high applied pressure is facilitated by a decrease in interparticle gap in the discontinuous region. This also enhances the significant contribution of electron

tunneling effect, thereby leading the composites to exhibit high conductivity at high applied pressures (Mohanraj et al., 2007).

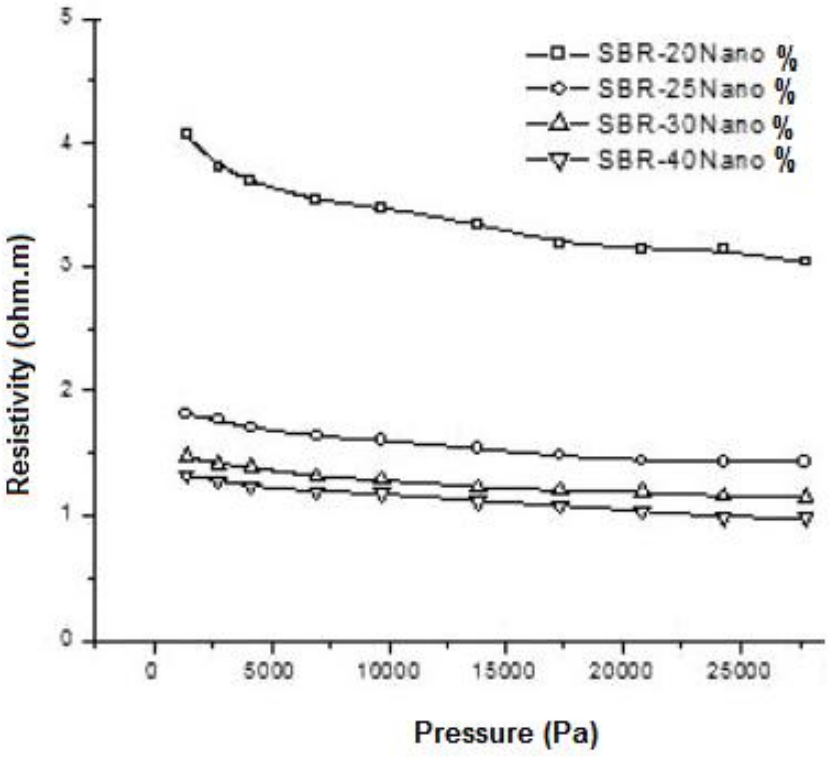

Figure 2.19 Effect of pressure on DC resistivity of SBR-nano composites (Mohanraj et al., 2007).

The variation of DC resistivity against time for all the composites under a constant compressive stress is shown in Figure 2.20. Once the samples are held under constant compression under fixed load, the resistivity of all the composites is found to decrease with time. Nevertheless, the rate of decrease slows down with time and becomes almost marginal, and attains a constant value after some time. It is found that this phenomenon is strongly observed in composites having lower loading of filler than in higher filler loading. This is because the systems having lower filler concentration contain only a fewer conductive networks and their destruction affects more significantly the change in magnitude of resistivity and in the case of high filler loading having large number of networks and average distance between filler aggregates is also small and so the effect of compression is marginal as the destruction and formation process has marginal effect. The polymer chain mobility in low filler loading is expected to be more than that in higher one. Also, the increase in

conductivity with time for compressed samples under constant strain shows that there is also a formation of a few new conductive networks in the system and this may be attributed to the slow chain mobility of polymer chains under compression (Mohanraj et al., 2007).

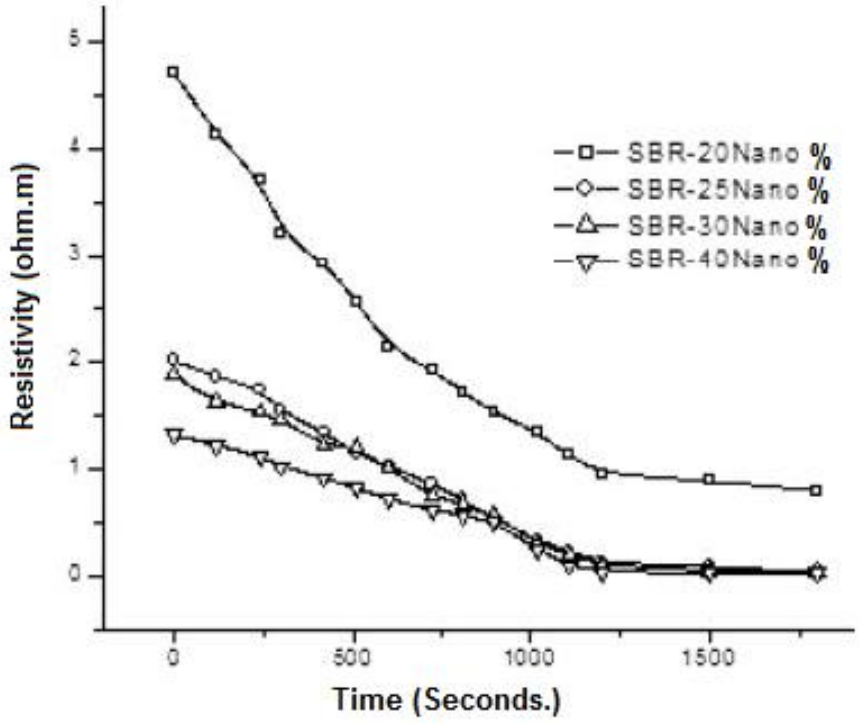

Figure 2.20 Effect of constant compressive stress on DC resistivity of SBR-nano composites (Mohanraj et al 2007).

2.3 Electrical Heating (Joule Heating)

Electrical heating is a process in which electrical energy is converted to heat. Common applications include space heating, cooking, water heating and industrial processes. An electric heater is an electrical appliance that converts electrical energy into heat. The heating element inside every electric heater is simply an electrical resistor, and works on the principle of Joule heating: an electric current through a resistor converts electrical energy into heat energy.

2.3.1 Ohm's Law and Joule's Law

When Georg S. Ohm (1787-1854) published "*Die galvanische Kette mathematisch bearbeitet"* in 1827, he described the theory and applications of electric current. For his achievements, the German scientist's name has been forever attributed to electrical science terminology: Ohm's Law (2.1) states the proportionality of current and voltage in a resistor and the SI unit of resistance is the Ohm (Ω).

$$V = IR \tag{2.1}$$

Ohm's work provides a direct correlation between the potential voltage drop, V, across a resistive (or Ohmic) material, R, and the electric current, I, flowing through the medium. In doing so, Ohm's Law is a fundamental concept that helped establish the basis of modern electrical theory. James Joule (1818-1889) coupled Ohm's Law with his own endeavors in relating heat to mechanical work. Joule worked with Lord Kelvin in developing the absolute temperature scale (Kelvin, K) and was also acknowledged for his contributions that eventually led to the First Law of Thermodynamics. His experiments initiated the concept of the mechanical equivalence of heat, which relates the energy required to raise the temperature of water by 1°F. Accordingly, the SI unit of work was named the Joule (J). However, Joule might be best remembered for his discovery of the relationship, appropriately named Joule's Law, between current flow and heat dissipation in a resistive element (2.2). Specifically, Joule found that the rate of thermal energy generated, ˙E, within a resistive material,

$$E = I^2R \tag{2.2}$$

is proportional to the square of the current, I, and directly proportional to the resistance, R. Together, Georg Ohm's and James Joule's accomplishments close the gap between electrical energy input (either as a voltage potential or an electric current) and thermal energy output.

When an electric field is applied to a material, the motion of electric charges within the material generates current flow. However, all materials exhibit some resistance, R, to this charge motion. Resistance, then, depends on both the resistive nature of a given material, called electrical resistivity, and the geometry of the material.

$$R = \rho \frac{L}{A} \tag{2.3}$$

Equation 2.3 explains that the resistance of a heating element is proportional to its length, L, and inversely proportional to its cross-sectional area, A. Furthermore, the the electrical resistivity, ρ, for a given material is a function of temperature.

The electrical conductivity, σ_e, is a measure of the material's ability to allow electrical current to flow and is defined as the reciprocal of resistivity.

$$\sigma_e = \frac{1}{\rho} \tag{2.4}$$

Table 2.2 Electrical Conductivities of Some Engineering Materials (Deshmukh, 2005)

Metals and Alloys	***Conductivity σ_e $(\Omega.m)^{-1}$**	**Non Metals**	***Conductivity σ_e $(\Omega.m)^{-1}$**
Silver	$6.3x10^7$	**Graphite**	10^5
Copper (cp)	$5.8x10^7$	**Germanium**	2.2
		Silicon	0.43
Gold	$4.2x10^7$	**Polyethylene (PE)**	10^{-14}
		Polystyrene (PS)	10^{-11}
Aluminum (cp)	$3.4x10^7$	**Diamond**	10^{-11}

* All conductivity datum listed in the table are measured at room temperature.

Quantified as $\Omega\ m^{-1}$, electrical conductivity (and thus resistivity) is an inherent material property that does not depend on geometry. Both conductivity and resistivity are functions of temperature. However, the difference in conductivity varies greatly between materials and helps categorize materials as conductors,

insulators, and semiconductors. Table 2.2 illustrates that pure metals have the highest conductivities, which explains their use as electrical heating materials. On the opposite end of the spectrum, the electrical insulators such as polyethylene (PE), polystyrene (PS), and diamond have very small conductivity values. Between these extremes, semiconductors such as graphite, germanium, and silicon have conductivities less than metals but much greater than insulators (Deshmukh, 2005).

2.3.2 Heating Elements

Heating elements are specially developed materials usually available in wire or strip form and can be given the desired shape by bending. Most utilized ones are in metallic form. Other types of heaters are made from nonmetallic materials such as silicide or carbide in ready-made forms such as rods or hairpins. Following are some of the desired properties of the materials to be used as heaters:

- High melting temperature
- Stability in the atmosphere
- Constant temperature coefficient (α) of resistivity
- Forming possibility or ready-made forms available
- Resistance to thermal and mechanical shocks

Resistance materials are available up to a maximum useful temperature of 2000°C. However, there is no one material for the whole range and all types of atmospheres. ach material has its own maximum useful temperature in a given atmosphere. For instance, a metal which can be used up to 1500°C in air (oxidizing) can be used only up to 1150°C maximum in a reducing atmosphere. (Deshmukh, 2005).

As summarized in Joule heating theory, flowing current generates heat, while heating environment heating element itself is also heated. Heating a heating element will change its resistance in terms of the changing temperature. Thermistors are temperature sensitive resistors that have a greater change than normal change in

resistance value when the temperature changes. The change in resistance is predictable with changes in temperature. The extreme sensitivity to temperature change enables a thermistor to perform many functions and is utilized in an increasing variety of thermal sensing, control and regulating applications.

The two basic types of thermistors generally available today are the NTC and the PTC types. The NTC thermistors are ceramic semiconductors that have a high negative temperature coefficient of resistance. NTC thermistors decrease in resistance as the temperature increases. PTC thermistors are positive temperature coefficient resistors generally made of polycrystalline ceramic materials that have a high positive temperature coefficient, which increases in resistance as the temperature increases. Similar behavior employed for ceramic material can be used for all types of heating elements.

2.3.2.1 Metallic Elements

Traditionally, metallic elements take the form of wire, strip or tape. This calls for reasonable ductility in the manufacturing process. For a given operating temperature, the element life tends to decrease with decreasing the cross-section of the element caused by progressive oxidation of the surface or reduction in mechanical strength and so, in practice, an optimum element thickness for economic life exists for each application. The choice of metal composition will depend on the operating temperature required, the material resistivity, the temperature coefficient of resistance, high temperature corrosion resistance, mechanical strength, formability, and cost. Metallic elements can be manufactured to close tolerances and, provided the material is in the fully annealed, slowly cooled condition, will have nominal resistivities within 5%.Whilst many metals and alloys are used as element materials, the most common for industrial applications are alloys based on nickel-chromium, iron-nickel-chromium alloys, or iron-chromium-aluminum alloys. All depend on an adherent non-spalling, self-sealing oxide layer forming on the surface of the alloy. Further oxidation is limited by diffusion of reacting species through this oxide layer.

The iron-chromium-aluminum alloys rely on an alumina film developing on the surface, whereas the nickel-iron-chromium alloys depend on chromium oxide.

Generally, the iron-chromium-aluminum alloys can operate at higher temperatures than the nickel-chromium based alloys, but are not as readily fabricated. The most exotic metals (platinum, tantalum, molybdenum, etc.) are used for special laboratory or high temperature vacuum work. Table 2.3 summarizes some of the characteristics of these materials. When used in a freely radiating state, the elements need to be supported on ceramic tubes, pins or correctly insulated metallic pins. If ceramic supports are chosen, it is important that they have sufficient mechanical strength to prevent sagging and have a sufficiently high electrical resistance at the working temperature to prevent excessive leakage current. Elements can also be supported in grooves in bricks, partially or fully embedded in ceramic fiber vacuum formed blocks or cast refractory blocks.

2.3.2.2 Sheated Elements

The elements may be protected from the working environment by the use of a suitable insulation layer separating the element from an outer sheath. In many domestic appliances, for example cooker rings, immersion heaters and kettle elements, a purified magnesium oxide powder separates the helical element coils from copper, stainless steel or nickel based alloy sheath material. In these cases the element is often rated in terms of watts per square centimeter of sheath.

Such mineral insulated elements are also used in industrial applications as cartridge heaters, radiant panels and immersion heaters. Thin strip or band heaters are available which use a mica insulation between the element and the sheath. Higher rated industrial units employ a protective metallic or thermally conducting ceramic sheath insulated from the elements by an air gap created by suitable ceramic supports and spacers. As before, careful consideration should be given to selection of materials for use in each application regarding the heat transfer, electrical and mechanical properties and corrosion characteristics.

2.3.2.3 Ceramic Elements

Silicon carbide, molybdenum disilicide, lanthanum chromite and hot zirconia are examples of ceramic materials which have sufficient electrical conductivity to act as element materials. The silicon carbide and molybdenum disilicide elements depend on a protective, self-sealing silica layer on the surface. These materials tend to be brittle and have to be handled with care, but they can achieve much higher temperatures and surface loadings in air than can conventional metal elements. They can also have unusual temperature coefficients of resistance as. The actual resistivity will depend on purity, grain size and method of manufacture. Careful selection of element size, shape and working resistance is required in practice, and advice regarding the choice of element, support, insulation and electrical supply characteristics should be sought.

Graphite is another recognized non-metallic element material which, of course, should be operated in the absence of oxygen or gaseous oxygen compounds such as steam and carbon dioxide. Ceramic elements generally consist of a hot zone either created by a thin section or a spiral cut supported by two or more cold ends which are either thicker in cross-section or which have been impregnated with a metallic phase to lower the resistance locally.

Table 2.3 Materials for resistance-heating elements (Jones, 2003)

Material	Θ(°C)	$\rho(10^{-8}/m)$	$\alpha(10^{-3}/K)$	Principal application
Nickel based alloys[1] 80 Ni/20 Cr	1200	108	+14	Furnaces, resistance heaters, mineral insulated elements for domestic and industrial use
60 Ni/15 Cr/bal Fe	1150	111	+18	Firebar and convector heaters. Domestic and furnace application up to 1100°C
35 Ni/20 Cr/bal Fe	1100	104	+29	Some domestic appliances and general heating equipment at moderate temperature.
20 Ni/25 Cr/bal Fe	1050	95	–	Terminal blocks
Iron based alloys[1] 22 Cr/5.8 Al/bal Fe	1400	145	+3.2	Furnaces for heating glass, ceramics, steel, electronics; crucible furnaces for melting/holding aluminum and zinc
22 Cr/5.3 Al/bal Fe	1375	139	–	Industrial furnaces
22 Cr/4.8 Al/bal Fe	1300	135	4.7	Furnaces for moderate temperatures, appliances
Exotic metals Platinum	1300	10.58	3.92	Laboratory furnaces, small muffle furnaces
90 Pt/10 Rh	1550	18.7	–	
60 Pt/40 Rh	1800	17.4	–	
Molybdenum[2]	1750	5.7	4.35	Vacuum furnaces, inert atmosphere furnaces
Tantalum[2]	2500	13.5	3.5	Vacuum furnaces
Tungsten[2]	1800	5.4	4.8	Incandescent lamps, vacuum and inert atmosphere furnaces
Nonmetallic materials Graphite[2]	3000	1000	-26.6	Vacuum, inert gas, reducing-atmosphere furnaces
Molybdenum disilicide	1900	40	1200	Glass industry, ceramic kilns, metal heat treatment, plus laboratory furnaces
Silicon carbide	1650	1.1×10^5	–	Furnaces for heat treatment of meals, ceramic kilns, conveyer furnaces
Lanthanum chromite	1800	2100	–	Laboratory furnaces and special ceramic kilns
Zirconia[3]	2200	–	–	Laboratory furnaces and special ceramic kilns

Θ, Maximum element operating temperature; ρ, electrical resistivity at 20°C; α, mean temperature coefficient of resistance at 20°C

1: Approximate compositions.

2: Not be used in atmosphere containing oxygen, oxides of carbon, water vapor, etc.

3: Becomes sufficiently conducting at temperatures in excess of 1000°C.

2.3.2.4 PMC Elements

Heating elements are widespread products in many applications for private and industrial use. As mentioned above CPCs are artificial conductive materials which are employed for many applications.

Theory based on joule heating can easily be integrated for CPCs similar to metallic elements. While designing a heating element with desired properties such as; high melting and working temperature, stability in the atmosphere, constant temperature coefficient (α) of resistivity, forming possibility or ready-made forms available, resistance to thermal and mechanical shocks must be taken in to account. As known melting or glass transition temperatures of polymer are lower than the metals and ceramics. Except this property others and more properties can be easily served by polymeric material. Corrosive resistance, plastic properties, flexibility, low cost and easy production can be listed for polymeric materials. Hence low temperature heating elements based on CPCs can be used for many applications.

The increasing demand of personal comfort at home or for leisure for example creates also a demand of light-weight and flexible heating modules with possibilities to be integrated easily. Even for industrial applications, more flexible heating modules are of interest for material treatments or process controls. Therefore, several approaches are studied worldwide to substitute heavy and less flexible metal wires/fibers by easily applicable CPCs. Furthermore, such printing or coatings technologies cover the whole surface, which are able to dissipate the generated temperature more evenly and avoid “hot wires”, with high temperature gradients. Therefore, the coated heating modules are more appropriate for applications near the skin thanks to thermal safety, which is useful especially in heating clothes (outdoor activities, snow sports, protective clothing for professionals, e.g. working in cold environments like cold stores or working in maintenance activities by all weather conditions, medical applications).

Although mentioned technology is researched for decades by many researchers, industrial or trade mark affords are deficient. A typical example of researches was reported by Opwis et al and depicted in Figure 2.21, applying a standard voltage of 24 V temperatures up to 170°C are practicable using poly(3,4-ethylene dioxythiophene) *p*-toluenesulfonic acid (PEDOT:PTSA) film on textile surfaces. Moreover, the desired temperature is easily adjustable by the absolute load and the applied voltage. These conductive textiles can be used, e.g., in carpets, electric blankets or automotive seat heaters (Opwis et al., 2012).

.

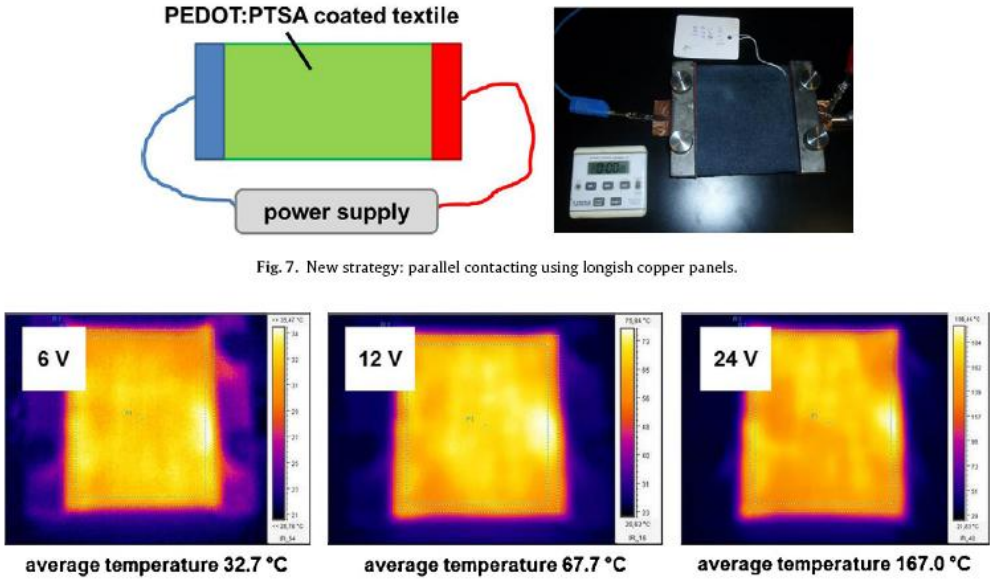

Figure 2.21 An example study for PMC heating elements (Opwis et al 2012).

Another example of PMC elements was studied by Isaji et al, by producing the composite films of ultra-high molecular weight polyethylene (UHMWPE) and branched low molecular weight polyethylene (LMWPE) used as matrix, and multi-walled carbon nanotubes (MWNTs) used as fillers. Results obtained by them are demonstrated in Figure 2.22 where the maximum surface temperature was reported up to 170°C using different fractions of polymer matrixes (Isaji et al., 2009).

In a published article related to PMC elements, we have concerned mainly with the production, characterization and industrial application of graphite-flake carbon black-reinforced polystyrene-matrix composite films deposited on glass-fiber woven fabrics as plane heaters. According to our results Planar heating of up to 60 °C was

observed with a 24-V DC power supply as showed in Figure 2.23 (Erol, & Celik, 2013).

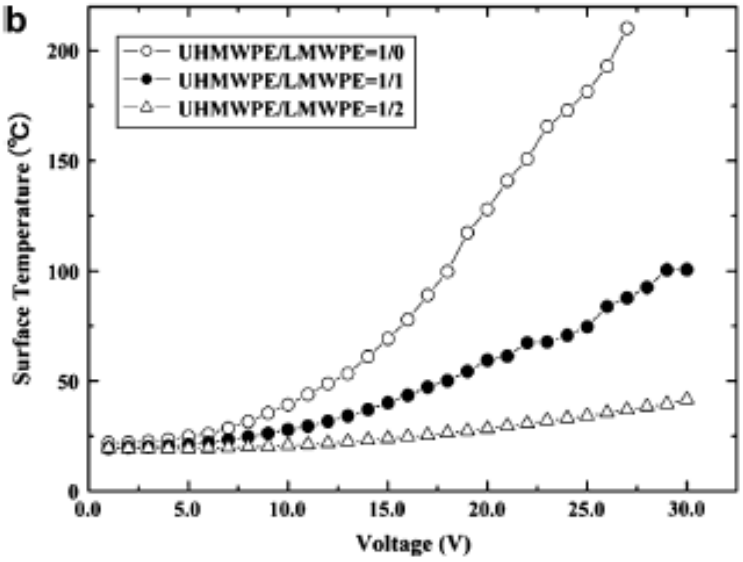

Figure 2.22 An example study for PMC heating elements (Isaji et al 2009).

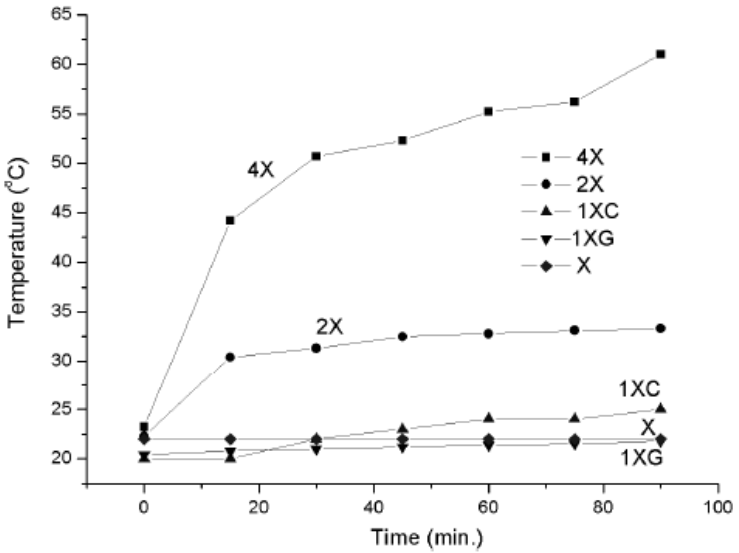

Figure 2.23 An example study for PMC heating elements (Erol, & Celik, 2013).

Finally it can be inferred that studies based on the PMC elements are limited and have a high potential for research and application. Also in comparison to metallic and ceramic types, ease in the design of composite structure, its flexibility in

forming, homogenous heat releasing, low cost and low weight can be listed as their advantages.

CHAPTER THREE
EXPERIMENTAL PROCEDURE

3.1 Purpose

The main purpose of this thesis can be summarized as; the production, characterization and application of nano scale carbon black and/or graphite reinforced styrene acrylic copolymer matrix nanocomposites. As mentioned in the previous chapters, addition of the conducting filler increases the conductivity of the composite materials. In addition also a flowing current through a conducting material releases heat energy which can be employed as space heating elements or devices. Based on the percolation phenomena effect of filler content or type on the structural, morphological, physical, and electrical and heat releasing properties will be investigated.

Co-percolation which can be defined as the optimum conductive content of both carbon black and graphite powders dispersed in the composite structure will be determined after the characterization processes. Co-percolation study is considered to assist the obtaining optimum electrical behaviors and reasonable mechanical properties, with decreased filler content and low cost. Finally the obtained optimum quality nanocomposite films with the mentioned considerations above can be used as low temperature heating elements or devices. By this way the films will be tested for different heating applications such as; floor heating pads (heat releasing carpets), saunas, boiler heaters, and etc.

3.2 Materials

In this study three main and two secondary materials were used to produce target nanocomposite film structure. Main components can be listed as matrix material and reinforcements. Secondary materials in other saying the substrates are polyester film and soda lime glass. The matrix material styrene acrylic copolymer emulsion (SACE) was purchased commercially from Ata Chemistry Inc. İzmir Turkey which is a milky water-polymer emulsion. SACE is generally used as binder for outdoor

paintings, concretes; fabric dyes since it has good resistance to water based corrosion and aggressive weather conditions. It has a pH value between 7 and 9 which can be electrochemically defined as basic. Also its viscosity value (Brookfield RVT 6/20 Viscosity) is found to be between 5000-10000 cps at 25ºC. Chemical structure of the copolymer in the emulsion is illustrated in Figure 3.1

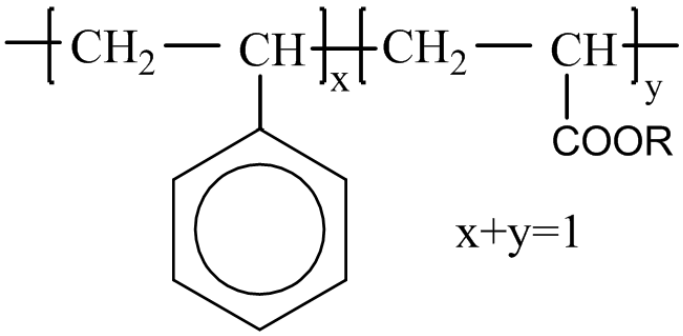

Figure 3.1 Chemical structure of styrene-acrylic copolymer.

Carbon black used in this research is purchased from Tupras Inc Kocaeli Turkey with initial particle size of 3-40 μm. Generally, carbon black (C) is produced by burning oil and natural gas. It has been used as a pigment and as reinforcing filler in rubber. Besides functioning in rubber, carbon black is also used as a UV stabilizer, antistatic and electromagnetic shielding agent, colorant, thermal antioxidant and conductive filler in plastics (Köysüren, 2008). Schematic structure of the carbon black is shown in Figure 3.2.

Graphite (G) powder, the other conducting agent in the structure with high purity >99,9 % and initial particle size of 3 - 38 μm was purchased from Selen Chemistry, Istanbul, Turkey. As well known, graphite is one of three natural forms of carbon (the other two are diamond and coal). It is found naturally in metamorphic rocks in the form of lump, crystalline flake, and amorphous. The majority of natural graphite is produced as flake graphite which can be further processed into powder graphite. Graphite has a layered, planar structure. In each layer, the carbon atoms are arranged in a honeycomb lattice with separation of 0.142 nm, and the distance between planes is 0.335 nm. Schematic structure illustration is shown in Figure 3.3.

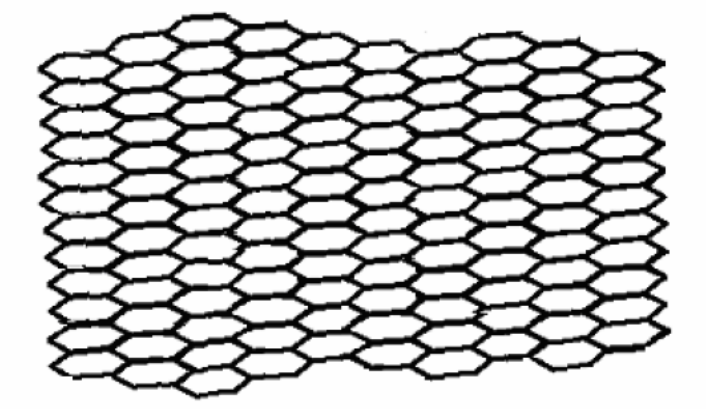

Figure 3.2 Schematic crystalline structure of carbon black (Köysüren, 2008).

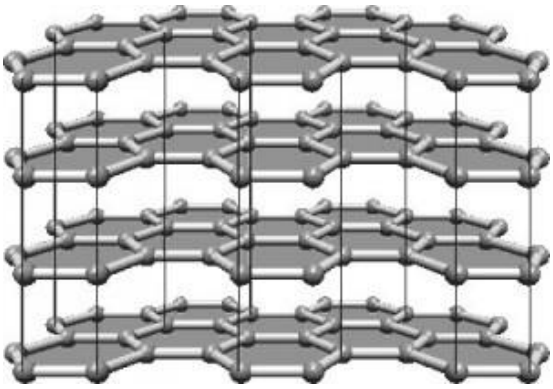

Figure 3.3 Schematic crystalline structure of graphite (Nano Enhanced Wholesale Technologies, 2013).

The powders were milled using a self-designed and produced industrial scale screw mill based on the Archimedes screw depicted in Figure 3.4 with variable sized ZrO_2 balls between 0.7 to 5 millimeters for different cycles hours to decrease the particle size. Basic elements of the mill can be listed as; engine that gives the rotational movement, a screw shaft which moves the milled powders and ZrO_2 balls from charge cone to collecting bucket and the stainless steel pipe covering the system. System works in a cycling manner, where a cycle can be defined as time through the charge cone and collecting bucket. Milling charge volumes were set as 1:1:1 for water: powder: air in agreement with general milling strategies. Milling process in this study was carried out up to the time when intended particle size of the C and G powders are obtained.

Subsequent to milling processes; obtained water-powder mixtures were filtered and dried to remove ZrO_2 balls and water, respectively. After that different specimen groups were defined including different amounts of milled powders (C and/or G) and matrix material (SACE). Homogenously stirred mixtures were spray deposited on mentioned substrates polyester film and soda lime glass with a air compressor driven deposition system.

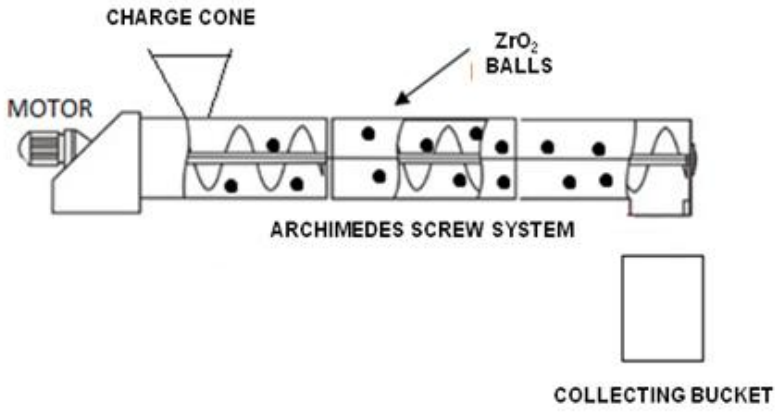

Figure 3.4 Screw mill based on Archimedes Screw Theory.

Polyester (PET) films have several wide range usage in industry as; flexible packaging and food contact applications, covering over paper, insulating material, electronic and acoustic applications etc. In this study, PET substrates with a thickness 50 μm (see Figure 3.5a) were chosen to satisfy the need of electrical insulation, flexibility and thermal stability (melting point ~270 ^{o}C).

Soda-lime glass, also called soda-lime-silica glass, is the most prevalent type of glass, used for windowpanes, and glass containers (bottles and jars) for beverages, food, and some commodity items. Soda-lime glass (Figure 3.5b) is relatively inexpensive, chemically stable, reasonably hard, and extremely workable, because it is capable of being re-softened and re-melted numerous times, and is ideal for recycling. Beside the general properties above soda lime glass substrates with dimension 20x20x4 mm^3 were chosen as substrates because of their rigidity, electrical insulation and low cost.

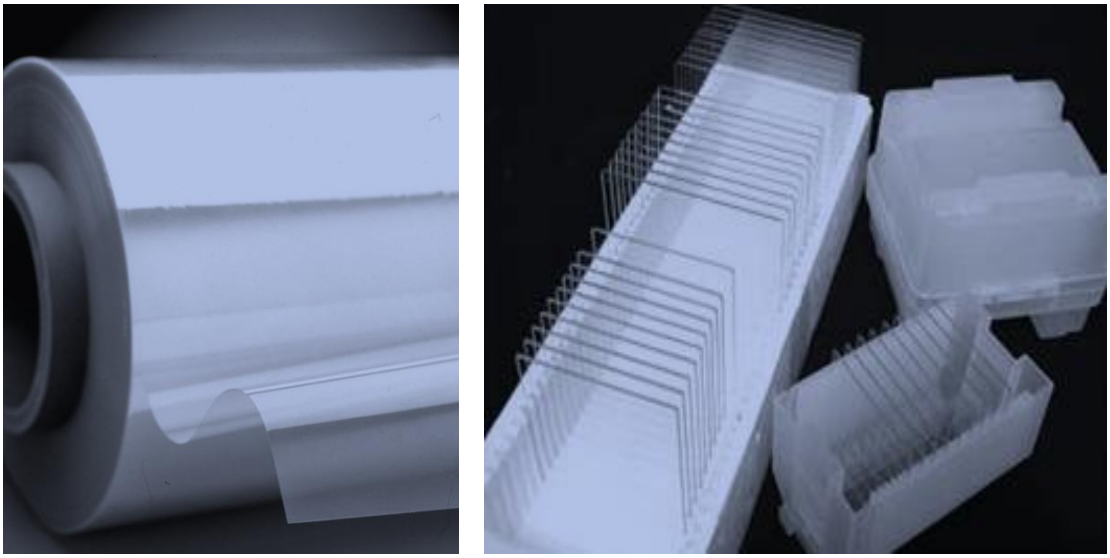

(a) (b)

Figure 3.5 Substrates such as (a) PET and (b) soda lime glass used in the experiments.

3.3 Production of Composite Coatings/Paints

In order to obtain the heat releasing conductive polymer composite (CPC) films, three classes of sample group were determined including milled G and/or C powders with SACE matrix material. Details and the ratios of the materials are listed in Table 3.1.

In addition, the samples listed in the Table 3.1 are the major ones which will be used for further structural, morphological, thermal and mechanical characterizations. However there are minor samples as with graphite ratios 1, 2, 3, 4, 10, 16, 17, 18, 19, 25 and 30 % wt. and with carbon black ratios 1, 2, 3, 4, 10, 16, 17, 18, 19, 25 and 30 % wt. produced to determine percolation threshold accurately. According to Table 3.1, main group of material classes are as graphite, carbon black and carbon-graphite based. In order to produce each sample, 500 milliliters of SACE matrix material was drop wise added in to a beaker. Afterwards the conductive fillers were added according to the ratios in Table 3.1 for every sample respectively. The mixture was stirred for 1 hour at room temperature in air to obtain homogenous composite structure using a mechanical stirrer as depicted in Figure 3.6.

Table 3.1 Definition and annotation about the samples

Material Class	Component (wt %)	Sample Code
Graphite Based Materials	0	G0
	10	G10
	20	G20
Carbon Black Based	0	C0
Materials	10	C10
	20	C20
Graphite-Carbon Black	5-1	G5-C1
Based Materials	5-3	G5-C3
	5-5	G5-C5
	10-1	G10-C1
	10-3	G10-C3
	10-5	G10-C5
	10-7	G10-C7

Homogenous mixtures of the samples were fed into the chamber of the air compression driven spray gun. Both soda lime glass and polyester substrates were cut in to the mentioned dimensions. Deposition process was performed in a fume hood at room temperature. Finally, gel films were dried at 80 C for 1 hour to obtain desired adhesion by using hot plate. All the summarized processes are schematically shown in Figure 3.7.

Figure 3.6 Mechanical stirrer

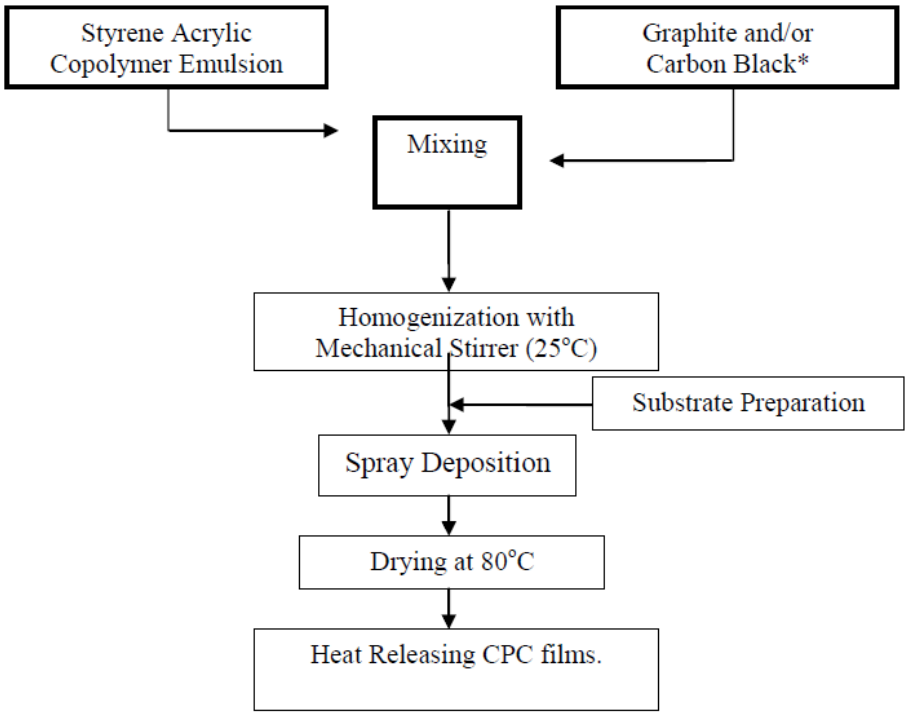

Figure 3.7 Flow chart for the production of heat releasing CPC films.

3.4 Characterization of Filler and Composite Films

3.4.1 Particle Size Distribution (PSD)

Theory based on the effect of particle size on the properties of the composite structure was discussed in previous chapters. In order to determine final hydrodynamic size of C and/or G powders a dynamic light scattering (DLS) technique based device Malvern Zeta Sizer Nano ZS90 (EMUM, DEU) was employed.

Small particles in suspension undergo random thermal motion known as Brownian motion. This random motion is modeled by the Stokes-Einstein equation. Equation 3.1 is given in the form most often used for particle size analysis.

$$D_h = \frac{k_B T}{3\pi\eta D_t} \tag{3.1}$$

The Stokes-Einstein relation (Equation 3.1) connects diffusion coefficient measured by dynamic light scattering to particle size. According to Equation 3.1 D_h, D_t, k_B, T, and η are the hydrodynamic diameter, the translational diffusion coefficient, Boltzmann's constant, thermodynamic temperature and dynamic viscosity, respectively.

The calculations are handled by instrument software. Nevertheless, the equation does serve as are important reminder about a few points. First sample temperature is important, as it appears directly in the equation. Temperature is even more important due to the viscosity term since viscosity is a stiff function of temperature. Finally, and most importantly, it reminds the analyst that the particle size determined by dynamic light scattering is the hydrodynamic size. That is, the determined particle size is the size of a sphere that diffuses the way as your particle. Thus as a result it can be inferred that exact size of the particle is also smaller that of the hydrodynamic one.

3.4.2 X-Ray Diffractometer (XRD)

X-ray diffraction (XRD) is one of the primary techniques to analyze all kinds of materials such as powders and crystals. XRD can provide information about crystalline structure and structural phases. It is extensively used to investigate the structural properties of heat releasing CPC nanocomposite coatings on substrates. Produced coatings were analyzed by means of XRD with a grazing angle attachment and an incident angle of 1° (Rigaku, D/Max-2200/PC). X-Ray radiation of CuKα was set at 40 kV and 36 mA with a scanning speed of 4° 2θ/min, from 3° to 90°.

3.4.3 X-Ray Photoelectron Spectroscopy (XPS)

X-ray photoelectron spectroscopy (XPS) is a quantitative spectroscopic technique that measures the elemental composition, empirical formula, chemical state and electronic state of the elements that exist within a material. XPS spectra are obtained by irradiating a material with a beam of X-rays whilst simultaneously measuring the

kinetic energy and number of electrons that escape from the top 1 to 10 nm of the material being analyzed (Figure 3.8). XPS requires ultra-high vacuum (UHV) conditions. It can be also used to analyze the surface chemistry of a material in its "as received" state, or after some treatment, for instance: fracturing, cutting or scraping in air or UHV to expose the bulk chemistry, ion beam etching to clean off some of the surface contamination, exposure to heat to study the changes due to heating, exposure to reactive gases or solutions, exposure to ion beam implant, exposure to ultraviolet light.

XPS detects all elements with an atomic number (Z) of 3 (lithium) and above. It cannot detect hydrogen and helium, because the diameter of these orbitals is so small, reducing the catch probability to almost zero. It is routinely used to analyze all solid materials (Crist, 2011). In the present study, produced samples were analyzed in elemental manner using XPS (Thermo-Scientific, Al-K_{α}, in EMUM-DEU).

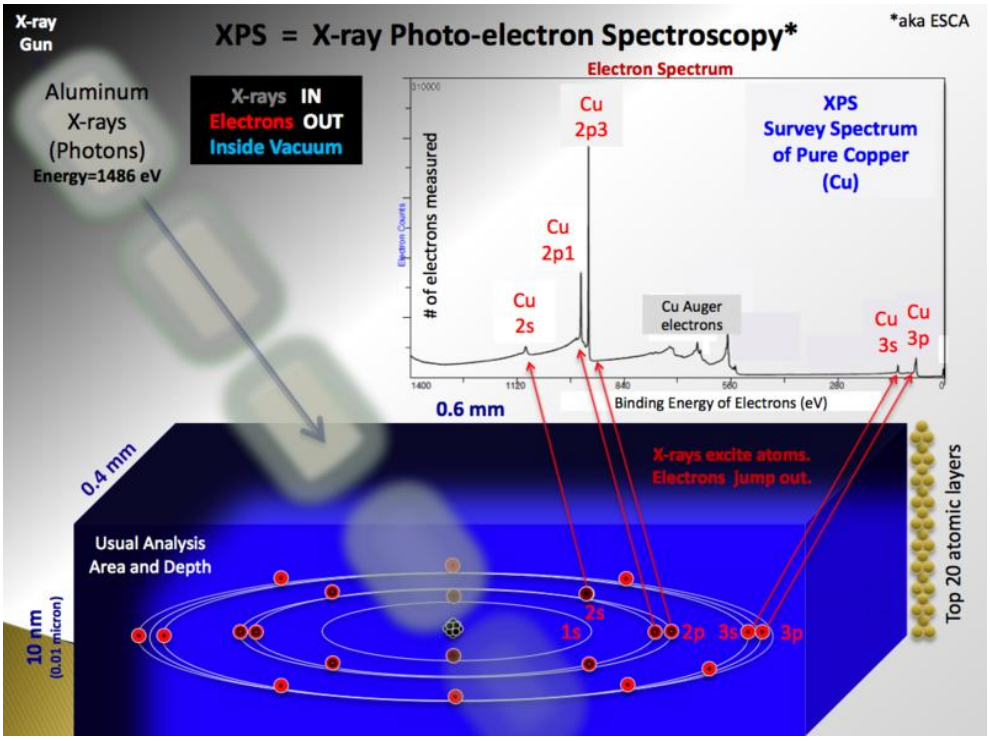

Figure 3.8 Rough schematic of XPS physics (Crist, 2011).

3.4.4 Fourier Transform Infrared Spectroscopy (FT-IR)

FT-IR is a powerful tool for identifying types of chemical bonds in a molecule by producing an infrared absorption spectrum that is like a molecular "fingerprint". Each different material is a unique combination of atoms, thus two different compounds never produce the exact same infrared spectrum. Therefore, infrared spectroscopy can result in qualitative analysis of every different kind of material. By interpreting the infrared absorption spectrum, the chemical bonds in a molecule can be determined. In principle, molecular bonds vibrate at various frequencies depending on the elements and the type of bonds. For any given bond, there are several specific frequencies at which it can vibrate. According to quantum mechanics, these frequencies correspond to the ground state (lowest frequency) and several excited states (higher frequencies). One way to cause the frequency of a molecular vibration to increase is to excite the bond by having it absorb light energy. For any given transition between two states the light energy (determined by the wavelength) must exactly equal the difference in the energy between the two states. The energy corresponding to these transitions between molecular vibration states is generally 1-10 kilocalories/mole which corresponds to the infrared portion of the electromagnetic spectrum. The results are generally plotted as a function transmittance or absorbance versus wavelength. The conversion between transmittance to absorbance data is: A= log (1/T) where A is absorbance and T is transmittance.

In addition to qualitative analysis, the size of the peaks in the spectrum is a direct indication of the amount of material present. With suitable software algorithms, infrared is also an excellent tool for quantitative analysis.

The technique of Attenuated Total Reflectance (ATR) has in recent years revolutionized solid and liquid sample analyses inasmuch as it combats the most challenging aspects of infrared analyses namely sample preparation and spectral reproducibility. An ATR accessory operates by measuring the changes that occur in a totally internally reflected infrared beam when the beam comes into contact with a sample as indicated in Figure 3.9.

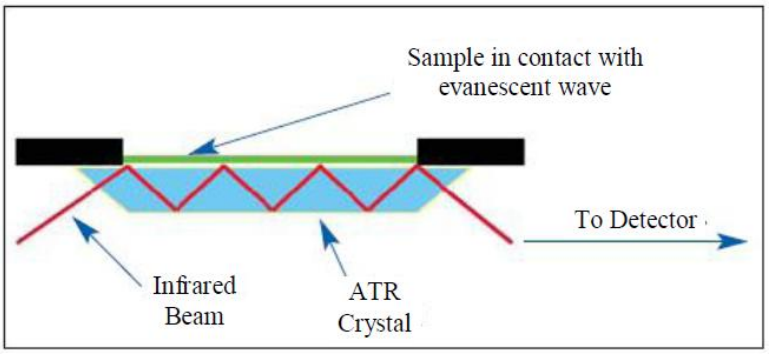

Figure 3.9 Schematic representation of an ATR system (Birlik, 2011)

The infrared spectra of the samples were recorded with a Perkin Elmer Spectrum BX instrument equipped with ATR apparatus in the spectra range between 4000 and 650 cm^{-1} with a resolution of 4 cm^{-1}. All of the samples were characterized by FT-IR by which % transmittance as a function of wavelength and % absorbance as a function of wave number curves can be obtained.

3.4.5 Scanning Electron Microscopy (SEM)

Scanning electron microscopy (SEM) is one of the most common analytical methods to examine surface morphology of the solid-state specimen. In SEM, a tiny high-energy electron beam is scanned across the sample surface. Series of radiations can be produced in terms of the interaction between the electron beam and the sample. Normally, two types of radiation are utilized for image formation: primary backscattered electrons and secondary electrons. Backscattered electrons reveal the compositional and topographical information of the specimen. The secondary electron images produce a depth of field which shows the surface topography. The signal modulation of the two types of radiation is viewed as images in the cathode ray tube (CRT) and provides the morphology, surface topology and composition of the specimen surface.

In this study, the surfaces of composites coatings/paints were examined by using JEOL JSM-6060 instrument operating at an accelerating voltage of 20 kV with several magnifications.

3.4.6 Differential Thermal Analysis-Thermal Gravimetric Analysis (DTA-TGA)

The thermal analysis of the polymeric mixture was studied under O_2 flowing by means of Shimadzu 60H Model Differential Thermal Analysis-Thermal Gravimetry (DTA-TG) in order to obtain information about the thermal behaviors of the CPC heat releasing films. Thermal data were analyzed using TA60 software program supplied with the instruments. In this experiment, heating regime was selected as 10 °C/min from 25 ^{o}C to 600 °C under nitrogen atmosphere.

DTA is a technique in which the difference in energy between the sample and the reference material is measured against time or temperature. The DTA curve is generally a plot of the difference in energy as the ordinate against temperature T, as the abscissa. By convention, in DTA endothermic peaks are drawn downwards and exothermic upwards (Ak, 2008). As for TG, it is a technique in which the mass of the sample is monitored against time or temperature while the temperature of the sample is programmed. A plot of mass loss or percent loss versus temperature or time can be obtained. The reaction is shown as one or more steps, each of which represents a mass change.

Temperature change in the samples brings about the chemical (phase transition, reduction, oxidation and decomposition) and physical (boiling, melting and sublimation) changes of a sample and these can be endothermic or exothermic. DTA is able to be used to study any process in which heat is absorbed or evolved. The number, shape and position of the various endothermic and exothermic peaks in DTA curve can be used for qualitative identification of the substance. Simultaneous techniques refer to the application of two or more techniques to a sample at the same time. In the present study, DTA-TG simultaneous techniques are used. It is an advantage to use simultaneous techniques because it saves time and sample and it gives an opportunity to set an experiment at the same conditions (Ak, 2008).

3.4.7 Mechanical Tests

Hardness is defined as the characteristic ability of a material to resist penetration or abrasion by other bodies. It has been nearly two centuries since the first hardness test was developed by Mohs in 1822. In that time, the state of the art has progressed from using reference materials to rank scratch relative resistance to the application of contact mechanics principles using instrumented, automated systems to probe mechanical properties on the nanometre scale.

Indentation testing is a simple method that consists essentially of touching the material of interest whose mechanical properties such as elastic modulus and hardness. Nanoindentation is simply an indentation test in which the length scale of the penetration is measured in nanometres (10^{-9} m) rather than microns (10^{-6} m) or millimetres (10^{-3} m), the latter being common in conventional hardness tests (Wheeler, J. M., 2009).

Nanoindentation hardness tests are generally made with either spherical or pyramidal indenters. Consider a Vickers indenter with opposing faces at a semi-angle of $\theta = 68°$ and therefore making an angle $\beta = 22°$ with the flat specimen surface. For a particular contact radius a, the radius R of a spherical indenter whose edges are at a tangent to the point of contact with the specimen is given by $\sin \beta = a/R$, which for $\beta = 22°$ gives $a/R = 0.375$. It is interesting to note that this is precisely the indentation strain at which Brinell hardness tests, using a spherical indenter, are generally performed, and the angle $\theta = 68°$ for the Vickers indenter was chosen for this reason (Fisher-Cripps, A. C. 2009).

The Berkovich indenter, in Figure 3.10.a, is generally used in small-scale indentation studies and has the advantage that the edges of the pyramid are more easily constructed to meet at a single point, rather than the inevitable line that occurs in the four-sided Vickers pyramid. The face angle of the Berkovich indenter normally used for nanoindentation testing is 65.27°, which gives the same projected area-to-depth ratio as the Vickers indenter. Originally, the Berkovich indenter was

constructed with a face angle of 65.03°, which gives the same actual surface area to depth ratio as a Vickers indenter. The tip radius for a typical new Berkovich indenter is on the order of 50–100 nm. This usually increases to about 200 nm with use. The Knoop indenter, in Figure 3.10.b,, is a four-sided pyramidal indenter with two different face angles. Measurement of the unequal lengths of the diagonals of the residual impression is very useful for investigating anisotropy of the surface of the specimen. The indenter was originally developed to allow the testing of very hard materials where a longer diagonal line could be more easily measured for shallower depths of residual impression. The cube corner indenter, Figure 3.11.c, is finding increasing popularity in nanoindentation testing. It is similar to the Berkovich indenter but has a semi-angle at the faces of 35.26° (Berkovich, 1951).

The Berkovich indenter is used routinely for nanoindentation testing because it is more readily fashioned to a sharper point than the four-sided Vickers geometry, thus ensuring a more precise control over the indentation process. The mean contact pressure is usually determined from a measure of the contact depth of penetration, h_c in such that the projected area of the contact is given by;

$$A = 3\sqrt{3}h_c^2 tan^2\theta \tag{3.2}$$

which for θ= 65.27°, evaluates to:

$$A = 24.494h_c^2 \approx 24.5h_c^2 \tag{3.3}$$

and hence the mean contact pressure, or hardness, is:

$$H = \frac{P}{24.5h_c^2} \tag{3.4}$$

The original Berkovich indenter was designed to have the same ratio of actual surface area to indentation depth as a Vickers indenter and had a face angle of 65.0333°.

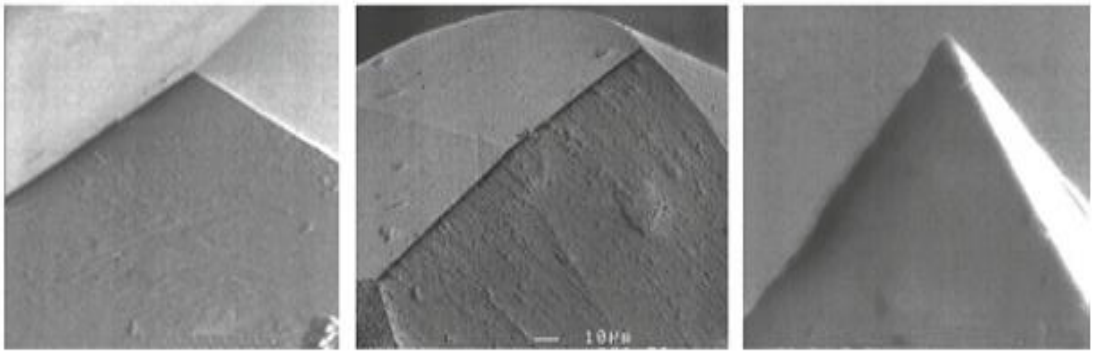

Figure 3.10 SEM images of the tips of (a) Berkovich, (b) Knoop, and (c) cube-corner indenters used for nanoindentation testing. The tip radius of a typical diamond pyramidal indenter is in the order of 100 nm (Fischer-Cripps, 2009).

For the calculation of modulus based on elastic contact theory, there are some differences in view of its indentation deformation. Figure 3.11 depicts the schematic representation of loading versus displacement during nanoindentation. In the figure, S represents the contact stiffness while h_c is the contact depth (Oliver & Pharr, 1992).

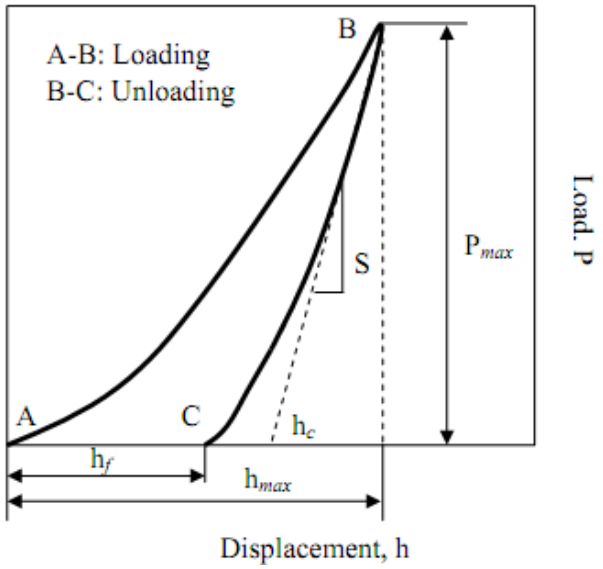

Figure 3.11 A schematic representation of load versus displacement during nanoindentation (Oliver & Pharr, 1992).

Nanoindentation measurements were performed using a nanoindentation system (IBIS, Fischer-Cripps Laboratories Pty Ltd., Australia) at EMUM-DEU. We have used a three-side pyramid (Berkovich) diamond indenter. The area function, which is

used to calculate contact area A_c from contact depth h_c, was carefully calibrated by using a fused silica sample, prior to the experiments.

Samples deposited on glass substrates were tested with a 0.6 mN force. As known the increase in the content of reinforcing element increase the mechanical properties such as, elastic modulus and yield strength but also increase in the brittleness. By this way thanks to mechanical and electrical tests optimized samples will be chosen for further applications.

3.4.8 Electrical Properties

A current–voltage characteristic is a relationship, typically represented as a chart or graph, between an electric current and a corresponding voltage, or potential difference. In electronics, the relationship between the DC current through an electronic device and the DC voltage across its terminals is called a current–voltage characteristic of the device. Electronic engineers use these charts to determine basic parameters of a device or material and to model its behavior in an electrical circuit. These characteristics are also known as I-V curves, referring to the standard symbols for current and voltage.

The "current-voltage characteristics" of an ideal resistor (resistance, heating element) are reasonably constant within certain ranges of current, voltage and power as it is a linear or ohmic device (Figure 3.8a). There are however, resistive elements (such as LDR's, thermistors, varistors, etc) whose I-V characteristic curves are not straight or linear lines but instead are curved or shaped and are therefore called nonlinear devices because their resistances are nonlinear resistances (Figure 3.8b).

The produced CPC films in this study are considered to be, conductive resistive heating elements. Hence the current voltage characteristics and resistance values are very important. And also in order to find out where the conductivity is provided, in other saying when the percolation threshold is exceeded, resistance measurements of the samples with graphite ratios 1, 2, 3, 4, 10, 16, 17, 18, 19, 25 and 30 % wt. and

with carbon black ratios 1, 2, 3, 4, 10, 16, 17, 18, 19, 25 and 30 % wt. were afforded using the experimental setup including a Keithley 2400 electrometer and copper film terminals as seen in Figure 3.13. Keithley 2400 SourceMeter is a 20W powered instrument that allows sourcing and measuring voltage from ±5µV (sourcing) and ±1µV (measuring) to ±200V DC and current from ±10pA to ±1A. The multimeter capabilities include high repeatability and low noise.

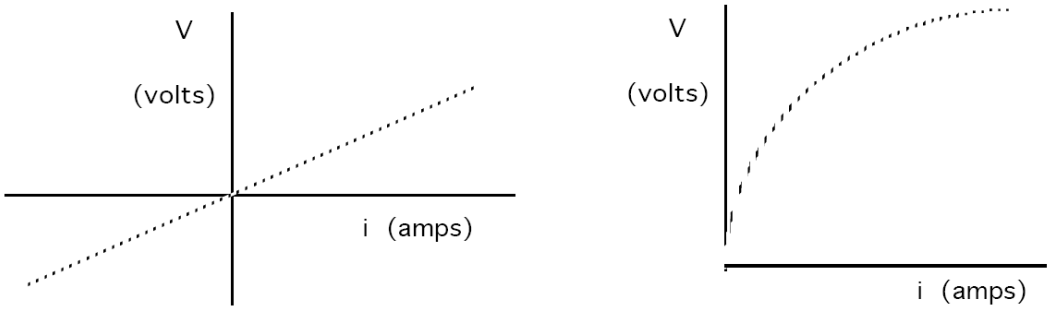

Figure 3.12 I-V characteristics for an ohmic (a) and non-ohmic (b) devices.

Voltage versus current and resistance versus time plots of the sample were recorded via computer software. Subsequent to measurements graphite and/or carbon black fractions versus respective resistance curves will be plotted to determine percolation thresholds of the sample groups in Table 3.1.

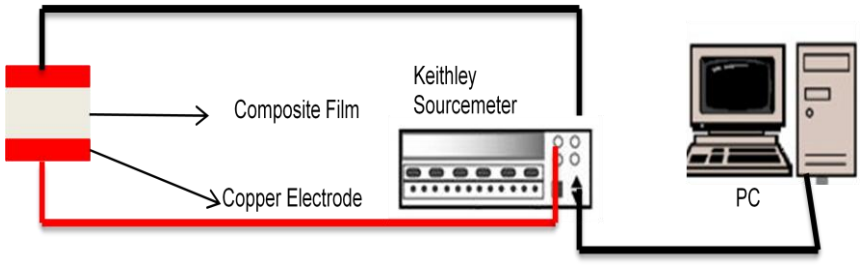

Figure 3.13 A schematic representation of electrical measurements setup.

3.4.9 Heating Properties

Surface temperature changes of a heating element versus time are significant issues. As mentioned before following the percolation threshold determination,

optimum samples above the threshold were characterized as the candidates of CPC film heating elements.

In order to determine the heating properties of the films an experimental setup including power supply (20 V), a thermal camera for contactless temperature measurements and copper film terminals schematized in Figure 3.14 was installed.

CPC films over PET substrates with proper conductivities (above the threshold) were cut in to 3x3 cm^2 dimensions, copper terminals were stacked on the parallel edges of the films using a conductive silver paste dye. Afterwards the terminals were connected to the power supply and time versus regional maximum temperatures and infrared thermographic maps were obtained with an infrared thermal imaging camera (Ti27, Fluke, USA). Finally temperature changes against time were plotted to present and compare the heating characteristics of the CPC films.

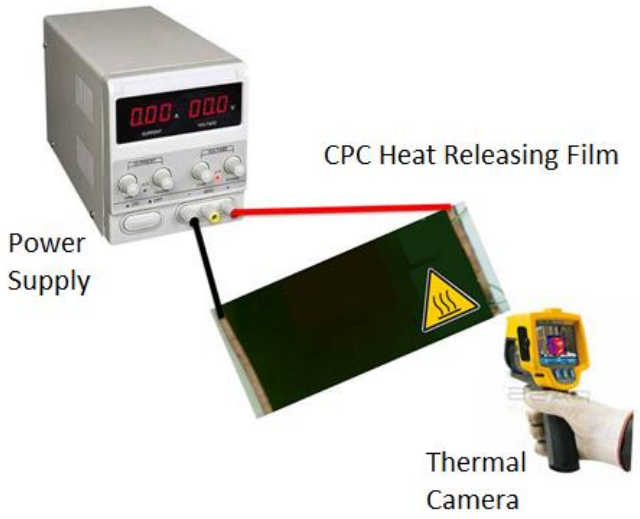

Figure 3.14 A schematic representation of heating properties setup.

3.4.10 Device Applications

As mentioned before one of the main aims of this study is the application of the produced materials as heating devices. Based on this aim, several prototype studies

were afforded with selected compositions of CPC heat releasing films. These devices can be listed as; heat releasing fabrics, portable home saunas, combi boilers and greenhouse heating systems.

In order to help indoor heating problems, macro scale CPC films were produced. The films were fixed under the carpets with the help of pocket sewn in the dimensions of the film. A thermostat with temperature controller was placed on to the structure. Tests were done in a 10 m^2 room to present the heating capability of the heat releasing carpet based on CPC films as a carpet.

Portable home saunas have an increasing potential in everyday life, medical and health issues. As distinct from traditional saunas portable ones are not steam supported. By this way they are mostly called as portable dry saunas. Portable dry saunas allow you to enjoy the benefits of a dry sauna (such as detoxification and muscle relaxation) without having to go to the expense or labor of building a whole sauna room in your home. According to this manner a prototype dry home sauna was produced using the CPC films.

Hot water requirement is an important issue for many boiler, electrical heating and etc. device try to overcome. As known, most of the electrical boilers or heat exchangers use metallic heating elements to heat or boil the water. But there are disadvantageous of this process in terms of corrosion and calcification.

In order to test the CPC films as boiler heating element tank of a commercial boiler was surrounded with macro scale CPC film and insulation materials. Comparative coefficients of performance (COP) tests were performed with a metallic element and our CPC films. The COP (sometimes CP) of a heat pump is the ratio of the heating or cooling energy provided over the electrical energy consumed. The COP provides a measurement of performance for heat pumps that is analogous to thermal efficiency for power cycles. Specifications of the heating elements to be compared are listed in Table 3.2.

Table 3.2 Some physical properties of the compared heating elements

Property	Metallic	CPC
Resistance *(ohm)*	42	38
Coefficient of heat conduction *(W/m.K)*	16.3	0.96
Mean surface area (mm^2)	7920	60000

In order to determine COP values an electrometer and a digital thermometer was utilized to record consumed electric energy (Q_2) and the temperature of the pure water, respectively. The energy supplied that used to increase the temperature of the pure water (Q_1) was calculated using basic thermodynamic equation as follows.

$$Q_1 = mc\Delta T \tag{3.5}$$

in which m, c and ΔT stand for mass, specific heat and temperature changes of pure water respectively. By this way to calculate the COP value for our system Equation 3.6 below is employed.

$$COP = \frac{Q_1}{Q_2} \tag{3.6}$$

Heating is a major concern to many commercial greenhouse producers. This is due primarily to the costs involved in the purchase and operation of heating equipment as well as the potentially disastrous effects of a poorly designed system. Similar to the previous prototype boiler system was employed also in greenhouse constructed in the Tinaztepe Campus next to department. Hot water was fluxed through the pipes and radiators to warm inside of the greenhouse. The system was tested in the manner of its capability to heat the space comparatively with the present heating systems especially in the freezing days. The green house and the boiler system is depicted in Figure 3.15.

(a) (b)

Figure 3.15 (a) The green house and (b) the prototype boiler systems.

CHAPTER FOUR
RESULTS AND DISCUSSION

4.1 Particle Size Distribution

Particle filled polymer composites have become attractive because of their wide applications and low cost. Incorporating inorganic mineral fillers into plastic resin improves various physical properties of the materials such as mechanical strength, modulus, flame retardancy, electrical and heat deflection temperature properties. In general the mechanical properties of particulate filled polymer composites depend strongly on size, shape and distribution of filler particles in the matrix polymer and good adhesion at the interface surface.

Stress concentration phenomena in mechanics can be employed to summarize the effect of the particle size on the mechanical properties. Following increasing filler particle size an increase in stress concentration and decrease in flexural strength is observed since the fillers behave as void or crack in the matrix structure. In this respect, composite with nano dimension fillers draw more attention for decades.

In order to decrease particle size of the fillers (carbon black and/or graphite) into nano scale, the milling operations briefly which are explained in the previous chapter were performed. Subsequent to milling process mean particle distributions of the obtained powders were measured using dynamic light scattering technique. Particle size distributions of graphite and carbon black powders were depicted in Figures 4.1 and 4.2 respectively after a 24 hours of milling operation.

As seen in Figure 4.1, particle size of graphite powders exhibits a distribution in a wide range from 60 nm to 2.7 μm. If the primary particle size distribution of the graphite particles (3 μm to 40 μm) taken into account, one can easily declare that an effective milling operation is performed. Distributions over 1 μm were thought to be agglomerated particles which will be supported using microstructure photographs.

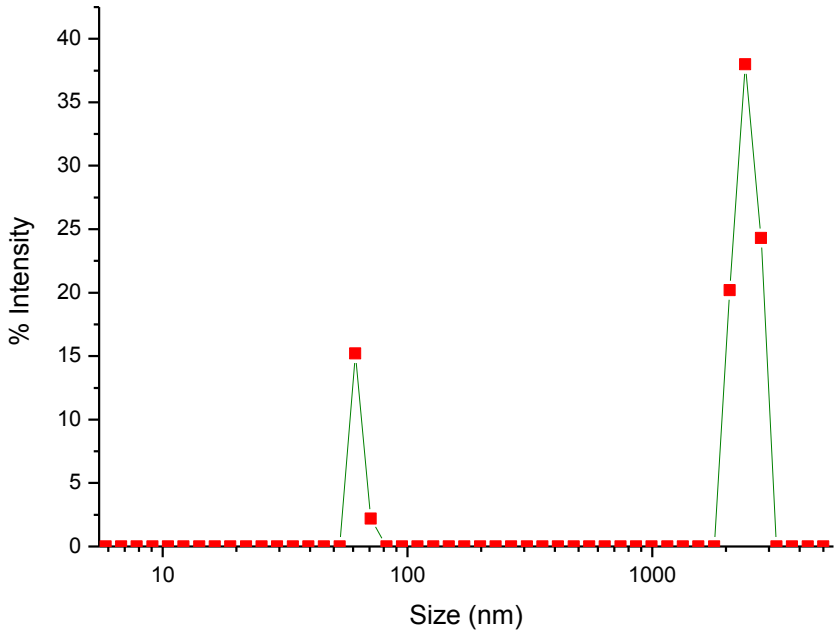

Figure 4.1 Particle size distribution of graphite powders.

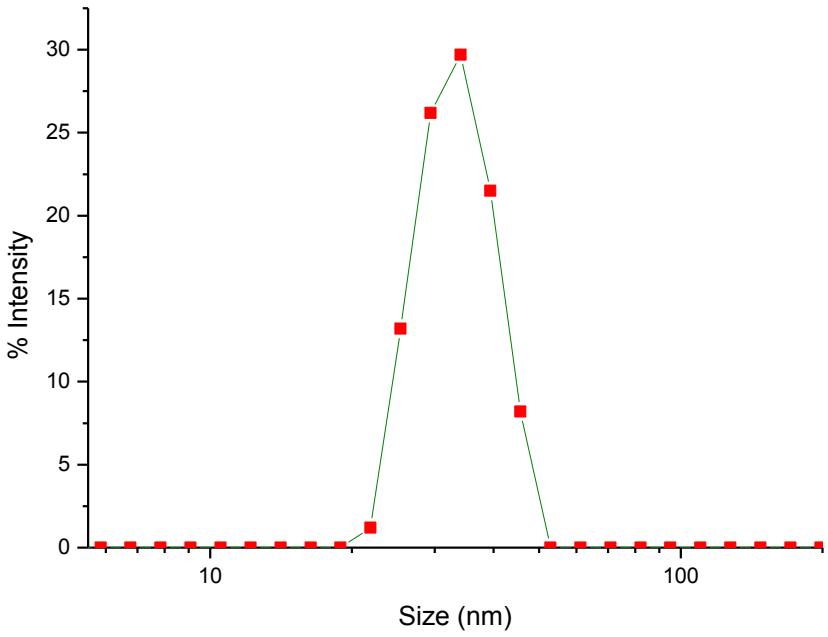

Figure 4.2 Particle size distribution of carbon black powders.

According to the carbon black particle size distributions depicted in Figure 4.2, it can successfully expressed that a monodisperse particle size distribution is obtained with a narrow range from 20 nm to 45 nm. Even though the same milling operation performed for both powders the effectivity of the carbon black powders milling was found to be higher since the primary particle size distribution is between 3-40 μm.

As known graphite is a self lubricating material due to its layered planar structure since these layers have a limited sliding motion. Thus it is considered that graphite structure made hard to mill it in to finer particle size (Shukor, & Saifudin, 2010). Beside this reality, both the milled powders were employed in heat releasing CPC film production.

4.2 Phase Analysis

XRD patterns of major samples of heat releasing CPC films listed in Table 3.1 were obtained via x-ray difractometer. XRD patterns of one component CPCs including just graphite and carbon black (G0, G10, G20, C0 C10C and C20) are depicted in Figure 4.3.

Second class of films (G5-C1,G5-C3,G5-C5, G10-C1, G10-C3, G10-C5, and G10-C7), including both carbon and graphite were structurally characterized using XRD. Patterns of this material classes were given in Figures 4.4 and 4.5 for 5 % and 10 % graphite series respectively.

As defined in the patterns, peaks 1, 2 and 3 correspond to the International Centre for Diffraction Data (ICDD) of polystyrene (053-1892), graphite (026-1077) and carbon black (026-1080) respectively. All the obtained data for the CPC films points out that; carbon black and graphite powders were encapsulated in the SACE matrix without any chemical and structural change. In addition, it can be declared that obtained results were found to be in a good agreement with the literature (Wang et al., 2007, Erol, & Çelik 2013).

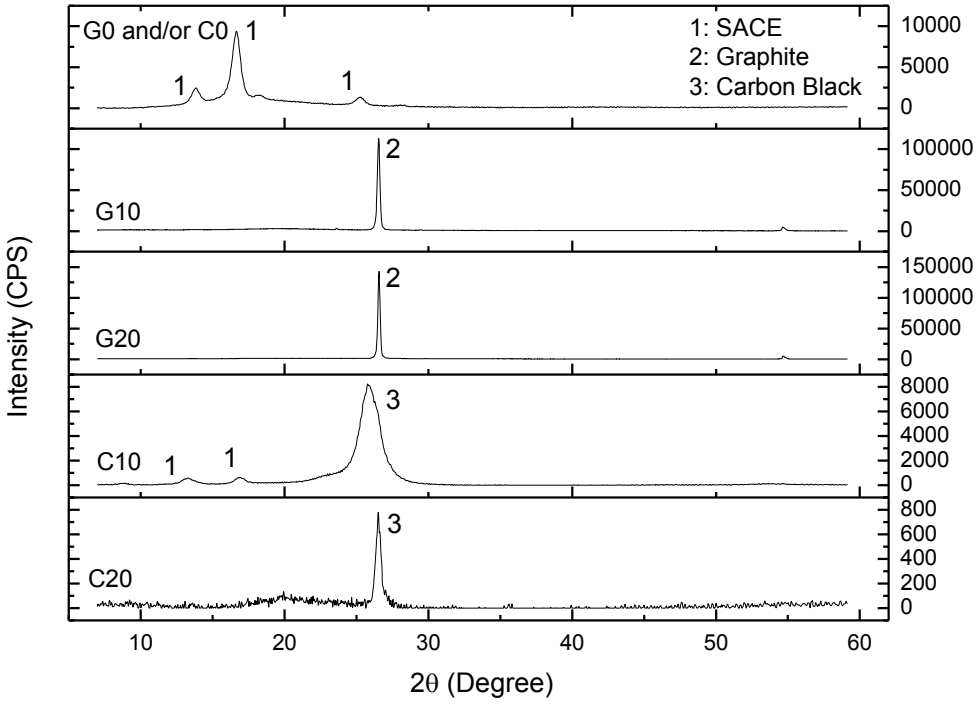

Figure 4.3 XRD patterns of carbon black and graphite reinforced CPC films.

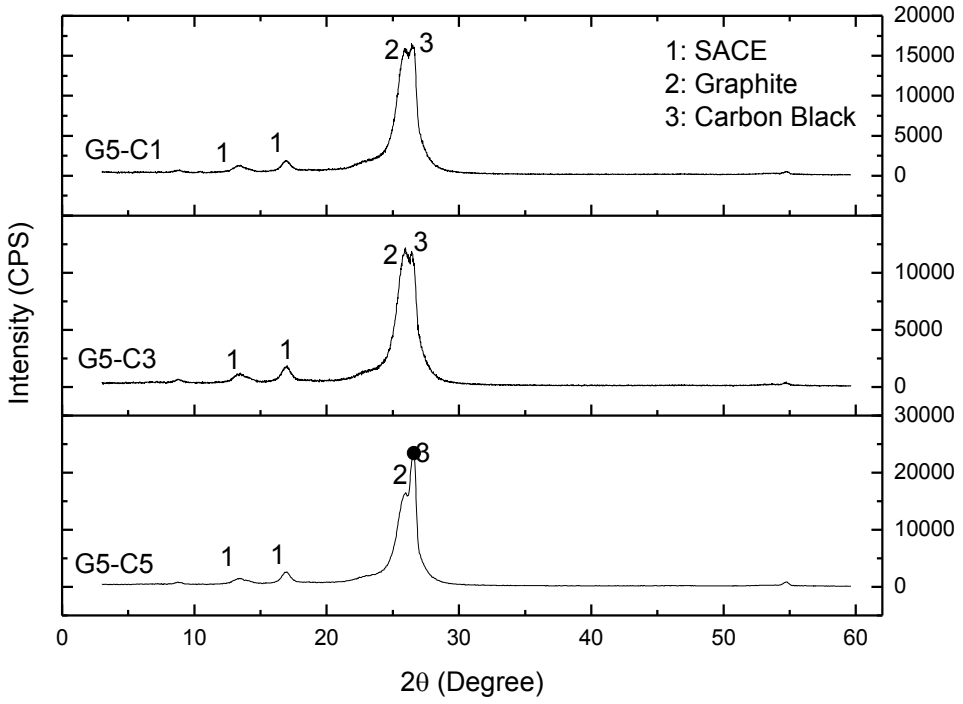

Figure 4.4 XRD patterns of binary graphite and carbon black reinforced CPC films (5 series).

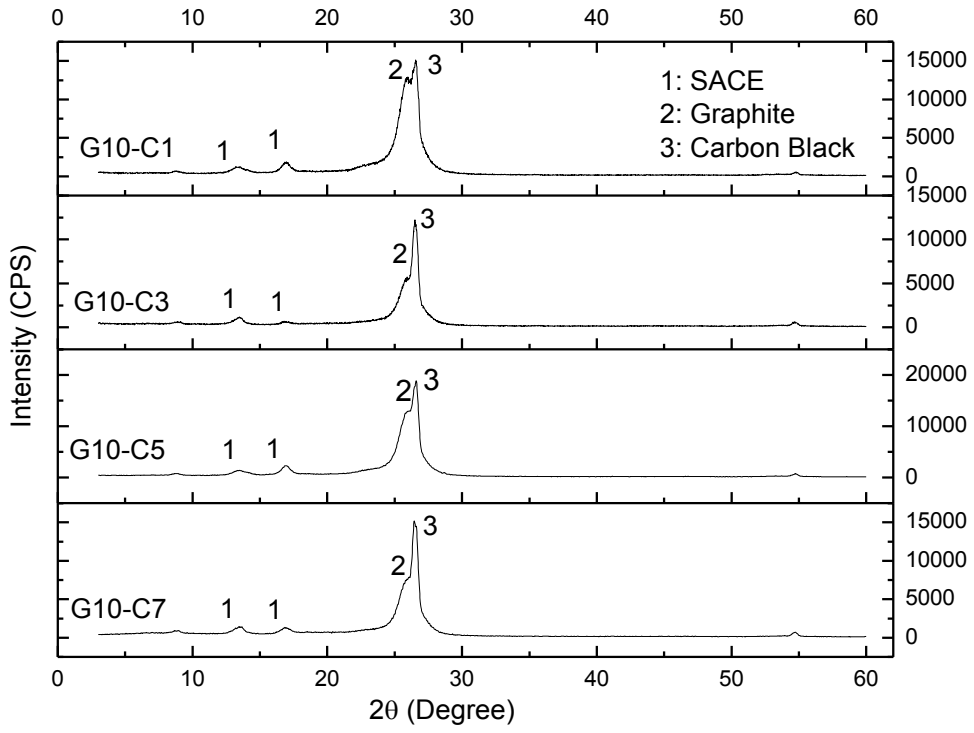

Figure 4.5 XRD patterns of binary graphite and carbon black reinforced CPC films (10 series).

4.3 Elemental Analysis

Elemental analysis of CPC films were determined with the help of XPS. The samples coded C10, G20, G5-C5 and G10-C7 were decided to be elementally surveyed inasmuch as they will be enough to represent properties of the corresponding material class and the results are plotted in Figures 4.6, 4.7, 4.8 and 4.9, respectively.

The XPS results of all samples indicated that; major elemental component of the films is carbon in C1S form. Surveys are obtained as a result of C-C bonds (284.0-286.0 eV) in the structures of carbon black and graphite as displayed in Figures 3.2 and 3.3 respectively. As known SACE structure (Figure 3.1) also includes C-C bonds, thus the increase in the percentage of C1s which is about 85-87 % was provided. Oxygen content obtained in the results indicates the content of oxygen in SACE structure (Wang et al., 2006).

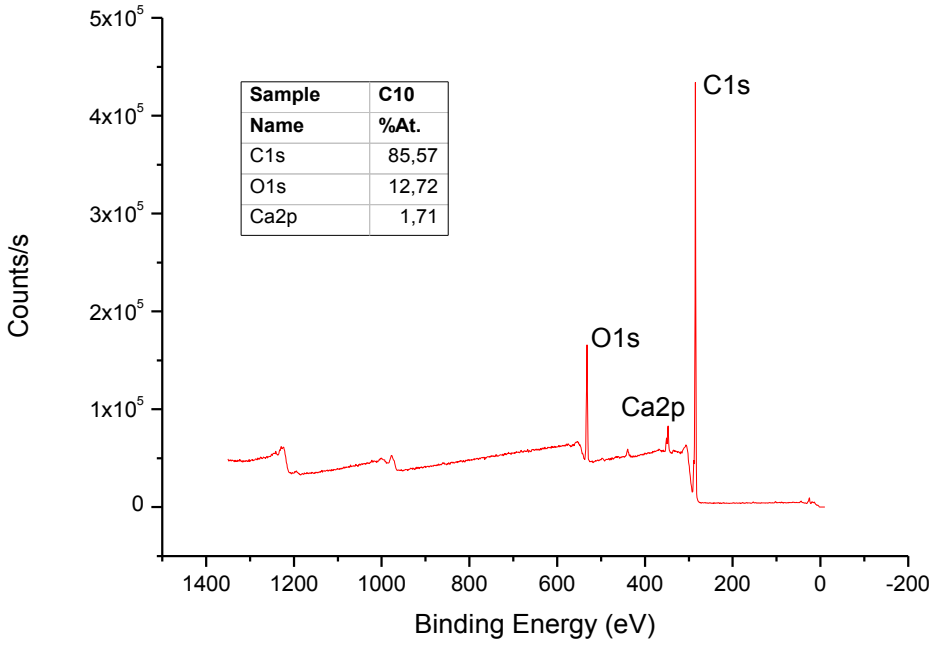

Figure 4.6 XPS result of sample C10

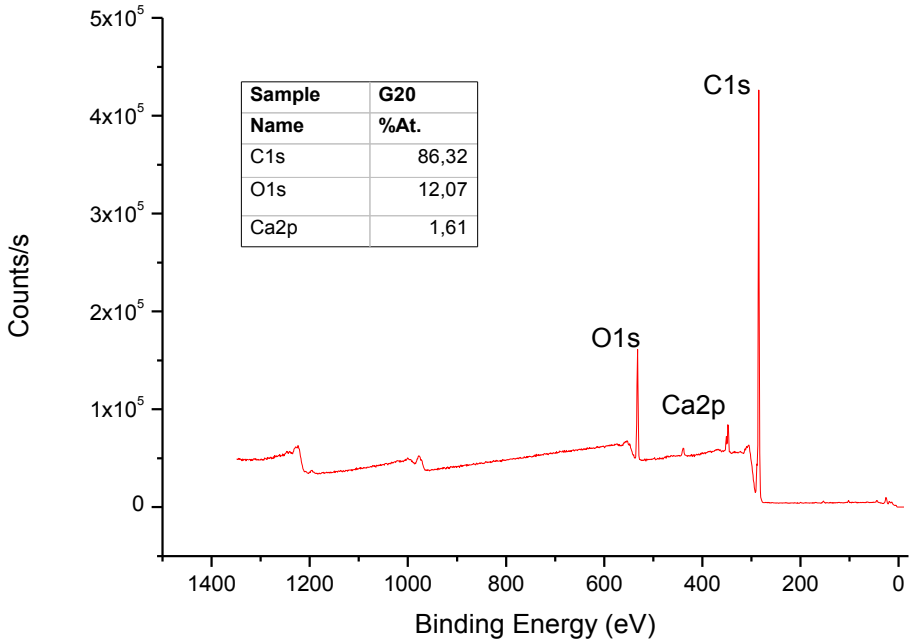

Figure 4.7 XPS result of sample G20

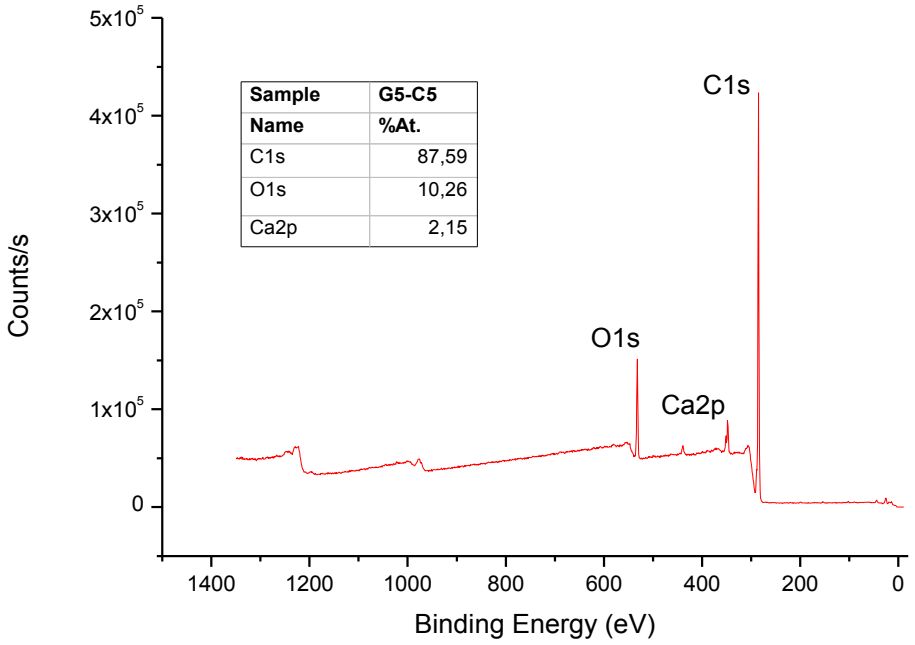

Figure 4.8 XPS result of sample G5-C5

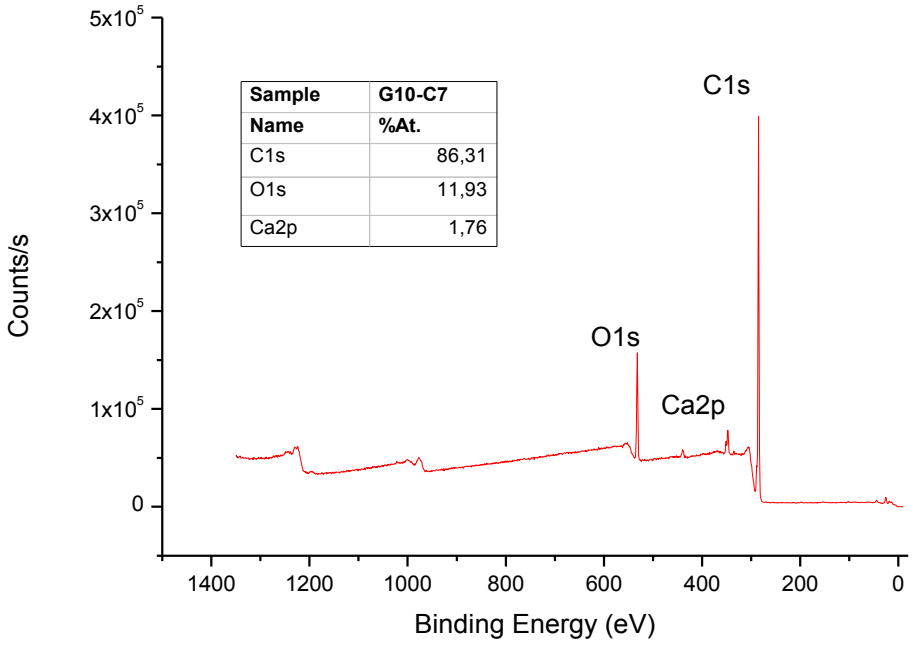

Figure 4.9 XPS result of sample G10-C7

As explained in the experimental study section, SACE is diluted using city water without any distillation since one of the aim of the thesis is to transfer this technology in to bulk production by considering the processing costs. By this way it is thought that the content of Ca is because of the water used. As reported in a study it is stated out that little amount of Ca can be found in the ash content of some graphite powders (Gilmanshina et al., 2012).

4.4 Spectroscopic Analysis

To provide a sound basis for empowering XPS results and illuminating the structure here, the principal concepts and experimental data concerning FTIR-ATR spectra of heat releasing CPC films were revealed and discussed separately below. Spectra of the samples including just graphite and carbon black (G0, G10, G20, C0 C10C and C20) are depicted in Figure 4.10. In order to depict binary effect of carbon black and graphite spectra of samples C10, G20, G5-C5 and G10-C7 are given in Figure 4.11.

First of all, it must be noted that graphite and carbon black are infra red inactive, because of their symmetric structure (Kim, & Kim 2010, Peng, 2013). The absence of the bands at 3440 cm^{-1} and 1640 cm^{-1} (O-H bond stretching modes of absorbed water) proves that the drying is successfully performed.

Matrix medium used in the thesis is a styrene-acrylic copolymer which has characteristic wavenumbers as 3060, 1730, 1490, 1455, 1385, 1243, 1160, 1065, 1029, 812, 760 and 705 cm^{-1} (Papliaka et al. 2010). The obtained results are in a good agreement with literature. As mentioned elsewhere because of the IR inactivity of carbon black and graphite, no significant change was obtained with increasing carbon black and/or graphite content in the CPC films.

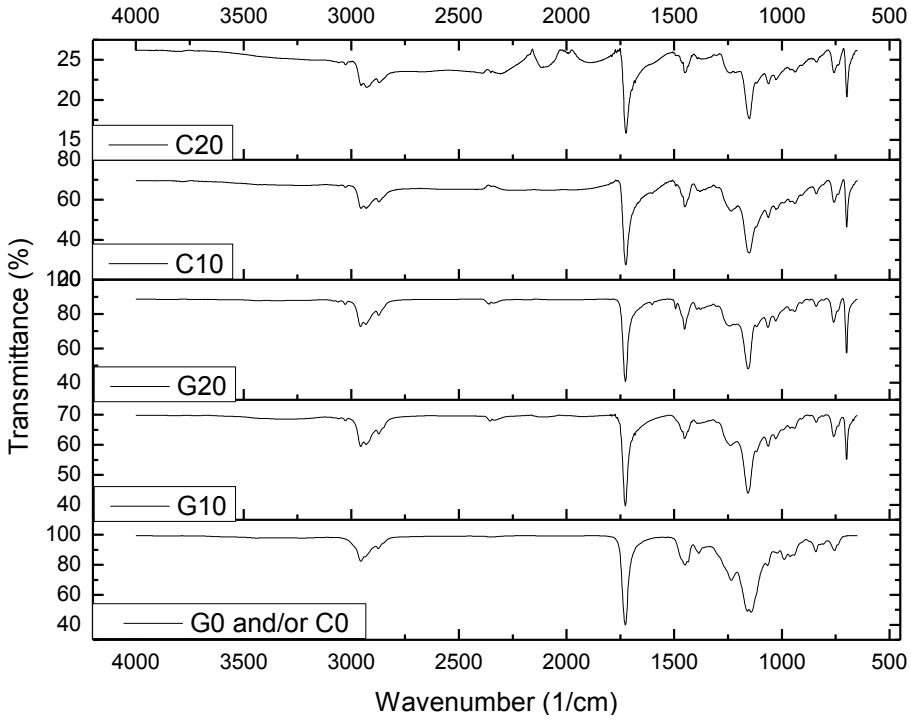

Figure 4.10 FTIR-ATR spectra of carbon black and graphite reinforced CPC films.

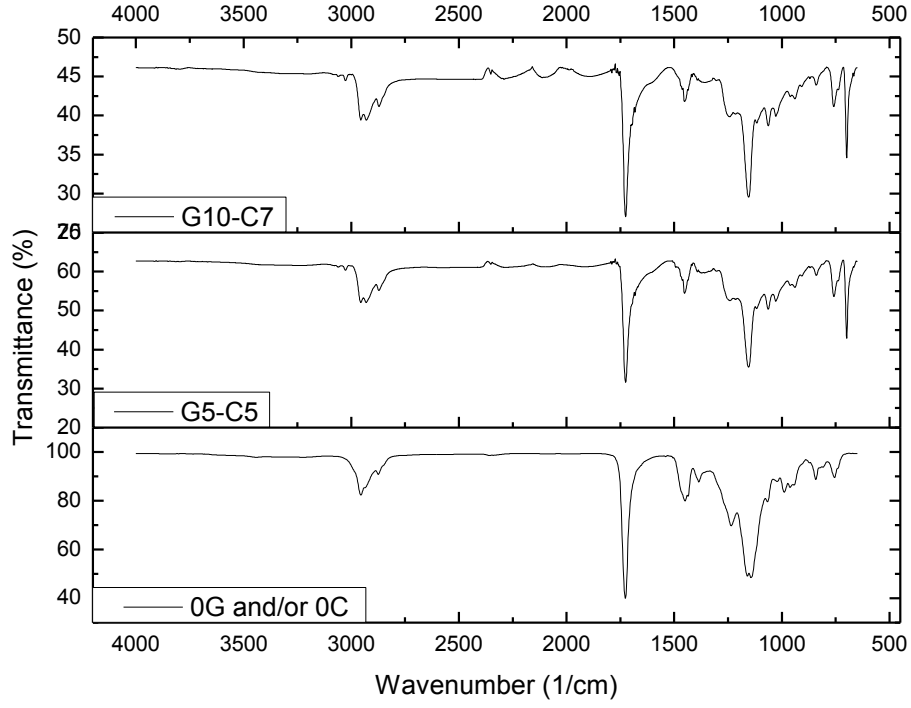

Figure 4.11 FTIR-ATR spectra of binary graphite and carbon black reinforced CPC films

4.5 Microstructure and Morphology Analysis

Microstructure can be defined generally as the structure of a material as determined by any of the available microscopic techniques. The microstructure of a material (which can be broadly classified into metallic, polymeric, ceramic and composite) can strongly influence the physical properties such as strength, toughness, ductility, hardness, corrosion resistance, high/low temperature behavior, wear resistance, and so on, which in turn govern the application of these materials in industrial practice.

In order to determine the microstructure of the produced CPC films SEM photographs were taken. Electron microscopy samples from G0 (or C0), G 10, G20, C10, C 20 for one component class, 5 and 10 series of binary CPC films were determined. Secondary electron images of the sample G0 (or C0) are given in Figure 4.12.

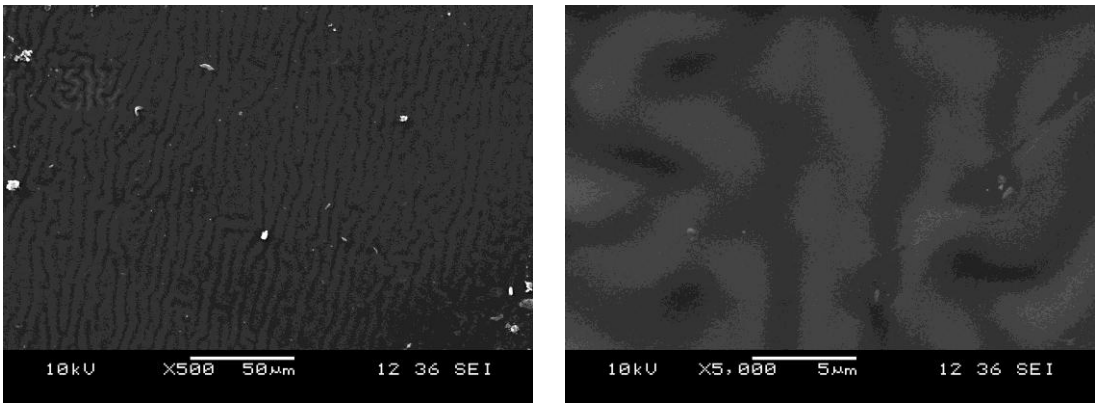

(a) (b)

Figure 4.12 SEM micrographs of sample without any filler (a) general and (b) detail view.

As seen in Figure 4.12, film without any filler has a rough surface including round valley and hills. If spray deposition, the technique used for film deposition, is taken into consideration, low surface quality was thought to be a result of flow of deposited emulsion over the substrate.

Electron micrographs of samples G10, G20, C10 and C20 are given in Figure 4.13 with general and detail views. In general views similar valley-hill structure are also

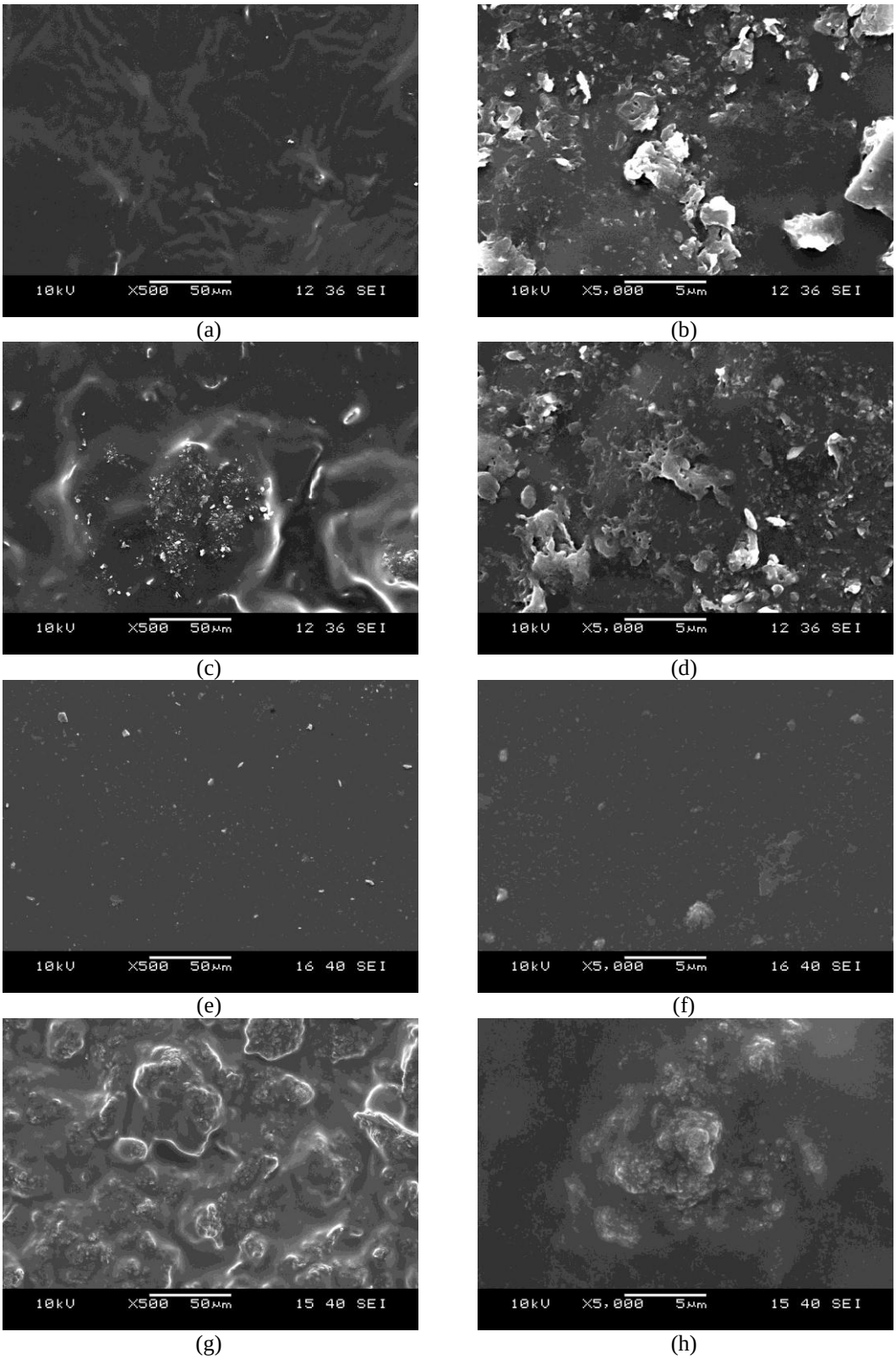

Figure 4.13 SEM micrographs of samples G10, G20, C10 and C20 (a, c, e and g are general b, d, f and h are detail views).

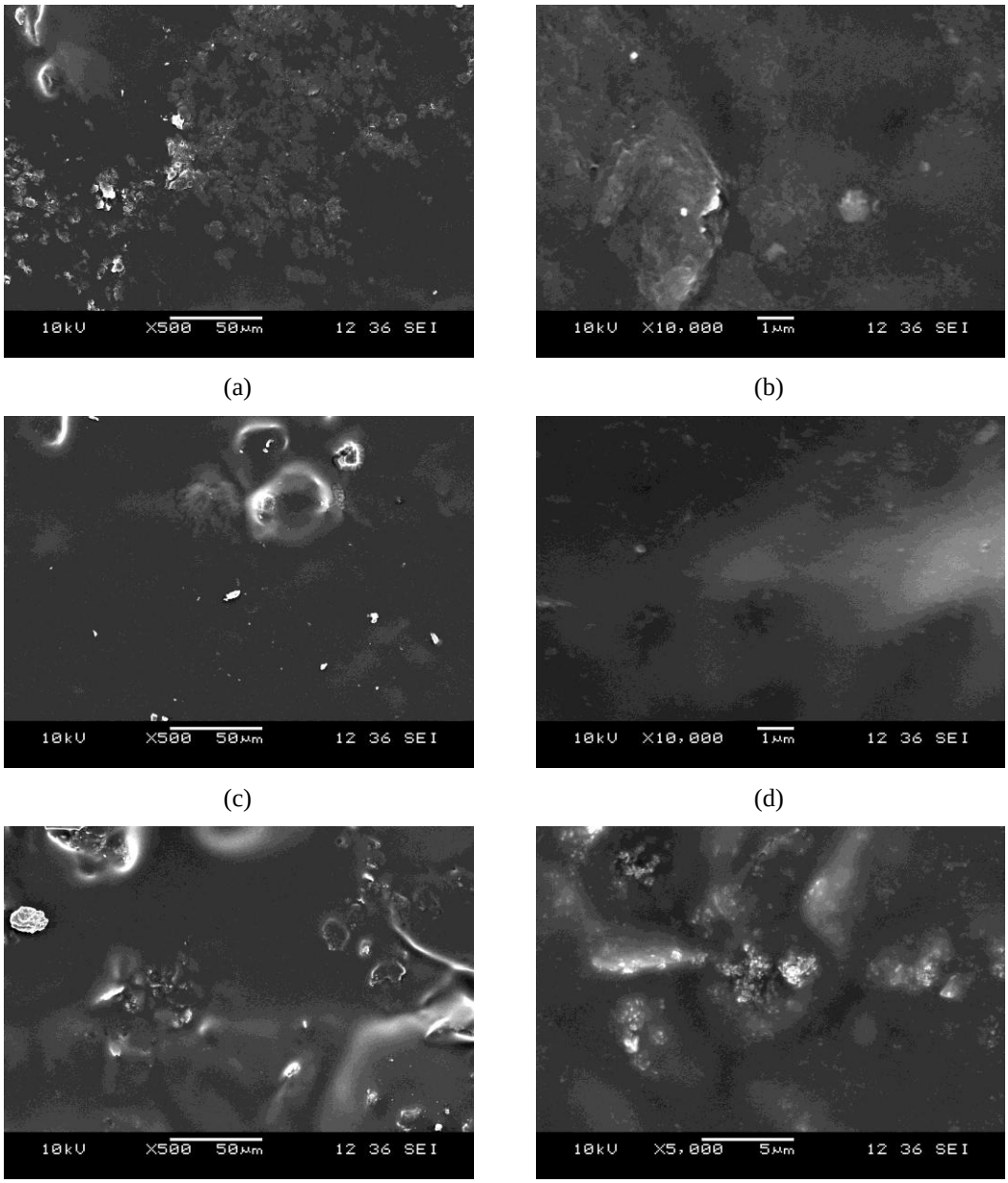

Figure 4.14 SEM micrographs of samples G5-C1, G5-C3 and G5-C5 (a, c and e are general, b, d, and f are detail views).

obtained for filler loaded films. Samples including just carbon black have smoother surfaces than the graphite loaded ones. It can be inferred that; CPC films including smaller particle sized fillers have smoother surfaces if the particle size distribution results considered. In addition; the plate like structure of the graphite particles with large particle size are observed as agglomerates and deposition islands. Beside the

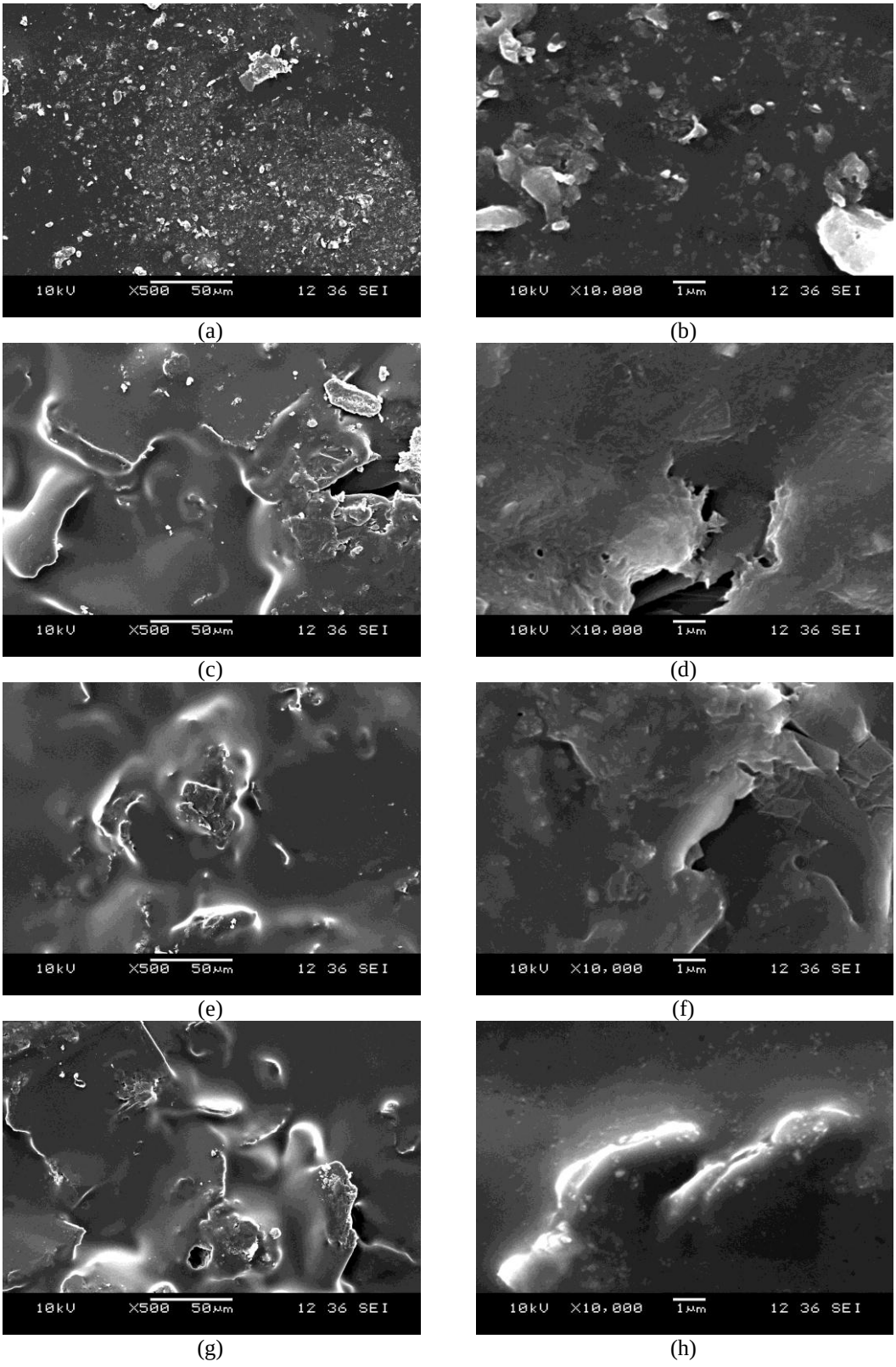

Figure 4.15 SEM micrographs of samples -C1, G10-C3, G10-C5, G10-C7 (a, c, e and g are general b, d, f and h are detail views).

surface roughness, the good coating and coverage capability of the matrix emulsion can be determined using the micrographs.

Micrographs of binary samples; G5-C1, G5-C3, G5-C5 and G10-C1, G10-C3, G10-C5, G10-C7 were represented in Figures 4.14 and 4.15 respectively. Binary samples which include both carbon black and graphite are the key point of the thesis. Aim of the thesis can be summarized as to produce composites including both carbon black and graphite with a concentration lower than the composites including just carbon black or graphite over the percolation threshold (see electrical properties for details). In other way; using binary samples will provide the replacement of the matrix with carbon black which has lower resistivity than the polymeric matrix. According to this aim; if the micrographs of the binary samples are taken into account, it can be expressed that graphite powders or agglomerates are found to be successfully surrounded with carbon blacks powders.

4.6 Thermal Analysis

The thermal stability of the CPC samples G20, C20, G5-C5 and G10-C7 was illustrated by differential thermal analysis (DTA) and thermo-gravimetric analysis (TGA). The TGA curves of the samples were represented in Figure 4.16. Generally it is possible to determine glass transition temperature, volatile removal temperature, organic burnt out temperature and melting point using DTA/TG device. However the obtained curves indicate that; any distinct energy or weight loss peaks corresponds to mentioned reactions was not observed except decomposition temperature (the temperature where the composite structure lose its integrity). The decomposition temperatures of the samples G20, C20, G5-C5 and G10-C7 was determined as; 407, 400, 395 and 404 ^{o}C respectively. It is thought that the little increase in the decomposition temperature was found to be increasing with the amount of graphite in the structure. The absence of volatile removal peak can be addressed into FTIR results which indicate that CPC films do not have water content owing to drying process.

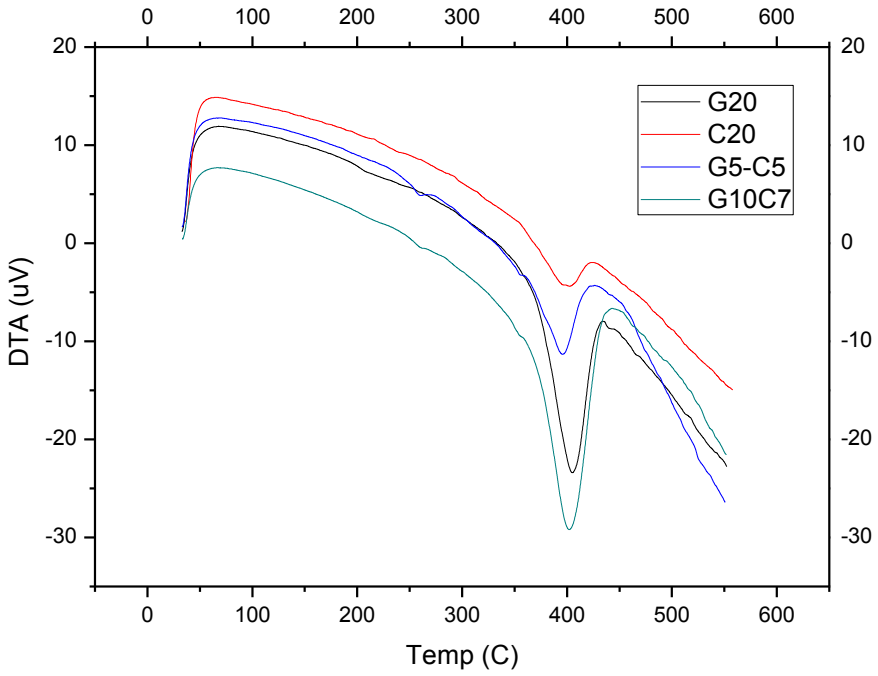

Figure 4.16 Differential thermal analysis of the samples

TG analysis, which gives information about the weight loss of CPC films against increasing temperature were depicted in Figure 4.17. Based on the results, it can be inferred that; increasing graphite contend slightly decrease the weight loss (see information Table in the graph). Similar to the DTA results, any other weigh loss temperature could not be observed. Both DTA and TG analysis were found to be in a good agreement with a study on thermal properties of styrene acrylic copolymers (Sadeghi, 2006).

If the aim of the thesis is taken into account, the role of thermal analysis becomes more important. Depending on the obtained result, it can be briefly expressed that; the obtained decomposition temperatures which is about (400 ^{o}C) are higher and more sufficient than the indented operation temperatures of the CPC heating elements.

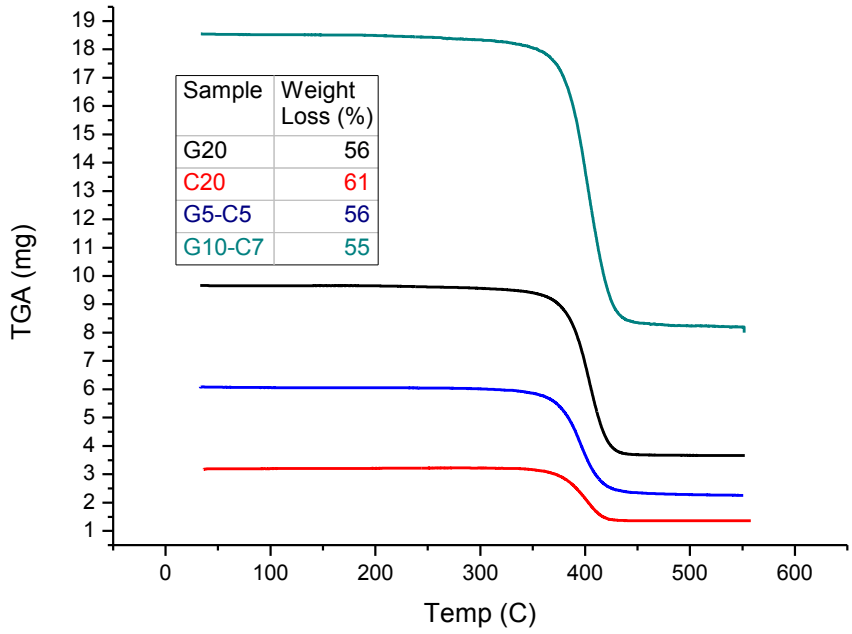

Figure 4.17 Thermogravimetric analysis of the samples

4.7 Mechanical Properties

Mechanical characterization of the produced films is another area where depth sensing indentations are being applied extensively. As mentioned before to measure the properties of the film without any substrate effect, the depth of indent made should be approximately 10 % of the thickness of the film. It is also a well known fact that surface roughness effects hardness measurements, if the surface roughness are much smaller than the indentation size. As a result of these in order to accompany the optimum quality mechanical characterization for coatings, thickness and roughness of the structure must be taken in to account. Due to the fact that; approximate thickness and roughness of the films were measured as 25 µm and 2 µm respectively. Hence the load 0.6 mN was determined as the optimum force for the appropriate indentation dept.

Using previously mentioned limitations load versus displacement nanoindentation measurements are plotted in Figure 4.18 for samples; G20, C20, G5-C1, G5-C5,

G10-C1 and G10-C7. Nine indents were applied for each sample and the results were presented as arithmetic mean values because of the heterogeneous structure of composites. According to obtained results, it can be reported that all plots were found to be coherent to schematic representation curve given in Figure 3.11. The obtained results indicates that; increase in the filler amount; results decrease in the penetration depth of the indenter.

Modulus of elasticity and hardness are dependent to the volume fraction of the filler for a two-phase composite. These rule of mixtures equations predict that the elastic modulus and hardness should fall between the values for matrix and the filler. Modulus of elasticity and hardness of the materials were calculated using the load displacement curves and given in the chart represented in Figure 4.19. According to the chart, it can be expressed that; increasing filler content increases the mechanical properties as modulus of elasticity and hardness.

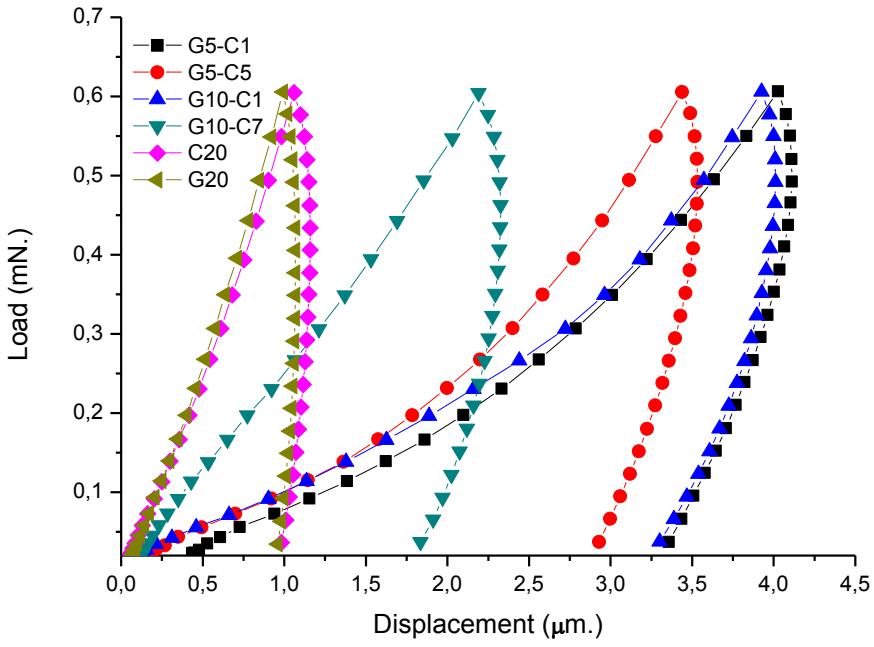

Figure 4.18 Load versus displacement plots of the samples.

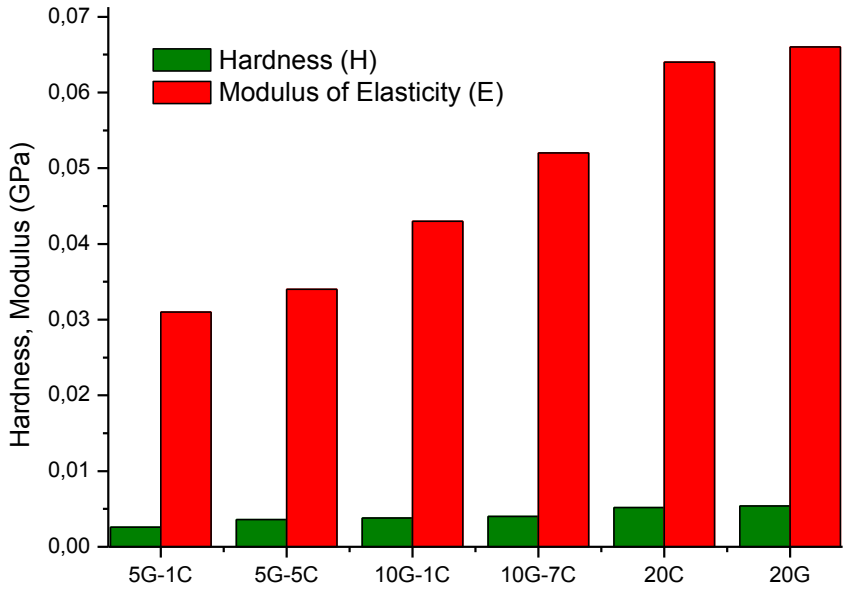

Figure 4.19 Hardness and modulus of elasticity values of the samples.

4.8 Electrical Properties

Electrical properties of a heat releasing CPC film are the most important parameters for further device applications and material innovations. Due to the major samples listed in Table 3.1, the minor samples were also employed characterization. Time versus resistance measurements were afforded using the experimental setup mentioned in Chapter 3. Increasing the graphite content-resistance and carbon black content-resistance graphs were plotted using the data obtained from these resistance measurements as represented in Figures 4.20 and 4.21, respectively.

As depicted in Figure 4.20, the resistance values of the films were measured as about 10^{10} ohm up to 15 (% wt.) graphite content. It should be kept in mind that when the graphite content slightly passed over 15 (% wt.) a sharp drop in the resistance is observed. As theoretically defined beforehand, the percolation threshold for graphite based samples was experimentally determined as ≈16 (% wt.). According to the curve, composites including graphite lower than 16 (% wt.) can be

named as insulator, in contrary to conductor composites including graphite content higher that 16 (wt. %).

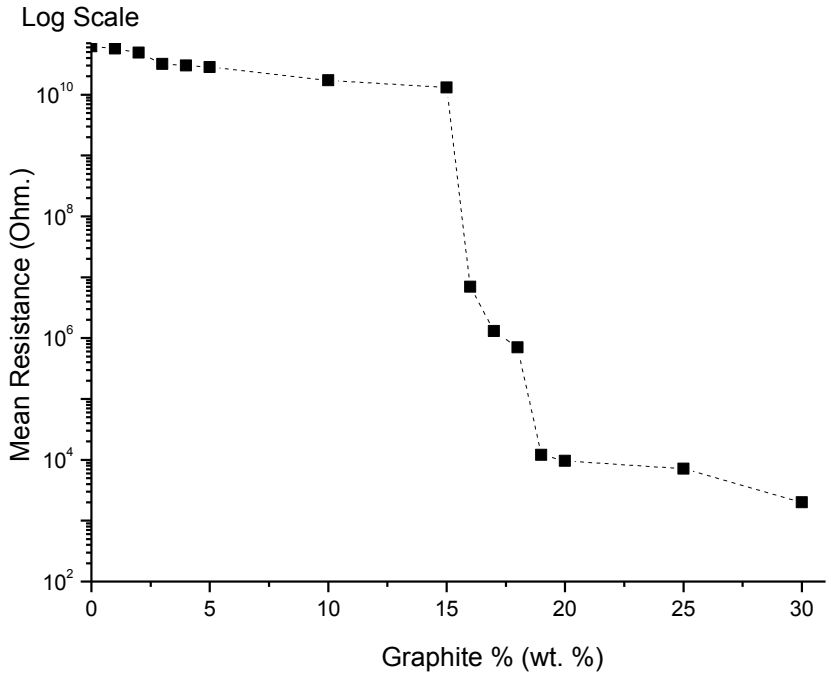

Figure 4.20 Mean resistance versus graphite content.

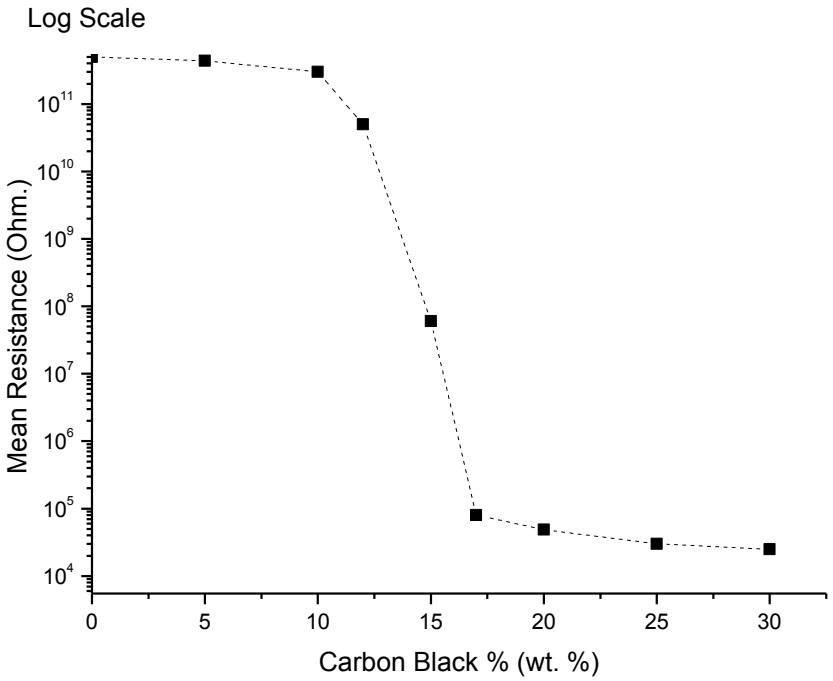

Figure 4.21 Mean resistance versus carbon black content.

Similar experiments were also performed for carbon black reinforced composites. According to the graph plotted in Figure 4.21, percolation threshold of carbon black based composited was determined as 13 (wt. %). Although a percolation threshold was obtained in a lower content of filler, the resistance values over the percolation was found to be ten times larger than to graphite based composites.

Percolation threshold can be defined as the critical conductive filler content where the applied electrical potential is enough for electron tunneling to occur. In other words, the critical distance between graphite powders are obtained, so the electrons can flow. With this manner; in order to decrease the distance between the powders or to increase tunneling potential, both graphite and carbon black including samples were produced as previously defined 5 and 10 series samples. Same electrical characterization experiments were performed for both 5 and 10 series as plotted in Figures 4.22 and 4.23 respectively.

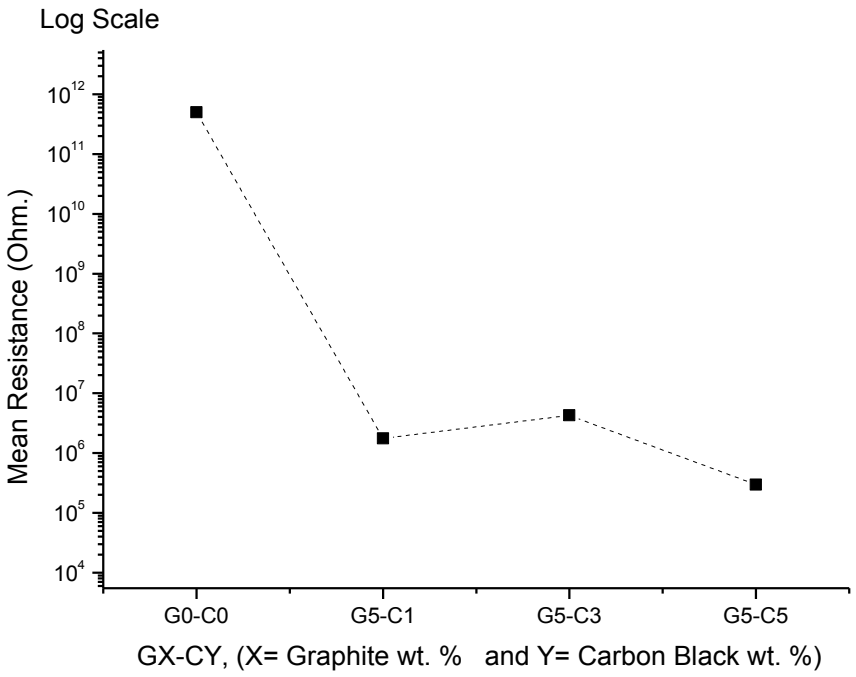

Figure 4.22 Mean resistance values of 5 series samples.

As seen on the electrical measurement results for 5 and 10 series samples; it can be realized that lower resistances (higher conductance) were obtained if compared to

results of both just graphite or carbon black filled composites. For example the resistivity obtained at 17 (wt %) graphite and carbon black are in 10^4 and 10^5 order respectively. Same order of resistance values was also obtained with samples G5-C5, G10-C1, G10-C3, G10-C5 and G10-C7. Based on this result, it can be inferred that the main aim of this thesis was successfully accomplished using lower content of filler than samples of just graphite and just carbon black filled composites.

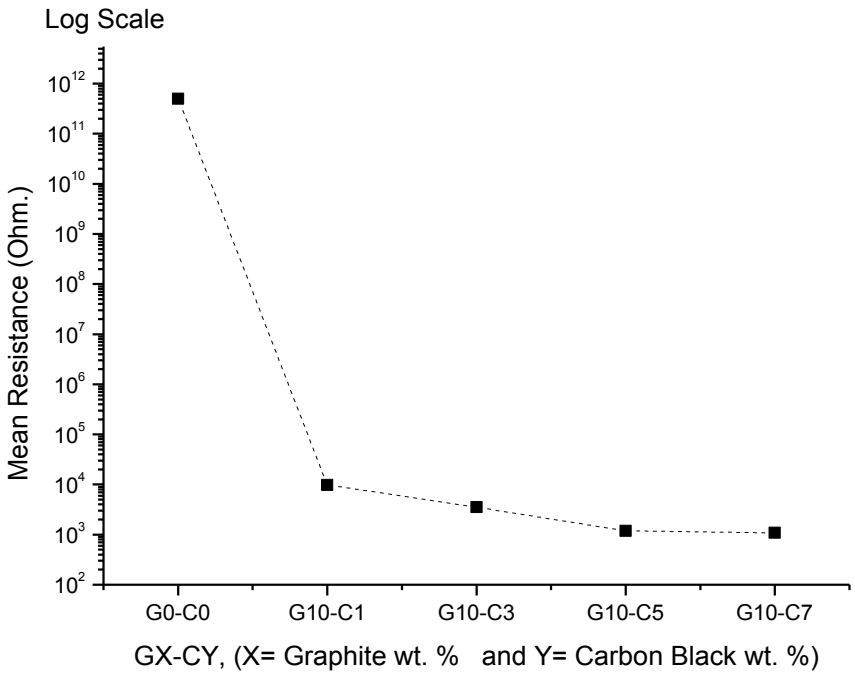

Figure 4.23 Mean resistance values of 10 series samples.

The resistance drop obtained in 5 and 10 series samples can be defined as co-percolation where both graphite and carbon black samples cooperatively (synergetic effect) provide electrical conductivity. The physical principles of the conductivity obtained with co-percolation is theoretically reported in literature (Aneli et al., 2011). Model composite microstructure is demonstrated by them as seen in Figure 4.24. Synergism of binary fillers is connected with the features of the composite morphology. In particular, this phenomenon is explained by the type of interdisposition of two types of filler particles in the polymer matrix. For instance, microstructure of a composite which contains carbon black and graphite may be schematically presented as a conglomerate of particles of the fillers, “injected” into the polymer matrix. It should be noted that carbon black particles possessing lower

electric conductivity form a secondary structure, looking like bridges between conducting particles of graphite, including them into the general conductive system. If it is presented as an electrical scheme of parallel consequent connected resistant elements, it becomes possible to explain the reason of a significant improvement of electrically conducting properties of the composite. Finally it can be expressed that the theory developed by Aneli et al was experimentally proved.

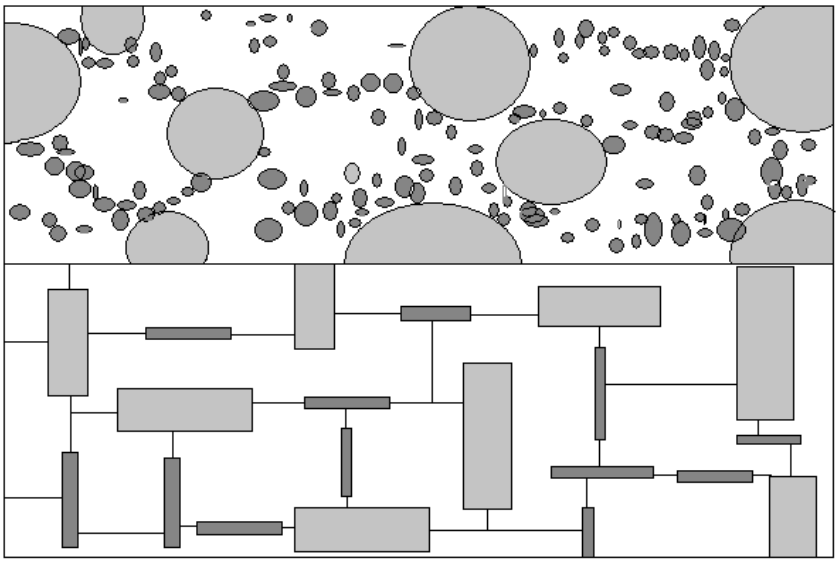

Figure 4.24 Two-dimensional model of the composition based on polymers with a binary filler (graphite + carbon black) (top) and equivalent direct current scheme (bottom). Big circles - graphite particles; small circles - carbon black particles; big rectangles – resistance of graphite particles; small rectangles – resistance of carbon black particles (Aneli et al., 2011).

In order to clarify the innovations provided by co-percolation, the advantages of them must be noted. If long term plan for process transferred to mass production, the decrease in the filler content will provide a significant decrease the production costs.

4.9 Heating Performances

Heating performance tests of samples were performed using the experimental setup mentioned in Chapter 3 including adjustable power supply (0-60 V. DC),

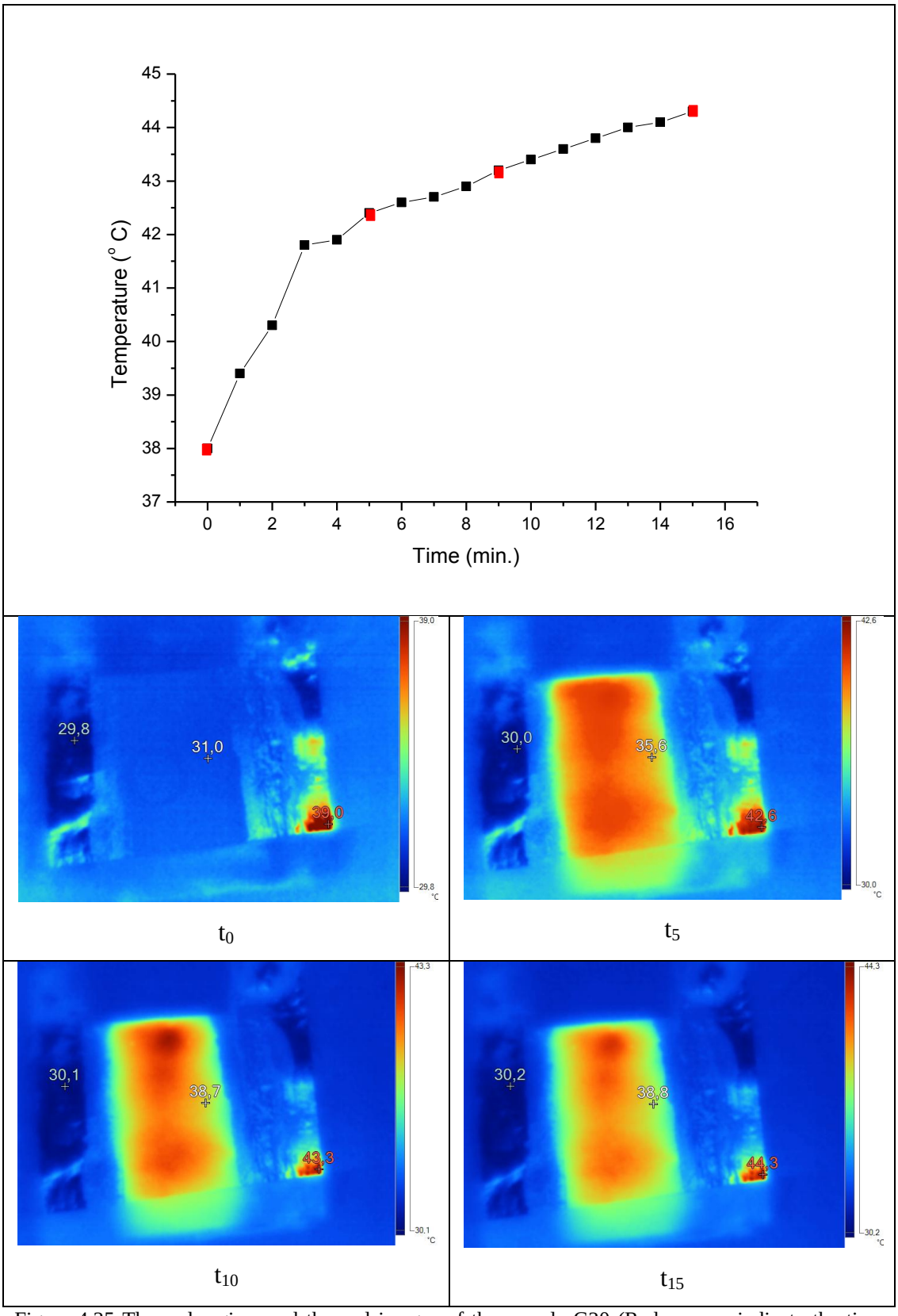

Figure 4.25 Thermal regime and thermal images of the sample G20 (Red squares indicate the time when the images are taken).

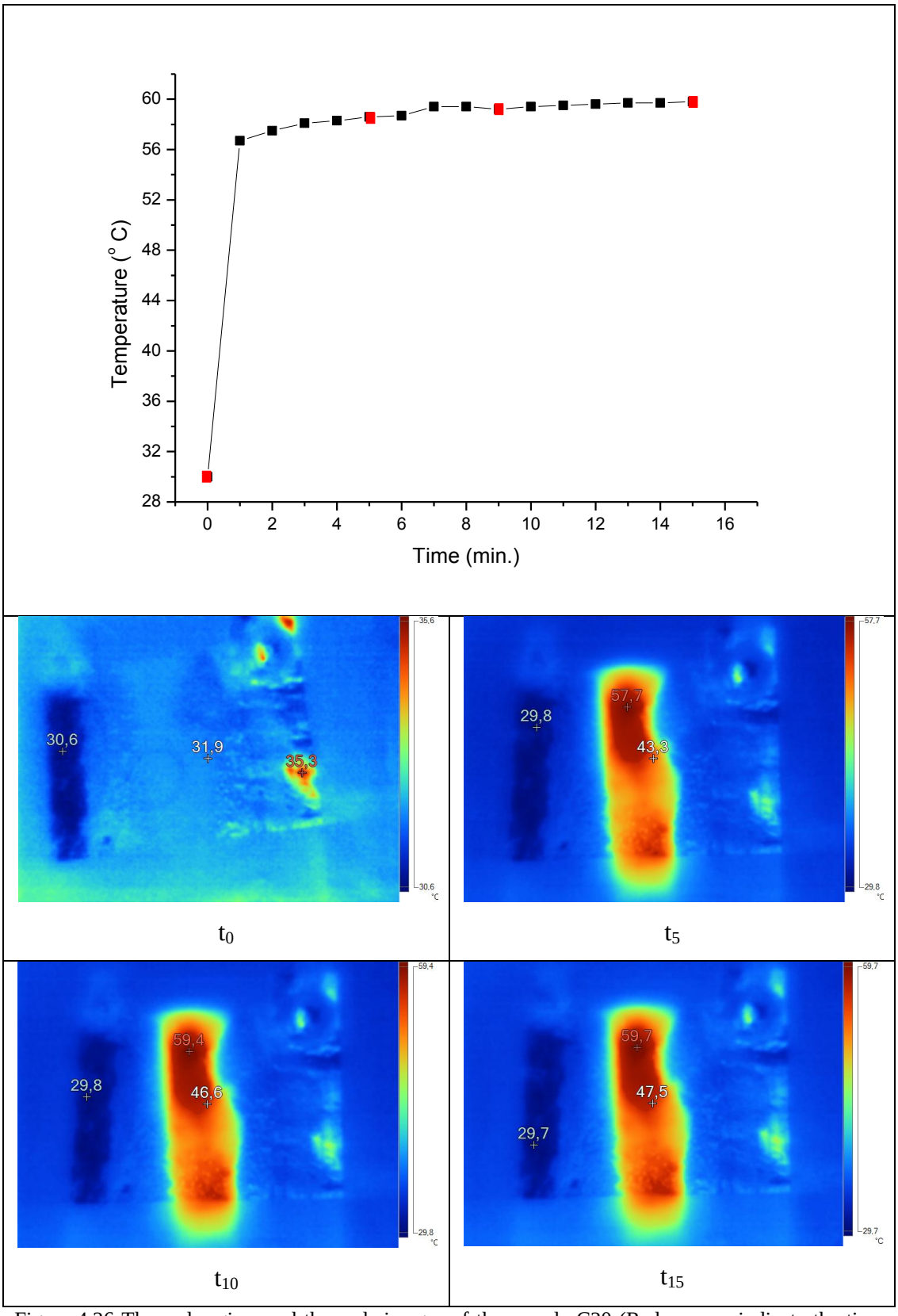

Figure 4.26 Thermal regime and thermal images of the sample C20 (Red squares indicate the time when the images are taken).

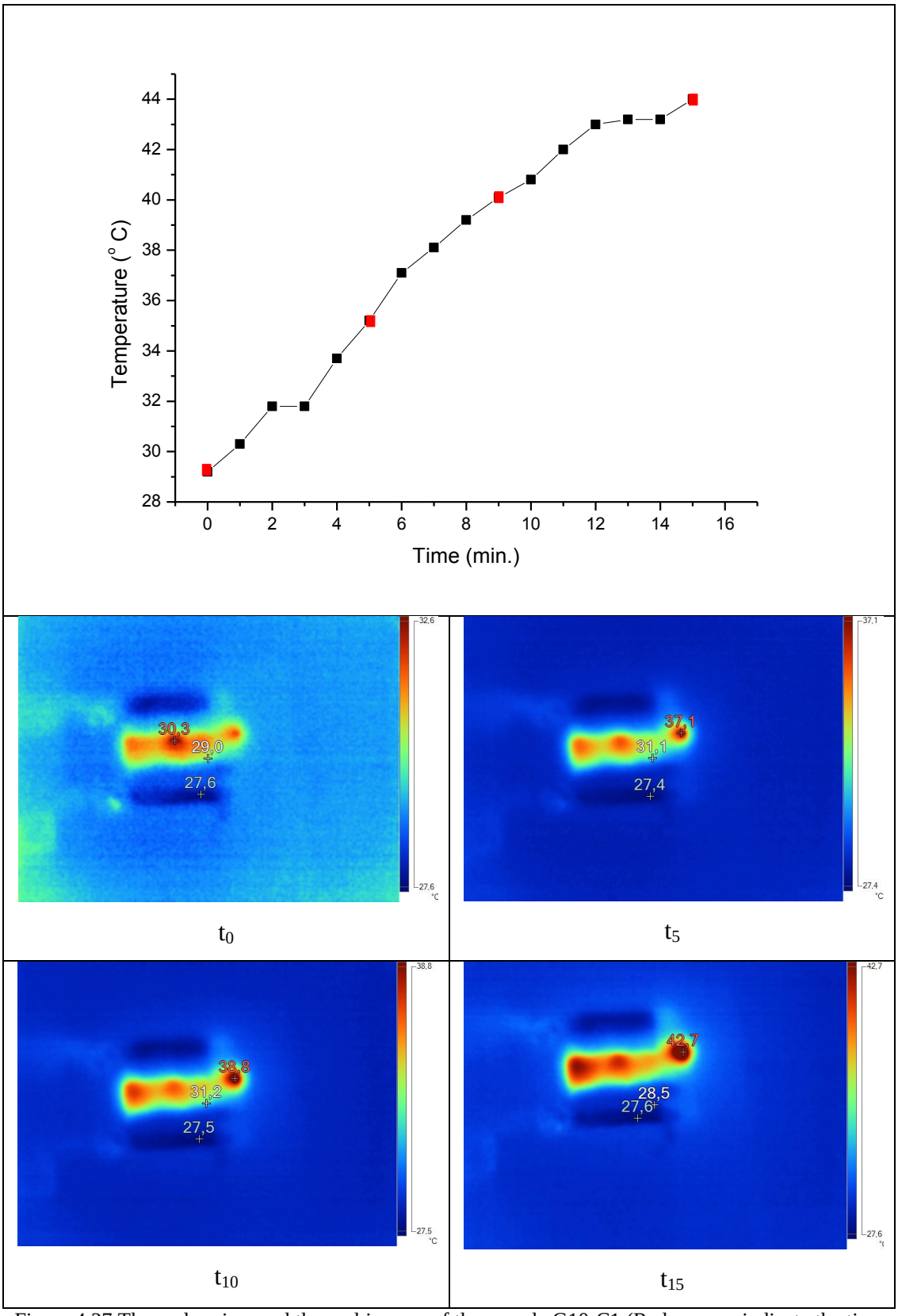

Figure 4.27 Thermal regime and thermal images of the sample G10-C1 (Red squares indicate the time when the images are taken).

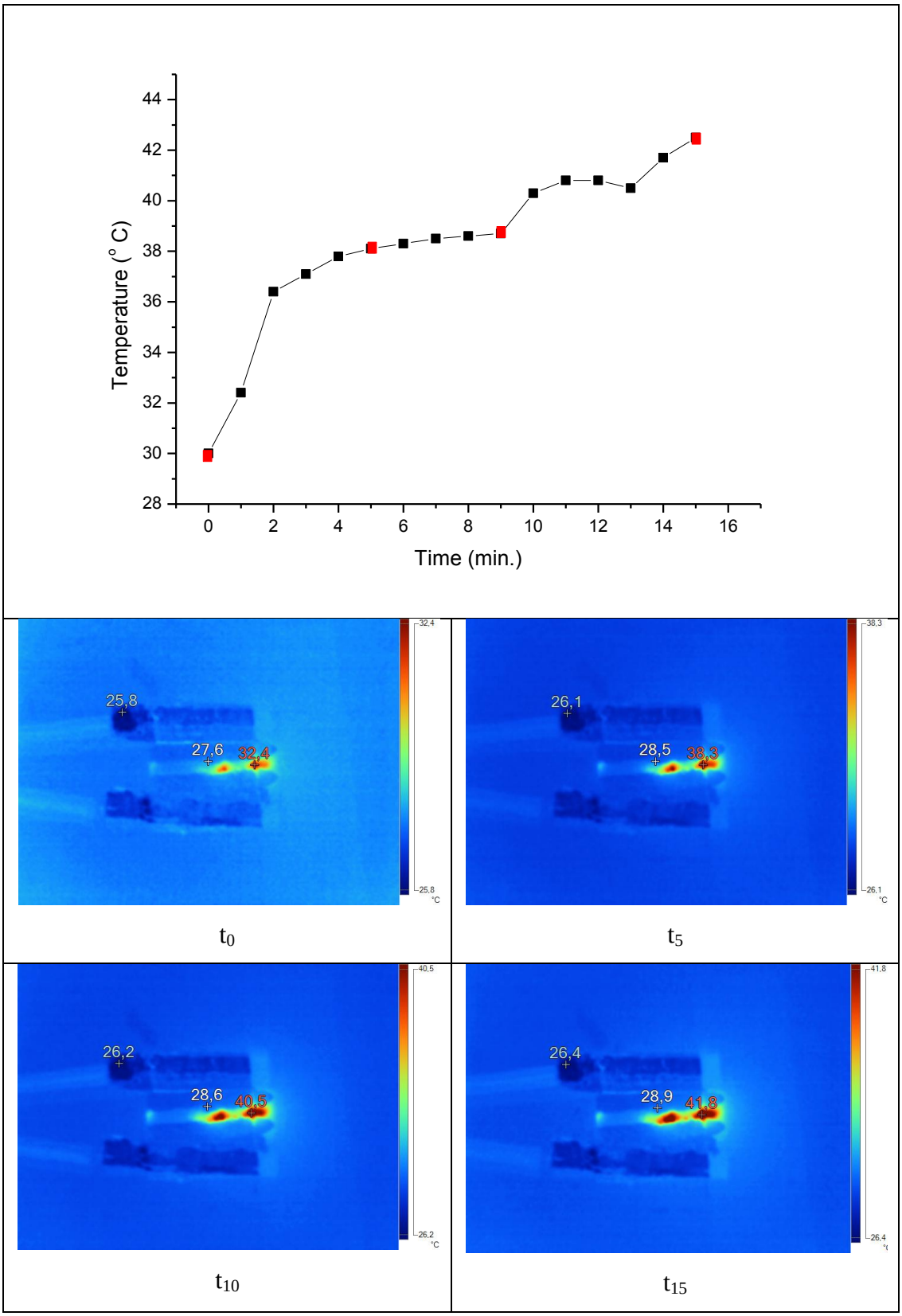

Figure 4.28 Thermal regime and thermal images of the sample G10-C3 (Red squares indicate the time when the images are taken).

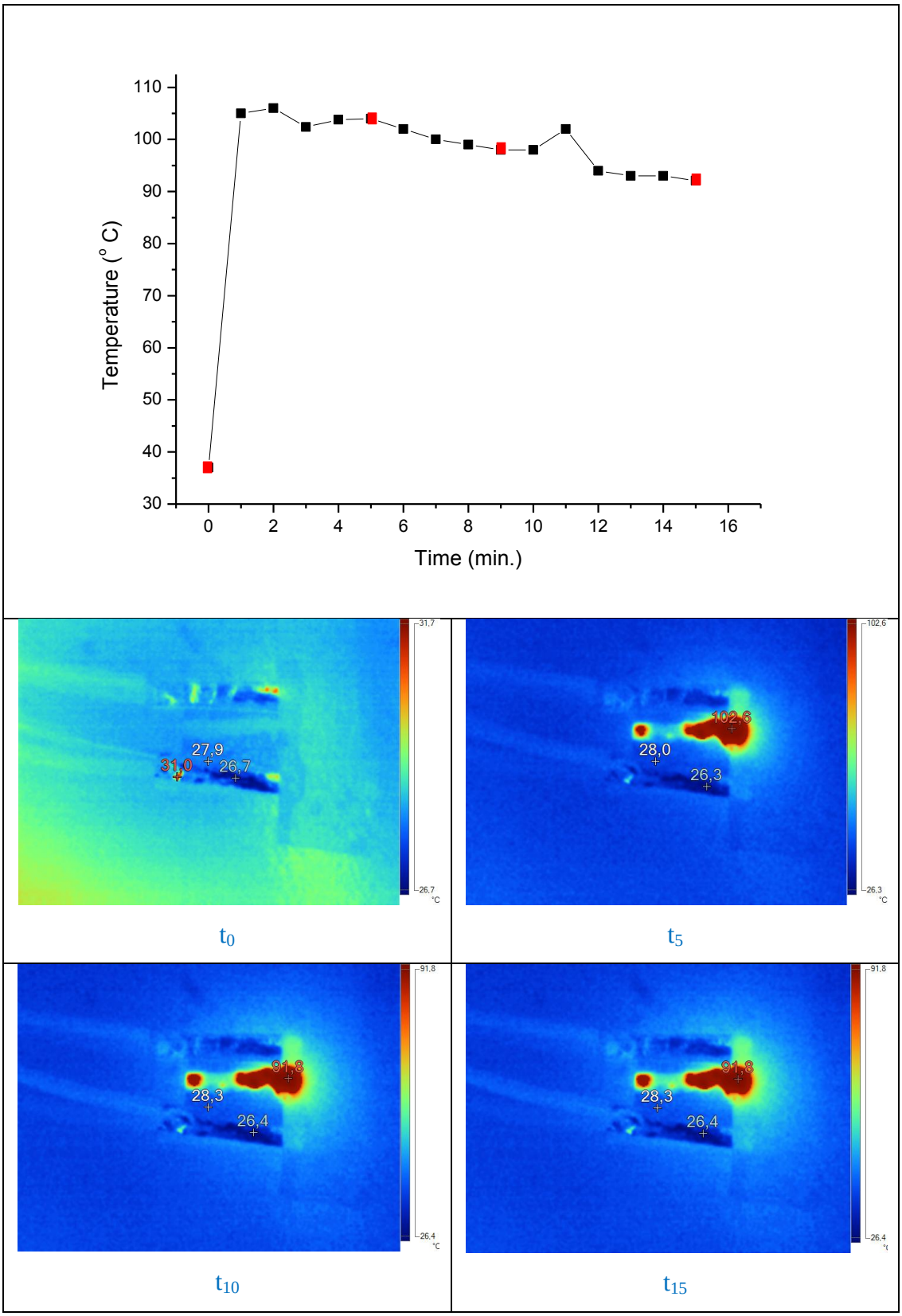

Figure 4.29 Thermal regime and thermal images of the sample G10-C5 (Red squares indicate the time when the images are taken).

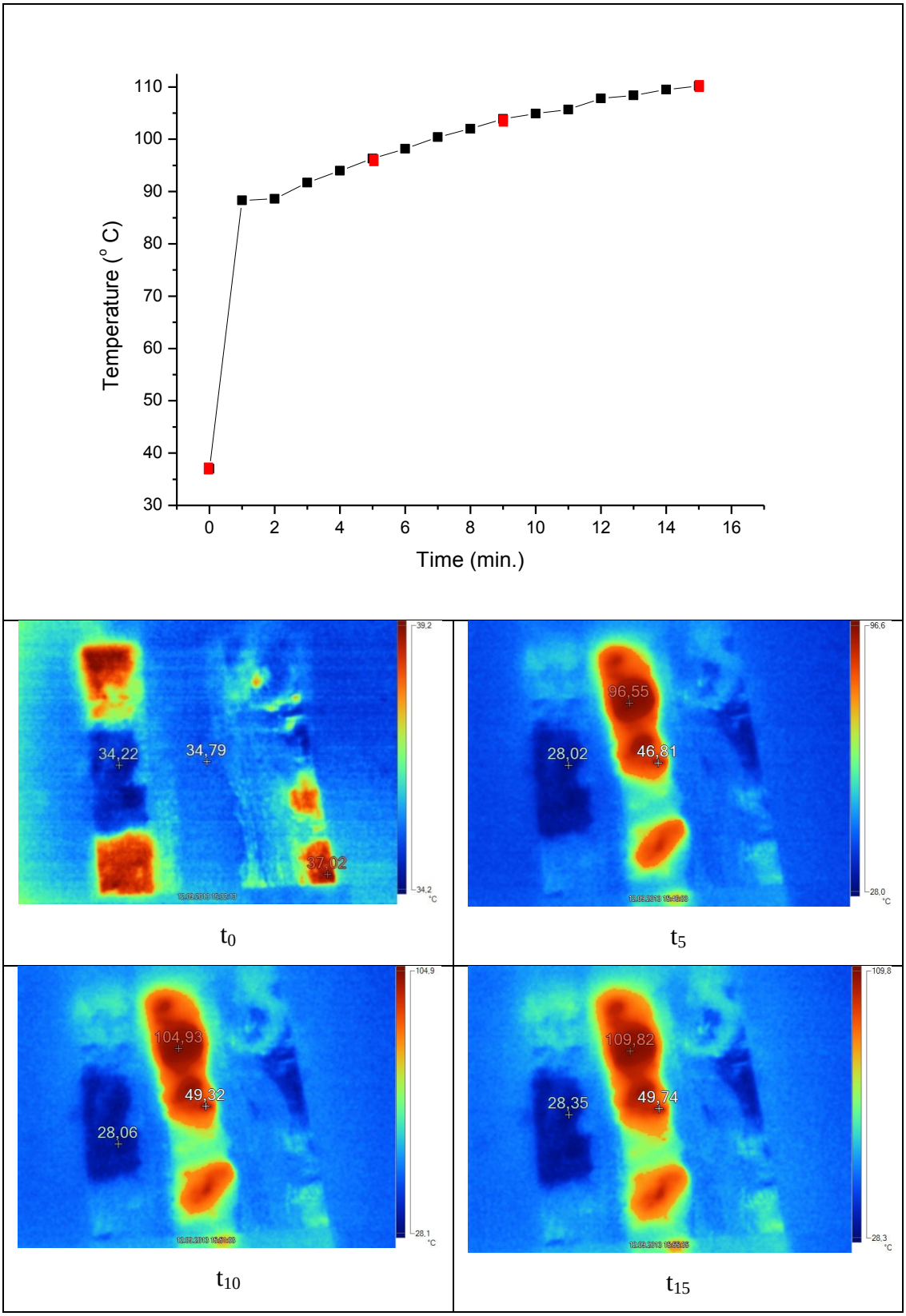

Figure 4.30 Thermal regime and thermal images of the sample G10-C7 (Red squares indicate the time when the images are taken)

thermal camera and timer. Time versus surface temperatures of the optimum samples with optimum electrical properties determined in the previous title were measured and thermal images were taken for every five minutes. Thermal regimes and thermal images of the samples G20, C20, 10G-1C, 10G-3C, 10G-5C and 10G-7C were plotted in Figures 4.25, 4.26, 4.27, 4.28, 4.29 and 4.30 respectively.

Due to the different resistance of the samples; a 4mA constant current (variable voltage) was adjusted in power supply to make heating results comparable. Hence the performance of the films were determined using the same current flow. Depending on the obtained results; it can be expressed that sample with minimum resistance (G10-C7) was found to be the best heating element with the maximum obtained temperature on the surface. Comparable result are given in the chart depicted in Figure 4. 31.

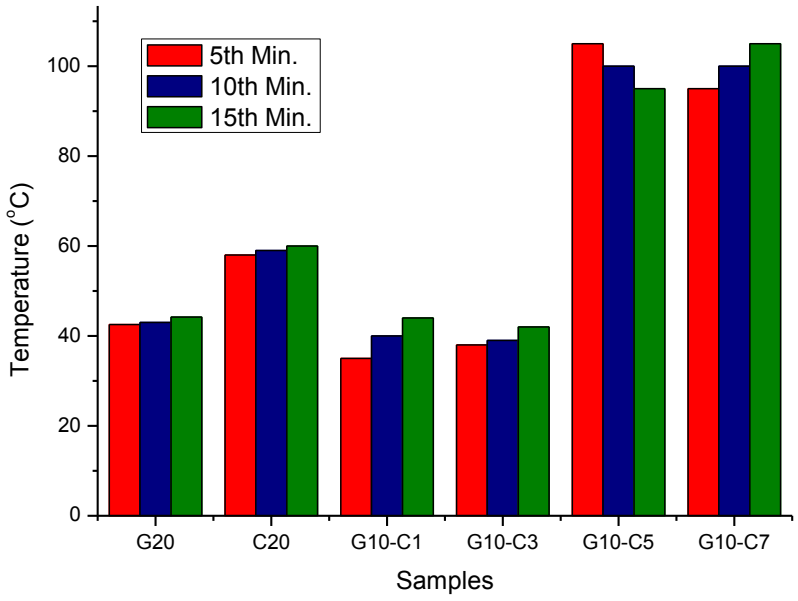

Figure 4.31 Comparative surface temperatures of the samples for different durations.

The maximum temperature of the surface can be defined as the place where resistance is the lowest in the surface of the film. In this context, thermographs taken with thermal camera will help us on the determination the heat releasing homogeneity of the films. A general assessment based on the thermal camera images

were done in Table 4.1. Based on the results, it must be again noted that the temperatures obtained on the surface was performed using constant current. If one increases the applied current the maximum obtained temperature of the film will be found to be increased.

Table 4.1 General assessment of heating experiments

Sample	T_{max} (^{O}C)	ΔT(^{O}C)*	HR Homogeneity*	Potential Application
G20	45	1	High	Heat releasing fabrics
C20	60	10	Medium	Portable saunas
G10-C1	47	10	Medium	Heat releasing fabrics
G10-C3	42	13	Medium	Heat releasing fabrics
G10-C5	103	60	Low	Boilers , central heating
G10-C7	110	20	High	Boilers , central heating

*Heat releasing homogeneity is determined by (T_{max} /ΔT) and $\Delta T=T_{max}-T_{min}$

As a general discussion on; co-percolation process which is the key point of the thesis was also supported by the heating performances. Co-percolation samples were determined as the optimum samples where homogeneous and higher temperature needed. Subsequent to heating performance tests with small size samples, applications were performed using real size samples based on the determined potentials listed in Table 4.1.

4.10 Applications

In the scope of the thesis, four applications was investigated. These are heat releasing fabrics, portable home saunas, combi boilers and greenhouse heating systems. Before listing the application results, it must be noted that; composites can be applicable in a wide range where one needs heating.

Smart textiles; nowadays is a promising research area since they have been employed as radar absorbing material, self cleaning and antibacterial clothes, unwrinkled fabrics and so on. Another application which is accomplished by us is heat releasing fabrics which is not reported in literature as industrial or trade scale. A coating was produced with the same scale of a carpet with G20 composition as

depicted in Figure 4.32. An adjustable thermostat was added in to the circuit to control. The thermostat temperature is determined as 40 ^{o}C. In a 13 ^{o}C temperature day; a 10 m^{2} room temperature is kept about 20-22 ^{o}C. Beside the numerical results; it must be noted that heat releasing from the floor over a large surface is more comfortable than any electrical heater using IR radiation. Depending on the thermodynamic laws, it is known that warm air move upwards and replace with cold air. Hence people using floor heating feels more comfortable than any other heating equipment working in a higher position (i.e. air conditioner and IR radiators.).

Figure 4.32 Heat releasing carpet application.

Another application performed in this thesis is the portable home saunas. Portable home saunas are newbie technology generally used for heat therapies in house or special health centers. Beside the fact that; similar to heat releasing carpets; samples of C20 were produced and concealed between polyester pockets. The prototype sauna produced in this study is depicted in Figure 4.33 with basic units as foldable siding, flooring and top cover. System was tested using thermometer to decide inner temperature. In only 5 minutes; the temperature is raised up to 50 ^{o}C where the ambient temperature was about 18 ^{o}C. Medical and pharmaceutical tests which are very important but out of the scope of the thesis, must be afforded to utilize a portable home sauna as a therapy unit.

Figure 4.33 Portable Home Sauna (1: Flooring, 2:Up cover and 3: Foldable Siding.)

Third important application performed in this study is the combi or boiler systems. Present devices or systems using electrical energy to heat up water for any requirement almost uses metallic heating elements reported in previous chapters. Beside the disadvantageous of metallic elements as low corrosion resistant and importability coefficient of performance (COP) tests were performed to compare a metallic heating element and heat releasing CPC film with G10-C7 composition. Prior to COP tests, some physical properties must be known as listed in Table 3.2. Consumed electrical energy, supplied heat energy and COP values against time were determined using a electric meter, Equations 3.5 and 3.6, respectively. The obtained results are listed in Table 4.2.

Table 4.2 COP test results.

Element	Time (min)	Consumed Electrical Energy (J)	Temperature of Water (^oC)	Supplied Heat (J)	COP
Metallic	0	0	29	0	1.08
	30	1774.8	75	1922.8	
CPC	0	0	29	0	1.18
	30	1630.8	75	1922.8	

If the data listed in Table 4.2 are taken in to account, the CPC sample was found to be 10 % more efficient than a typical metallic heating element. Based on the results, it can be inferred that CPC film which surrounds the boiler wall extensively releases a homogenous heat in comparison to metallic element which supply heat from a local surface. If further investigations and innovations are considered, the test results are promising for replacement of metallic films with if heat insulation and boiler wall material selections were successfully afforded. If the relative efficiency against metallic element is increased, many effective devices and systems can be easily transformed to CPC based ones.

Based on the results obtained in the boiler systems; make us to think about heating a green house or a house by only replacing heat generating heart of a central heating coils system with CPC based one. With this manner, a boiler mounted inside the green house depicted in Figure 3.15 and hot water circulation were afforded. Studies on this application are yet limited and innumerable since several measurements were performed in winter time. Inside temperature was kept at 20^oC for subzero ^oC nights.

In conclusion all application studies performed in the scope of the thesis were found to be successful. But an important point of the results must be noted that tests were afforded with prototype samples or systems. Generally results indicate that devices based on CPC technology can be mass produced with highly sensitive quality control processes. In addition to above; the number of these reported four application can be increased since CPCs are easily applicable where low temperature heating are required.

CHAPTER FIVE
CONCLUSIONS AND FUTURE PLANS

In conclusion it must be noted that; production and industrial applications of heat releasing electronic nanocomposite materials for heating systems was successfully afforded as titled in the thesis. In order to express and summarize this success based on the obtained results; general assessments outlined as follows:

1) Prior to production process; conductive fillers graphite, carbon black were milled with a self designed ball mill. As a result of milling operations; both graphite and carbon black powders were fined from micron to nanosclae successfully and adapted in to the matrix structure with desired compositions.

2) All the structural and chemical data obtained from XRD, XPS and FTIR analysis for the CPC films points out that; carbon black and/or graphite powders were encapsulated in the SACE matrix without any chemical and structural change with a good agreement to literature.

3) In the samples including just carbon black or graphite, beside some agglomerations, relatively homogenous structures were observed in the SEM analysis. Intended theoretical structure; for binary samples to be employed in copercolation was demonstrated in Figure 4.24. It can be expressed that the desired structures were successfully obtained if the SEM images of the binary samples were taken in to account where the bigger graphite plates were surrounded smaller carbon black agglomerates.

4) Thermal properties of a heat releasing conducting polymer must be considered because the thermal fluctuations at operation. DTA/TG analysis of the samples were afforded to determine decomposition temperatures. The decomposition temperatures of the films with different fractions of graphite and/or carbon black were determined about 400 ^{o}C. Little temperature changes were observed with different filler fractions. Similar to DTA results, TG alaysis were found to be indicating weight

losses about 56 %. The obtained decomposition temperatures are higher and more sufficient than the desired operation temperatures of the CPC heating elements.

5) Although mechanical analysis of the CPC films are less important than the other analysis mostly related to the heating element efficiency, they were performed to determine the mechanical limits of the films to be employed in several heating applications. In addition it is a fact that all the mechanical properties of the films were found to be increasing with the increasing content of the filler as expressed in the rule of mixtures for composites.

6) Electrical properties of a heat releasing CPC film are the most important parameters for further device applications and material innovations. Percolation thresholds of the samples were determined as 15 and 13 (wt. %) for graphite and carbon black filled composite films respectively. In order to decrease composition where the conductivity begins; copercolation studies were successfully applied. Composition of conductivity were decreased thanks to synergetic effect of graphite and carbon black. In order to clarify the innovations provided by co-percolation, the advantages of them must be noted. If long term plan for process transferred to mass production, the decrease in the filler content will provide a significant decrease the production costs.

7) Heating performances against time were performed using constant current to make the efficiency of the films comparable. Maximum temperatures were found to be between 45 and 110 ^{o}C which indicates different types of applications. In addition to maximum temperature heat releasing homogeneity is an important parameter for a wide surface film heating element. Films with less filler content was found to be less homogeneous as listed in Table 4.1. It must also be noted that test were employed with a constant current, which means the increasing current will increase the maximum surface temperatures between the limits reported in DTA analysis.

8) In the scope of the thesis four applications was investigated. These are heat releasing fabrics, portable home saunas, combi boilers and greenhouse heating

systems. All the applications were successfully performed using prototype devices which were designed and produced by us. Beside these applications it must be noted that; composites can be applicable in a wide range of area where one needs heating.

As denoted in the title of the thesis; heat releasing CPC films were successfully produced and utilized in some applications. The obtained result indicates that the performed study which has some innovations about the heating technology. Hence the systems can be easily adapted in to the present heating devices. This high potential of the results must be transferred in to industrial scale of production with the design of an integrated production unit were substrates, matrix and fillers were fed and CPC films were obtained at the end.

In addition to the mass production plans, graphite used in the study can be replaced by the graphene powder since limited milling was performed with graphite. Graphene can be described as a one-atom thick layer of the layered mineral graphite. High-quality graphene is very strong, light, nearly transparent, and an excellent conductor of heat and electricity. Its interaction with other materials and with light, and its inherently two-dimensional nature, produce unique properties.Due to fact that smarter CPCs can be used many device application. And the idea of producing a heating element for house or space heating can be transformed to micro scale to heat any device or circuits with its charming potential for high technology application.

REFERENCES

Advani, S. G., & Hsiao, K. T. (2012). *Manufacturing techniques for polymer matrix composites (PMCs)*. Cambridge: Woodhead Publishing Limited.

Ak, N. F. (2008). *Production of hydroxyapatite coating by Sol-Gel technique on 316L stainless steel and its corrosion properties*. Izmir: Dokuz Eylul University, The Graduate School of Natural and Applied Sciences.

Al-Saleh, M., Saadeh, W. H., & Sundar, U. (2013). EMI shielding effectiveness of carbon based nanostructured polymeric materials. *Carbon, 60,* 146–156

Aneli J., Gennady Z., & Omar M. (2011). Physical principles of the conductivity of electrically conductive polymer composites. *Chemistry, 5*, 1-8.

Atay, H. Y., & Celik, E. (2010). Use of Turkish huntite/hydromagnesite mineral in plastic materials as a flame retardant. *Polymer Composites. 31*, 1692–1700.

Baniassadi, M., Addiego, F., Laachachi, A., Ahzi, S., Garmestani, H., Hassouna, F., et al. (2011). Using SAXS approach to estimate thermal conductivity of polystyrene/zirconia nanocomposite by exploiting strong contrast technique. *Acta Materialia, 59,* 2742–2748.

Belashi, A. (2011). *Percolation modeling in polymer nanocomposites.* Toledo: The University of Toledo.

Berkovich, E.S. (1951). Three-faceted diamond pyramid for micro-hardness testing. *Industrial Diamond Review. 11, 127,* 129-133.

Birlik, I. (2011). *Synthesis of superconducting films and improvement of their flux pinning properties with barium zirconate nanoparticles using chemical solution*

deposition method. Izmir: Dokuz Eylul University, The Graduate School of Natural and Applied Sciences.

Bloor, D., Donnelly, K ., Hands, P. J., Laughlin, P., & Lussey, D. (2005). A metal–polymer composite with unusual properties. *Journal of Physics D: Applied Physics, 38*, 2851–2860

Cheang, P., & Khor, K. A. (2003). Effect of particulate morphology on the tensile behaviour of polymer/hydroxyapatite composites. *Materials Science and Engineering A3,45*, 47- 54.

Chen, D., Yang, J., & Chen, G. (2010). The physical properties of polyurethane/graphite nanosheets/carbon black foaming conducting nanocomposites. *Composites: Part A, 41*, 1636–1638.

Chun, K. Y., Oh, Y., Rho, J., Ahn, J. H., Kim, Y. J., Choi, H. R., et al. (2010). Highly conductive, printable and stretchable composite films of carbon nanotubes and silver. *Nature Nanotechnology, 5*, 853–857.

Colloca, M., Gupta, N., & Porfiri, M. (2013). Tensile properties of carbon nanofiber reinforced multiscale syntactic foams. *Composites: Part B, 44*, 584–591.

Crist, B.V. (2011). *X-ray photoelectron spectroscopy.* Retrieved June 10, 2010, from http://en.wikipedia.org/wiki/X-ray_photoelectron_spectroscopy

Dai, L. (2004). *Intelligent macromolecules for smart devices from materials synthesis to device applications*. London: Springer-Verlag Limited.

Davtyan, S. P., Berlin, A., Agabekov, V., & Lekishvili, N. (2012). Synthesis, properties, and applications of polymeric nanocomposites. *Journal of Nanomaterials, Article ID 215094*, 3 pages

Deshmukh, Y. V. (2005). *Industrial heating, principles, techniques, materials, applications, and design*. Florida: CRC Press.

Ercin, G.H., Camanho, P.P., Xavier , J., Catalanotti, G., Mahdi, S., & Linde, P. (2013). Size effects on the tensile and compressive failure of notched composite laminates. *Composite Structures, 96*, 736–744.

Erol, M., & Çelik, E., (2013). Graphite-flake carbon-black/polystyrene composite films as plane heaters. *Materials and Technology*, *47*, 25–28.

Fisher-Cripps, A. C. (2009). *Nanoindentation* (3rd.). Australia; Fischer-Cripps Laboratories Pty Ltd.

Gilmanshina, T. R., Mamina, L. I., & Galina, A. K. (2012). The technology of getting cryptocrystalline graphite having low ash content mined in the deposits of Krasnoyarsk Territory. *Journal of Siberian Federal University. Engineering & Technologies, 4*, 419-432.

Girotto, C., Rand, B. P., Genoe, J., & Heremans, P. (2009). Exploring spray coating as a deposition technique for the fabrication of solution-processed solar cells. *Solar Energy Materials & Solar Cells, 93*, 454–458.

Griebel, M., & Hamaekers, J. (2004). Molecular dynamics simulations of the elastic moduli of polymer–carbon nanotube composites. *Computer Methods in Applied Mechanics and Engineering, 193*, 1773–1788.

Gupta, A., & Choudhary, V. (2011). Electromagnetic interference shielding behavior of poly(trimethylene terephthalate)/multi-walled carbon nanotube composites. *Composites Science and Technology, 71*, 1563–1568.

Hamilton, V., Ricardo, L. B., & Roberto, M. T. (2003). Ionic transport in conducting polymers/nickel tetrasulfonated phthalocyanine modified electrodes. *Polymer, 44* 5369–5379.

Hao, X., Gai, G., Yang, Y., Zhang, Y., & Nanb, C. (2008). Development of the conductive polymer matrix composite with low concentration of the conductive filler. *Materials Chemistry and Physics, 109*, 15–19.

Isaji, S., Bin, Y., & Matsuo, M. (2009). Electrical conductivity and self-temperature-control heating properties of carbon nanotubes filled polyethylene films. *Polymer, 50,* 1046–1053.

Jeon, J., Lee, H. B. R., & Bao, Z. (2013). Flexible wireless temperature sensors based on Ni microparticle-filled binary polymer composites. *Advanced Materials, 25*, 850–855.

Jing, X., Zhao, W., & Lan L. (2000). The effect of particle size on electric conducting percolation threshold in polymer/conducting particle composites. *Journal of Materials Science Letters, 19*, 377– 379.

Jones, P. L. (2003) *Electroheat and materials processing, electrical engineer's reference book*. Oxford; Elsevier,

Kim, O., & Kim, S. (2010). Noncolvalent functionalization of graphene with end-functional polymers, *The Royal Society of Chemistry, 1*, 1-4.

Klemperer, C., J., & Mahara, D. (2009). Composite electromagnetic interference shielding materials for aerospace applications. *Composite Structures*, *91*, 467–472.

Köysüren, Ö. (2008) P*reparation and characterization of conductive polymer composites, and their assessment for electromagnetic interference shielding materials and capacitors.* Ankara: Middle East Technical University.

Lee, S. H., Kim, J. H., Choi, S. H., Kim, S. Y., Kimb, K. W., & Youn, J. R. (2009). Effects of filler geometry on internal structure and physical properties of polycarbonate composites preparedwith various carbon fillers, *Polymer International, 58*, 354–361

Li, J., & Kim, J. K. (2007). Percolation threshold of conducting polymer composites containing 3D randomly distributed graphite nanoplatelets. *Composites Science and Technology*, *67*, 2114–2120.

Lu, W., Lin, H., Wu, D., & Chen, G. (2006). Unsaturated polyester resin/graphite nanosheet conducting composites with a low percolation threshold. *Polymer, 47*, 4440-4444.

Lucintel – Global Management Consulting & Market Research Firm (2013). Retrieved June 15, 2013, from, http://www.lucintel.com/Lucintel-GlobalCompositeMarketAnalysis-ACMA2012-EducationalSession.pdf

Mahmoudian, M. R., Alias, Y., Basiruna, W. J., & Ebadid, M. (2013). Effects of different polypyrrole/TiO_2 nanocomposite morphologies in polyvinyl butyral coatings for preventing the corrosion of mild steel. *Applied Surface Science, 268*, 302–311.

Mazumdar, S. K. (2001). *Composites manufacturing, materials, product, and process engineering*, Florida; CRC Press LLC.

Michler, G. H. (2008). *Electron microscopy of polymers*. Berlin: Springer-Verlag Heidelberg.

Mohanraj, G. T., Dey, P. K., Chaki, T. K., Chakraborty, A., & Khastgir1, D. (2007). Effect of temperature, pressure, and composition on DC resistivity and AC conductivity of conductive styrene–butadiene rubber–particulate metal alloy Nanocomposites. *Polymer Composites, 28*, 696–704.

Morais, A. B. (2006). Prediction of the longitudinal tensile strength of polymer matrix composites. *Composites Science and Technology*, *66*, 2990–2996.

Moreno, I., Navascues, N., Irusta, S., & Santamaría, J. (2012). Silver nanowires/polycarbonate composites for conductive films. *Materials Science and Engineering IOP Conf. Series, 40*, 012001.

Moulson, A. J., & Herbert, J. M. (2003). *Electroceramics, Materials, Properties, Applications.* (Second edition). Chichester:Wiley.

Nam, I. W., Kim, H. K., & Lee, H. K. (2012). Influence of silica fume additions on electromagnetic interference shielding effectiveness of multi-walled carbon nanotube/cement composite. *Construction and Building Materials, 30*, 480–487.

Nano Enhanced Wholesale Technologies (2013). Retrieved June 18, 2013 from http://www.nano-enhanced-wholesale-technologies.com/faq/carbon-forms.htm.

Oliver, W.C., & Pharr, G.M. (1992). An improved technique for determining hardness and elastic modulus using load and displacement sensing indentation experiments. *Materials Research Society*, *7*, 1564-1583.

Opwis, K., Knittel, D., & Gutmann, J. S. (2012). Oxidative in situ deposition of conductive PEDOT:PTSA on textile substrates and their application as textile heating element. *Synthetic Metals, 162*, 1912–1918.

Oxford Vacuum Science Ltd, (2013), Retrieved June 18, 2013 from http://www.oxford-vacuum.com/background/thin_film.htm.

Papliaka, Z., E., Konstantinos S., A., & Evangelia A. V. (2010). Study of the stability of a series of synthetic colorants applied with styrene-acrylic copolymer, widely used in contemporary paintings, concerning the effects of accelerated ageing. *Journal of Cultural Heritage, 11,* 381–391.

Peng C.,, Chuxin Z., Ming L., & Jianqing W. (2013). Preparation of silica encapsulated carbon black with high thermal stability. *Ceramics International, 39,* 7247-7253.

Przemyslaw, L., Aneta, L., Sylwia, K., Regina J., & Jerzy, K. (2011) Obtaining and properties of polyolefin composites metamaterials with copper micro- and nanoflakes, *Polimery,* 56, 4, 324-327.

Research and Markets (2013). Retrieved June 19, 2013, from http://www.researchandmarkets.com/reports/607616/advances_in_polymer_technology_highlights_of

Sadeghi, S., & Mohammad, T. (2006). Synthesis, characterization and thermal stability study of styrene-based ionomers programmed heating experiments, *Iranian Journal of . Chemistry and. Chemical Engineering. 25,* 1-5.

Schneider, C., Kazemahvazi, S., Akermo, M., & Zenkert, D. (2013). Compression and tensile properties of self-reinforced poly(ethyleneterephthalate)-composites. *Polymer Testing 32,* 221–230.

Shukor, M. S, & Saifudin, H., Y. (2010). Properties determination of self-lubricating algraphite composites. *Journal of Advanced Manufacturing and Technology, 4,* 1-5.

Seo, M. K., Rhee. K. Y., & Park, S.J. (2011). Influence of electro-beam irradiation on PTC/NTC behaviors of carbon blacks/HDPE conducting polymer composites. *Current Applied Physics, 11*, 428-433.

Shen, J., Champagne, M. F., Yang, Z., Yu, Q., Gendron, R., & Guo, S. (2012). The development of a conductive carbon nanotube (CNT) network in CNT/polypropylene composite films during biaxial stretching. *Composites: Part A, 43*, 1448–1453.

Shih, W. P., Tsao, L.C., Lee. C.W., Cheng, M. Y., Chang, C., Yang, Y. J., et al. (2010). Flexible temperature sensor array based on a graphite-polydimethylsiloxane composite. *Sensors, 10*, 3597-3610.

Sivakkumara, S.R., Koa, J. M., Kim, Y. D., Kim, B.C., & Wallace, G.G. (2007). Performance evaluation of CNT/polypyrrole/MnO_2 composite electrodes for electrochemical capacitors. *Electrochimica Acta, 52*, 7377–7385.

Strumpler, R., & Glatz-Reichenbach, J. (1999) "Conducting polymer composites," *Journal of Electroceramics, 3*, 4, 329-34.

Teh, P. L., Ng, H. T., & Yeoh, C. K. (2011). Recycled copper as the conductive filler in polyester composites. *Malaysian Polymer Journal, 6*, 98-108.

Timurkutluk, B., Celik, S., Timurkutluk, C., Mat, M. D., & Kaplan, Y. (2012). Novel electrolytes for solid oxide fuel cells with improved mechanical properties. *International Journal of Hydrogen Energy, 37*, 3499 - 3509.

Varelaa, H., Brunoa, R. L., & Torresib, R.M. (2003). Ionic transport in conducting polymers/nickel tetrasulfonated phthalocyanine modified electrodes. *Polymer, 44*, 5369–5379.

Wacker Chemie AG, (2013), Retrieved June 18, 2013 from http://www.wacker.com/cms/en/products-markets/pl_composites/pl_comp_appl/handlayup.jsp?country=TR&language=tr

Wan, Y., Xiong, C., Yu, J., & Wen, D. (2005). Effect of processing parameters on electrical resistivity and thermo-sensitive properties of carbon-black/styrene–butadiene–rubber composite membranes. *Composites Science and Technology, 65*, 1769–1779.

Wang, L., Wang, D., Zhu, G., Li, J., & Pan, F. (2011). Thermoelectric properties of conducting polyaniline/graphite composites. *Materials Letters, 65*, 1086–1088.

Wang, Z., Han, E., & Ke, W. (2006). Effect of acrylic polymer and nanocomposite with nano-SiO_2 on thermal degradation and fire resistance of APP-DPER-MEL coating. *Polymer Degradation and Stability, 91*, 1937-1947.

Wanga, N., Zhang, J., Fang, Q., & Hui, D. (2013). Influence of mesoporous fillers with PP-g-MA on flammability and tensile behavior of polypropylene composites. *Composites Part B, 44*, 467–471.

Ward, J. K., & Koros, W. J. (2011). Crosslinkable mixed matrix membranes with surface modified molecular sieves for natural gas purification: II. Performance characterization under contaminated feed conditions. *Journal of Membrane Science, 377*, 82– 88.

Western Carolina University (2013). Retrieved June 18, 2013 from http://paws.wcu.edu/ballaaron/www/met366/modules/module5/mod5.htm.

Wheeler, J. M. (2009). *Nanoindentation under dynamic conditions*. England: Clare College, University of Cambridge.

Wu, C.S. (2011). Polyester and multiwalled carbon nanotube composites: characterization, electrical conductivity and antibacterial activity. *Polymer International, 60*, 807–815.

Xu, S., Wen, M., Li, J., Guo, S., Wang, M., Du, Q., et al. (2008). Structure and properties of electrically conducting composites consisting of alternating layers of pure polypropylene and polypropylene with a carbon black filler. *Polymer, 49*, 4861–4870.

Yang, Q., Wu, C. N., Saito, T., & Isogai, A. (2012). Cellulose–clay layered nanocomposite films fabricated from aqueous cellulose/LiOH/urea solution. *Carbohydrate Polymers* (Article in Press).

Zhao, X., Koos, A. A., Chu, B. T. T., Johnston, C., Grobert, N., & Grant, P. S. (2009). Spray deposited fluoropolymer/multi-walled carbon nanotube composite films with high dielectric permittivity at low percolation threshold. *Carbon, 47*, 561 –569.